Australian Water Resources Council

Technical Paper No. 66

Movement of non-reactive solute through the unsaturated soil zone

DEPARTMENT OF NATIONAL DEVELOPMENT AND ENERGY
AUSTRALIAN WATER RESOURCES COUNCIL

Research Project No. 78/109

MOVEMENT OF NON–REACTIVE SOLUTE THROUGH THE UNSATURATED SOIL ZONE

by M.J. Jones and K.K. Watson

School of Civil Engineering
The University of New South Wales

Australian Water Resources Council
Technical Paper No. 66

AUSTRALIAN GOVERNMENT PUBLISHING SERVICE
CANBERRA 1982

Published for the Department of National Development and Energy on behalf of the Australian Water Resources Council by the Australian Government Publishing Service.

CIP Information

Jones, Malcolm J.
Movement of non—reactive solute through the unsaturated soil zone.

Bibliography.
Research project no. 78/109.
ISBN 0 642 89064 1.

1. Soil absorption and adsorption — Mathematical models.
I. Watson, K:K. (Keith Kingsford). II. Australian Water Resources Council. III. Title. (Series: Australian Water Resources Council technical paper ; no. 66).

631.4'32'0724

The AWRC Technical Paper series presents information resulting from research projects supported by the Water Research Program of the Australian Water Resources Council, which is funded by the Commonwealth Government. The report is presented in accordance with the general policy of providing for the wide dissemination of research findings arising out of the Council's research program. Publication of the report in this series does not signify that the contents necessarily reflect the views and policies of the Australian Water Resources Council or the Commonwealth or State Governments. Details of other publications in the series are given at the back of this report.

Printed by C. J. THOMPSON, Commonwealth Government Printer, Canberra

R81/7

ABSTRACT

The significance of computer-based numerical methods in describing non-reactive solute movement through the unsaturated soil zone is discussed and an implicit finite difference model of water movement in unsaturated soils is outlined. The development of an explicit finite difference model of solute movement is then described in detail and its use in conjunction with the soil water model explained. The solute model is verified by comparing the numerical results with a quasi-analytical solution developed for a constant-valued hydrodynamic dispersion coefficient. Further verification of the model is then undertaken using experimental data for solute movement during horizontal absorption under constant concentration and constant flux conditions. The experimental results and the numerical solutions provide the basis for a detailed analysis of the hydrodynamic dispersion coefficient in relation to velocity-dependent effects. The use of the model in simulating solute movement during an intermittent water application regime is described using a sandy loam as the porous material. An extensive annotated bibliography is included as an Appendix to the report.

ACKNOWLEDGEMENTS

The authors warmly acknowledge the advice and assistance of several colleagues, in particular Mr. D.G. Doran and Dr. J.D. Fenton from The University of New South Wales and Dr. D.E. Smiles and his staff from the C.S.I.R.O. Division of Environmental Mechanics. The Division of Environment Mechanics carried out the experimental program for this study and this assistance was appreciated. Mrs. Julie Chapman typed the manuscript and we extend our thanks to her for her skill, patience and thoroughness.

CONTENTS

LIST OF FIGURES

LIST OF SYMBOLS

A	Amplification factor	
$\bar{A}$	Complex conjugate of the amplification factor	
A_i, B_i, C_i, D_i	Coefficients for the tridiagonal equations	
C_s	Specific water capacity $[\partial\theta/\partial h]$	m^{-1}
$D(\theta)$	Soil water diffusivity	m^2s^{-1}
D_m	Molecular diffusion coefficient of KCℓ in solution	m^2s^{-1}
D_p	Molecular diffusion coefficient	m^2s^{-1}
D_h	Mechanical dispersion coefficient	m^2s^{-1}
D_e	Combined (effective) dispersion coefficient	m^2s^{-1}
F, F^*	Coefficients in solute finite difference equation	m^2s^{-1}
G	Coefficient in solute finite difference equation	ms^{-1}
J	Total solute flux	meq $m^{-2}s^{-1}$
K	Unsaturated hydraulic conductivity	ms^{-1}
L	Length of soil column	m
M	Integral in Smiles' analytical solution	
N	Number of equal space intervals in the one-dimensional grid	
R_c	Cell Reynolds number $[c/d]$	
S	Sorptivity	$ms^{-\frac{1}{2}}$
T	Reduced time ordinate $[v_o^2 t]$	m^2s^{-1}
V	Amplification function of the Fourier components	
W	Reduced velocity (solute finite difference model)	ms^{-1}
X	Reduced space ordinate $[v_o x]$	m^2s^{-1}
a,b	Experimental constants	
c	Solute concentration	meq m^{-3}
$\bar{c}$	Normalized solute concentration	
g	Coefficient in analytical studies	$ms^{-\frac{1}{2}}$
h	Soil water potential	m
q	Volumetric (Darcy) flux of solution	ms^{-1}
t	Time	s
v	Pore water velocity	ms^{-1}
$\bar{v}$	Average pore water velocity	ms^{-1}
v_o	Constant water flux at wetting surface	ms^{-1}
x	Horizontal flow direction ordinate	m
z	Vertical flow direction ordinate	m
Δt	Incremental time step (variable)	s
Δx, Δz	Incremental space step (constant)	m
α	Angle between $g(\lambda)$ and λ	
β	Experimental constant	m
θ	Volumetric water content	m^3m^{-3}
Ω	Coefficient in analytical studies	m
λ	Boltzman transformation parameter $[xt^{-\frac{1}{2}}]$	$ms^{-\frac{1}{2}}$
ϕ	Phase angle $[k\Delta z]$	
c	Courant number $[\Delta t.G/\Delta z]$	
d	Diffusion number $[\Delta t.F/(\Delta z)^2]$	
i	Complex number $[\sqrt{-1}]$	
k	Fourier wavenumber	
ℓ	Characteristic length	m

1 GENERAL INTRODUCTION

The unsaturated zone is the medium through which soluble salts and pollutants originating at the soil surface are conveyed to the groundwater system. In recent years the use of computer-based numerical models has enabled a study in detail to be made of a wide range of unsaturated flow systems involving the movement of 'pure' water. The stage has been reached where research workers are now extending such work to incorporate the simultaneous movement of solute or pollutant. The successful development of these studies will provide guidelines for environmental control in several problem areas. These include leaching strategies for saline soils, fertiliser and pesticide movement in agricultural systems and water quality changes during percolation through areas used for the landfill disposal of garbage.

The initial objective of the project was to develop and test a numerical system capable of describing the movement of solutes and pollutants through a soil profile to the water table under an intermittent water application regime. It became evident as the project developed that time constraints would require the above objective to be slightly modified by considering only solute movement. In addition, relatively shallow soil profiles have been simulated rather than the six-metre unsaturated zone of the local Botany Basin unconfined aquifer as originally envisaged.

During the past decade a comprehensive computer-based numerical approach to water movement in unsaturated soils has been developed in The School of Civil Engineering at The University of New South Wales. The range of initial conditions, boundary conditions and material properties able to be described by the computer program allows it to be used in simulating many naturally-occurring environmental systems. Chapter 2 in this report gives a brief summary of this water movement model emphasizing those aspects of particular interest in solute movement studies.

The development of the explicit finite difference model for non-reactive solute movement is described in detail in Chapter 3 with the related stability analysis being discussed in Chapter 4. The verification of the model for solute movement involving a constant-valued hydrodynamic dispersion coefficient is achieved by using a quasi-analytical solution developed for this purpose and described in Chapter 5. In the following three chapters the numerical solute analysis is checked against experimental results obtained for a fine sand for both horizontal absorption under constant concentration and constant flux conditions and for infiltration-redistribution. Finally, the ability of the model to simulate solute movement under intermittent conditions is discussed in Chapter 9 using Rubicon sandy loam as the porous material.

A significant and useful component of this report is Appendix A which provides an extensive annotated bibliography of literature in the solute movement field.

2 NUMERICAL ANALYSIS OF WATER MOVEMENT IN UNSATURATED SOILS

2.1 Introduction

One-dimensional vertical water movement in a rigid, homogeneous, porous, unsaturated material may be described by the equation

$$C_s(h)\,\frac{\partial h}{\partial t} = \frac{\partial}{\partial z}\left[K(h)\,\frac{\partial h}{\partial z}\right] + \frac{\partial}{\partial z}\left[K(h)\right] \qquad 2.1$$

where

h	soil water potential (expressed on a weight basis) relative to atmospheric pressure	$[L]$
t	time	$[T]$
z	flow direction ordinate, positive upwards	$[L]$
$C_s(h)$	$= \partial\theta/\partial h$ = specific water capacity	$[L^{-1}]$
θ	volumetric water content	$[L^3L^{-3}]$
$K(h)$	unsaturated hydraulic conductivity	$[LT^{-1}]$

Equation 2.1 is a convenient form of the unsaturated flow equation and has been used in solving a wide range of problems involving the hydrology of the unsaturated zone. Whisler and Watson (1968) described a computer-based numerical solution of equation 2.1 which used an implicit finite difference approach in the analysis. This computer program has been continually updated and, in its present form, is able to handle all types of constant and time-dependent boundary conditions, material variations including spatial heterogeneity, and intermittency in the application of water. The program has also been extended to allow the study of horizontal flow systems. For the latter development, equation 2.1 was modified to remove the gravity flow component giving

$$C_s(h)\,\frac{\partial h}{\partial t} = \frac{\partial}{\partial x}\left[K(h)\,\frac{\partial h}{\partial x}\right] \qquad 2.2$$

So that essentially the same computer program could be used in solving equation 2.2, the sign convention has not been changed. This results in the 'x' ordinate being positive in the direction opposing horizontal absorption.

2.2 Soil Water Hysteresis

Because of the marked hysteresis in $h(\theta)$ and therefore in $K(h)$, systems involving the intermittency of water application, such as in a series of infiltration-redistribution cycles, require the inclusion of a hysteresis model in the dataset. Three different hysteresis models have been developed for use with the general computer package - an interpolative model (Watson and Perrens 1973) and two domain models. The interpolative model is the simplest, and defines secondary and higher order scanning curves from the primary wetting and draining scanning curves. However its use is restricted to situations where the flow reversals are not too closely spaced in time. A model based on the dependent domain theory of hysteresis (Lees and Watson 1975) has a sounder physical basis, is more precise than the interpolative model and is not limited with regard to rapidly recurring intermittency. However, it suffers the disadvantages of requiring substantially more computer core storage and execution time. The second domain model, which is much simpler and requires less $h(\theta)$ data in its formulation, has recently been developed by Banerjee (personal communication).

In this study the timing of the infiltration-redistribution sequences in Chapter 9 is such that the interpolative hysteresis model can be safely used in the analysis.

2.3 An Implicit Finite Difference Model For Water Flow

To solve equation 2.1 (or equation 2.2) the space-time domain is written in incremental form as

$$z_i = (i - 1)\,\Delta z \qquad i = 1, 2, \ldots N, (N+1)$$

$$\Delta z = -L/N \qquad L = \text{Length of column}$$

$$t_j = \sum_{r=1}^{j} \Delta t_r \qquad j \geq 1$$

In order to avoid confusion, the following equations are developed for equation 2.1. The necessary changes for equation 2.2 are straightforward. The following approximations are made:

$$h(i+1,j+\tfrac{1}{2}) = \tfrac{1}{2}[h(i+1,j) + h(i+1,j+1)] \qquad 2.3a$$

$$h(i,j+\tfrac{1}{2}) = \tfrac{1}{2}[h(i,j) + h(i,j+1)] \qquad 2.3b$$

$$h(i-1,j+\tfrac{1}{2}) = \tfrac{1}{2}[h(i-1,j) + h(i-1,j+1)] \qquad 2.3c$$

and Taylor Series expansions used in both time and space. The central difference approximation to the L.H.S. of equation 2.1 then becomes

$$C_s \frac{\partial h}{\partial t}(i,j+\tfrac{1}{2}) = C_s(i,j+\tfrac{1}{2})[h(i,j+1) - h(i,j)]/\Delta t + 0(\Delta t)^2 \qquad 2.4$$

and for the space derivatives, using equations 2.3a, b, c

$$\frac{\partial h}{\partial z}(i+\tfrac{1}{2},j+\tfrac{1}{2}) = [h(i+1,j) + h(i+1,j+1) - h(i,j) - h(i,j+1)]/2\Delta z + 0(\Delta z)^2 \qquad 2.5a$$

$$\frac{\partial h}{\partial z}(i-\tfrac{1}{2},j+\tfrac{1}{2}) = [h(i,j) + h(i,j+1) - h(i-1,j) - h(i-1,j+1)]/2\Delta z + 0(\Delta z)^2 \qquad 2.5b$$

$$\frac{\partial}{\partial z}\left[K(h)\frac{\partial h}{\partial z}\right](i,j+\tfrac{1}{2}) = \left[K(i+\tfrac{1}{2},j+\tfrac{1}{2})\frac{\partial h}{\partial z}(i+\tfrac{1}{2},j+\tfrac{1}{2}) - K(i-\tfrac{1}{2},j+\tfrac{1}{2})\frac{\partial h}{\partial z}(i-\tfrac{1}{2},j+\tfrac{1}{2})\right]/\Delta z + 0(\Delta z)^2 \qquad 2.6$$

$$\frac{\partial}{\partial z}[K(h)](i,j+\tfrac{1}{2}) = [K(i+\tfrac{1}{2},j+\tfrac{1}{2}) - K(i-\tfrac{1}{2},j+\tfrac{1}{2})]/\Delta z + 0(\Delta z)^2 \qquad 2.7$$

On substituting equations 2.4 to 2.7 into equation 2.1,

$$C_s(i,j+\tfrac{1}{2})[h(i,j+1) - h(i,j)]/\Delta t =$$

$$\{K(i+\tfrac{1}{2},j+\tfrac{1}{2})[h(i+1,j) + h(i+1,j+1) - h(i,j) - h(i,j+1)]$$

$$- K(i-\tfrac{1}{2},j+\tfrac{1}{2})[h(i,j) + h(i,j+1) - h(i-1,j) - h(i-1,j+1)]\}/2(\Delta z)^2$$

$$+ [K(i+\tfrac{1}{2},j+\tfrac{1}{2}) - K(i-\tfrac{1}{2},j+\tfrac{1}{2})]/\Delta z + 0[(\Delta t)^2 + (\Delta z)^2] \qquad 2.8$$

Let $$K(i+\tfrac{1}{2},j+\tfrac{1}{2}) = [K(i+1,j) + K(i+1,j+1) + K(i,j) + K(i,j+1)]/4 \qquad 2.9a$$

$$K(i-\tfrac{1}{2},j+\tfrac{1}{2}) = [K(i,j) + K(i,j+1) + K(i-1,j) + K(i-1,j+1)]/4 \qquad 2.9b$$

The terms of equation 2.8 are collected and arranged in the general form

$$A_i\, h(i-1,j+1) + B_i\, h(i,j+1) + C_i\, h(i+1,j+1) = D_i \qquad 2.10$$

where all the terms at the old (known) time level (j) are contained in the right hand side, D_i. The coefficients of equation 2.10 are then

$$A_i = - K(i-\tfrac{1}{2},j+\tfrac{1}{2})/2(\Delta z)^2 \qquad 2.11$$

$$C_i = - K(i+\tfrac{1}{2},j+\tfrac{1}{2})/2(\Delta z)^2 \qquad 2.12$$

$$B_i = C_s(i,j+\tfrac{1}{2})/\Delta t - A_i - C_i \qquad 2.13$$

$$D_i = - A_i\, h(i-1,j) + [C_s(i,j+\tfrac{1}{2})/\Delta t + A_i + C_i]\, h(i,j)$$

$$- C_i\, h(i+1,j) + 2\Delta z[A_i - C_i] \qquad 2.14$$

Equation 2.10, expanded for each of the (N-1) internal node points of the finite difference grid of N intervals in the z direction, represents a set of (N-1) nonlinear tridiagonal simultaneous equations in (N+1) unknowns. The solution of these equations requires the application of a top and bottom boundary condition to eliminate the terms in h(1,j+1) and h(N+1,j+1) respectively. The method of solution of the tridiagonal equations used in the program is the well known Thomas Algorithm, details of which are given in Appendix B. The algorithm involves two passes through the equations, a preparatory sweep followed by a solution sweep in the reverse direction.

To remove the nonlinearity in the equations, an iteration process is used in which an initial estimate of the h(i,j+1) values at each point is made and used to determine the coefficients A_i, B_i, C_i and D_i. The initial condition is used as the first set of h(i,j) values and also as the first estimate of h(i,j+1) values to evaluate A_i, B_i, C_i and D_i. The resulting set of linear

algebraic equations is solved using the Thomas algorithm to obtain an improved set of h(i,j+1) values. This improved estimate of h(i,j+1) is in turn used to get new values of A_i, B_i, C_i and D_i and a second improved estimate of the h(i,j+1) values is obtained. The process is continued until satisfactory convergence occurs. The solution to the problem proceeds in steps of Δt_r along the t axis. A variable timestep is used to achieve an overall optimal progression, based upon the time rate of change in h values at each node and the number of iterations required for convergence.

All boundary conditions are specified by the formulation of both a preparation and a solution equation for each case. The former equation is used to eliminate terms in h(1,j+1) or h(N+1,j+1) from the tridiagonal equations, and the latter to determine a solution for h(1,j+1) or h(N+1,j+1) after the tridiagonal equations have been solved.

2.4 Conclusion

As indicated in the Introduction, the computer program based on the implicit finite difference model outlined above has been successfully applied to a wide range of unsaturated one-dimensional flow problems. The applications involve various boundary conditions including surface ponding, steady and time-dependent precipitation at the soil surface, redistribution and drainage, a stationary or moving water table and a controlled flux from the profile (for example, Whisler and Watson 1968 and 1969, Watson et al 1973, Watson and Perrens 1973, Webb and Watson 1977, Ayers and Watson 1977). Other systems studied include scale heterogeneous media (Whisler et al 1972), intermittent surface flux involving soil water hysteresis (Watson and Perrens 1973, Lees and Watson 1975), air compression effects in bounded profiles (Watson and Curtis 1975) and stratified profiles (Watson and Whisler 1976). The model has also been used to simulate the rainfall-runoff process (Watson and Lees 1975) and has been linked with a steady-state drainage equation to analyse tile drainage systems.

The soil water program package provides the external controls and, in addition provides the necessary data on soil water content and flux distributions at each timestep. These are used as input for the solute movement analysis described in Chapter 3.

3 NUMERICAL ANALYSIS OF NON-REACTIVE SOLUTE MOVEMENT

3.1 Introduction

The mass transport of solutes in porous media is generally assumed to be the net effect of convection (viscous movement of the soil water), diffusion (thermal motion of the solute within the water) and mechanical dispersion (solute mixing due to pore water velocity distributions). Diffusion is the only process that can occur when the soil water is not mobile.

The differential equation describing solute movement under isothermal, unsteady state conditions in one dimension in unsaturated porous materials, when the solute is assumed to be non-reactive and sufficiently dilute so that density changes can be neglected, is written as

$$\frac{\partial(c\theta)}{\partial t} = \frac{\partial}{\partial z}\left[D_e(\theta,v)\,\frac{\partial c}{\partial z}\right] - \frac{\partial}{\partial z}(qc) \qquad 3.1$$

where

c	solute concentration of the soil solution	$[ML^{-3}]$
$D_e(\theta,v)$	longitudinal combined diffusion-dispersion coefficient	$[L^2T^{-1}]$
q	volumetric (Darcy) flux of solution	$[L^3L^{-2}T^{-1}]$

In the above equation, D_e is defined as a function of θ and v (pore water velocity) following for example Bresler (1973). Other workers (e.g. Davidson et al., 1975) use a different form of equation 3.1, where D_e is replaced by θD_e. Our choice of definition is particularly useful when comparing the numerical model performance with the analytical solution of Chapter 5.

3.2 A Brief Discussion of Hydrodynamic Dispersion

Detailed studies have been carried out in recent times on understanding the nature of miscible displacement in porous media (see reviews by Biggar and Nielsen, 1967 and Fried and Combarnous, 1971). It is apparent that an adequate quantitative and predictive theory of dispersion in partially saturated porous media does not exist (Wilson and Gelhar, 1974).

The components of hydrodynamic dispersion are qualitatively described below following Fried and Combarnous (1971).

Mechanical Dispersion

This occurs when fluid flows through a porous medium with a non-uniform velocity distribution resulting from pore boundary effects. Zero velocity on the solid surfaces creates a velocity gradient in the fluid phase (Fig 3.1(a)), variations in pore dimensions cause discrepancies between the maximum pore velocities along the pore axes (Fig 3.1(b)), and the streamlines fluctuate with respect to the mean direction of flow (Fig 3.1(c)).

Many experiments and theoretical studies have shown that the magnitude of the mechanical dispersion coefficient D_h in a given porous medium depends upon the average flow velocity. For saturated steady state conditions it has been shown (Ogata 1970) that often D_h can be taken to be

$$D_h(v) = \beta|\bar{v}| \qquad 3.2$$

where $\bar{v}$ is the average pore water velocity [LT^{-1}]
β is an experimental constant, a function of the characteristics of the porous medium [L]

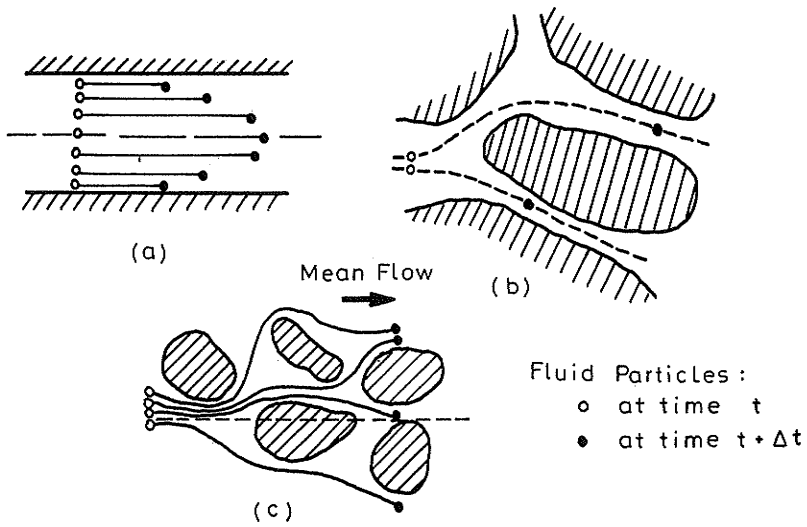

Fig 3.1 The components of dispersion

Bresler (1973) assumed that a similar relationship held for unsteady unsaturated flow conditions. Many other workers have used this relationship (Passioura, 1971, De Smedt & Wierenga, 1978, Davidson et al, 1975).

Diffusion

The physiochemical dispersion is termed molecular diffusion. It results from the chemical potential gradient, which is correlated to the solution concentration. Fig 3.2 illustrates the two different diffusion mechanisms. Inside a streamtube, the concentration gradient tends to vanish as in (a), whilst between adjacent streamtubes there is a mass transfer by diffusion [see (b)]. These two mechanisms produce a longitudinal and a transverse effect, as in mechanical dispersion [see (c)].

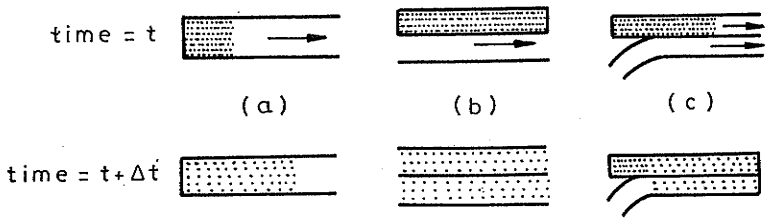

Fig 3.2 The way diffusion appears in dispersion

Diffusion of solute in a uniform body of water can be described macroscopically by Fick's first law. In soils, the molecular diffusion coefficient D_p is less than the equivalent coefficient in a free water system D_m and is dependent upon the water content (Bresler, 1973). The relationship is of the type

$$D_p(\theta) = D_m \, a \exp(b\,\theta) \qquad 3.3$$

where a and b are empirical constants characterising the soil. Bresler (1973) follows Olsen and Kemper (1968) and uses b = 10 and 'a' ranging from 0.001 to 0.005 depending upon the surface area of the particular soil (clay to sandy loam).

Effective Dispersion Coefficient

In general, molecular diffusion and mechanical dispersion occur simultaneously, each contributing to the final hydrodynamic dispersion of the solution. It is usually assumed that solutes are transported by convection at some average velocity of solution, and dispersed about the mean position of the front. For a fine sand material, this assumption is supported by the work of Watson and Jones (1981*a*).

Mathematically, mechanical dispersion can be treated as a diffusion process. The joint effect of diffusion and dispersion is given by combining their mathematical expressions to give

$$D_e = (D_h + D_p) \qquad 3.4$$

where D_e is the effective dispersion coefficient (function of θ,v)
D_h is the mechanical dispersion coefficient (function of v)
D_p is the molecular diffusion coefficient (function of θ)

3.3 A Convective Transport Model

The first published numerical model capable of simulating simultaneous one-dimensional flow of water and solute in unsaturated soils under unsteady flow conditions was that of Bresler and Hanks (1969).

It was assumed that solute was non-reactive, dispersive flow so small compared to convective flow that it could be neglected, and further that no sources (or sinks) were present. Water flow computations were considered to be independent of solute concentration and isothermal conditions applied. The model permits computation of the solute concentration-depth profile at any time during a wetting or drying cycle (including infiltration, redistribution and evaporation). The derivation of this model is not given here, as full details are in the referenced paper.

This convective model was programmed and tested as part of the project, but discarded as unsuitable for further development for the following reasons:-

(i) the solution technique introduces significant numerical dispersion;
(ii) quantitative effects of hydrodynamic dispersion cannot be traced;
(iii) simulations are restricted to 'semi-infinite' profiles;
(iv) the model is unsuited to further developments incorporating reactive solute transport.

3.4 A Convective - Dispersive Solute Model

Expanding equation 3.1

$$c \frac{\partial \theta}{\partial t} + \theta \frac{\partial c}{\partial t} = \frac{\partial}{\partial z} (D_e) \frac{\partial c}{\partial z} + D_e \frac{\partial^2 c}{\partial z^2} - q \frac{\partial c}{\partial z} - c \frac{\partial q}{\partial z} \qquad 3.5$$

Introducting the equation of continuity for one-dimensional flow of water in unsaturated soil

$$\frac{\partial \theta}{\partial t} = - \frac{\partial q}{\partial z} \qquad 3.6$$

Substituting equation 3.6 into equation 3.5 and rearranging gives

$$\frac{\partial c}{\partial t} = \frac{D_e}{\theta} \frac{\partial^2 c}{\partial z^2} - W \frac{\partial c}{\partial z} \qquad 3.7$$

where $$W = \left[\frac{q}{\theta} - \frac{1}{\theta} \frac{\partial D_e}{\partial z}\right] \qquad 3.8$$

At this point Davidson et al (1975) assume that $D_e\theta$ is independent of depth, thus reducing their form of equation 3.8 to

$$W = \left[\frac{q}{\theta} - \frac{D_e}{\theta^2} \frac{\partial \theta}{\partial z}\right] \qquad 3.9$$

The more general equation 3.8 is used in this study.

Solution of equation 3.7, which is a linear parabolic equation in the dependent variable c, requires specification of an initial condition and two boundary conditions for c.

At the surface, the total solute flux is given by

$$J = - D_e \frac{\partial c}{\partial z} + qc \qquad 3.10$$

where during infiltration, $J(1,t) = q(1,t)\ c_o(t) \qquad t > 0 \qquad 3.11$

and during redistribution/drainage, $J(1,t) = 0 \qquad t > 0 \qquad 3.12$

Initial conditions are $c(z,0) = c_n(z) \quad 0 \leq z \leq -L \quad t = 0 \qquad 3.13$

Where c_o is the solute concentration in the infiltrating water, $J(1,t)$ the solute flux applied at the surface, $c_n(z)$ the predetermined initial concentration profile, and L the length of the column.

At the lower boundary the appropriate condition for a 'semi infinite' column is

$$\lim_{z \to -\infty} c(z,t) = c(z,t=0) \quad t \geq 0 \qquad 3.14$$

If a finite column is considered, the condition favoured by most authors is

$$\frac{\partial c}{\partial z} = 0 \qquad \text{at } z = -L \qquad t > 0 \qquad 3.15$$

In this study the combined dispersion coefficient D_e has been taken to be of the form given by equation 3.4, but with the molecular diffusion component being a constant value. The complete problem as defined by equations 3.7 to 3.15 is solved numerically using an explicit finite difference approach.

3.5 Explicit Finite Difference Solute Model

The space-time domain is written in incremental form as

$$z_i = (i-1)\,\Delta z \qquad i = 1,2,\ldots N,(N+1)$$

$$\Delta z = -L/N$$

$$t_j = \sum_{r=1}^{j} \Delta t_r \qquad j \geq 1$$

A Taylor Series expansion of c(i,j) in the time dimension gives

$$c(i,j+1) = c(i,j) + \Delta t \frac{\partial c(i,j)}{\partial t} + \frac{(\Delta t)^2}{2} \frac{\partial^2 c(i,j)}{\partial t^2} + 0(\Delta t)^3$$

rearranging $$\frac{\partial c(i,j)}{\partial t} = \frac{c(i,j+1) - c(i,j)}{\Delta t} - \frac{\Delta t}{2} \frac{\partial^2 c(i,j)}{\partial t^2} + 0(\Delta t)^2 \qquad 3.16$$

The term $\partial^2 c/\partial t^2$ in equation 3.16 requires knowledge of c over three timesteps if a finite difference approximation of $0(\Delta t)^2$ is to be maintained. Since solute flow under unsaturated unsteady state conditions is dominated by convection in the cases being considered, an approximation to $\partial^2 c/\partial t^2$ assuming pure convection is reasonable. This approach follows Lantz (1971) and Bresler (1973).

Assuming zero dispersion, and putting $v = q/\theta$ reduces equation 3.7 to

$$\frac{\partial c}{\partial t} = -v \frac{\partial c}{\partial z} \qquad 3.17$$

Differentiating equation 3.17 with respect to both time and space

$$\frac{\partial^2 c}{\partial t^2} = -\frac{\partial v}{\partial t} \frac{\partial c}{\partial z} - v \frac{\partial^2 c}{\partial t\, \partial z} \qquad 3.18$$

$$\frac{\partial^2 c}{\partial t\, \partial z} = -\frac{\partial v}{\partial z} \frac{\partial c}{\partial z} - v \frac{\partial^2 c}{\partial z^2} \qquad 3.19$$

from equations 3.18 and 3.19

$$\frac{\partial^2 c}{\partial t^2} = v^2 \frac{\partial^2 c}{\partial z^2} + \left[v \frac{\partial v}{\partial z} - \frac{\partial v}{\partial t}\right] \frac{\partial c}{\partial z} \qquad 3.20$$

Combining equations 3.16 and 3.20 we obtain

$$\frac{\partial c(i,j)}{\partial t} = \frac{c(i,j+1) - c(i,j)}{\Delta t} - \frac{\Delta t}{2} v^2(i,j) \frac{\partial^2 c(i,j)}{\partial z^2}$$

$$- \frac{\Delta t}{2} \left[v(i,j) \frac{\partial v(i,j)}{\partial z} - \frac{\partial v(i,j)}{\partial t}\right] \frac{\partial c(i,j)}{\partial z} + 0(\Delta t)^2 \qquad 3.21$$

Substituting equation 3.21 into equation 3.7 gives

$$\frac{c(i,j+1) - c(i,j)}{\Delta t} = \left[\frac{D_e(i,j)}{\theta(i,j)} + \frac{\Delta t}{2} v^2(i,j)\right] \frac{\partial^2 c(i,j)}{\partial z^2}$$

$$- \left[W(i,j) - \frac{\Delta t}{2} \left\{v(i,j) \frac{\partial v(i,j)}{\partial z} - \frac{\partial v(i,j)}{\partial t}\right\}\right] \frac{\partial c(i,j)}{\partial z} + 0(\Delta t)^2 \qquad 3.22$$

It is clear from equation 3.22 that a first order approximation to the time derivative would introduce artificial dispersion and convection terms to the solute transport equation.

Taylor Series expansions in space about c(i,j) give

$$c(i-1,j) = c(i,j) - \Delta z \frac{\partial c(i,j)}{\partial z} + \frac{(\Delta z)^2}{2} \frac{\partial^2 c(i,j)}{\partial z^2} + 0(\Delta z)^3 \qquad 3.23$$

$$c(i+1,j) = c(i,j) + \Delta z \frac{\partial c(i,j)}{\partial z} + \frac{(\Delta z)^2}{2} \frac{\partial^2 c(i,j)}{\partial z^2} + 0(\Delta z)^3 \qquad 3.24$$

Adding equations 3.23 and 3.24 and rearranging gives

$$\frac{\partial^2 c(i,j)}{\partial z^2} = \frac{c(i+1,j) - 2c(i,j) + c(i-1,j)}{(\Delta z)^2} + 0(\Delta z)^2 \qquad 3.25$$

Subtracting equation 3.23 from 3.24 gives, on rearranging

$$\frac{\partial c(i,j)}{\partial z} = \frac{c(i+1,j) - c(i-1,j)}{2\Delta z} + 0(\Delta z)^2 \qquad 3.26$$

Combining equations 3.22, 3.25 and 3.26, an explicit finite difference approximation correct to $0[(\Delta z)^2 + (\Delta t)^2]$ is obtained for equation 3.7. Rearranging to give an expression for the unknown c(i,j+1) gives

$$c(i,j+1) = c(i,j) + \Delta t\, F(i,j) \left[\frac{c(i+1,j) - 2c(i,j) + c(i-1,j)}{(\Delta z)^2}\right]$$

$$- \Delta t\, G(i,j) \left[\frac{c(i+1,j) - c(i-1,j)}{2\Delta z}\right] + O[(\Delta t)^2 + (\Delta z)^2] \qquad 3.27$$

where
$$F(i,j) = \frac{D_e(i,j)}{\theta(i,j)} + \frac{\Delta t}{2} v^2(i,j) \qquad 3.28$$

$$G(i,j) = W(i,j) - \frac{\Delta t}{2} \{v(i,j) \frac{\partial v(i,j)}{\partial z} - \frac{\partial v(i,j)}{\partial t}\} \qquad 3.29$$

and using
$$\frac{\partial v(i,j)}{\partial z} = \frac{v(i+1,j) - v(i-1,j)}{2\Delta z} + O(\Delta z)^2 \qquad 3.30$$

$$\frac{\partial v(i,j)}{\partial t} = \frac{v(i,j+1) - v(i,j)}{\Delta t} + O(\Delta t) \qquad 3.31$$

Suitable finite difference approximations for the boundary conditions, equations 3.11, 3.12 and 3.15 are respectively

$$q(1,j+1)\, c_o = -D_e(1,j+1)\ \ c(1,j+1) + q(1,j+1)\, c(1,j+1) \qquad 3.32$$

$$\Delta c(1,j+1) = 0 \qquad 3.33$$

$$\Delta c(N+1,j+1) = 0 \qquad 3.34$$

where
$$\Delta c(1,j+1) = [-3c(1,j+1) + 4c(2,j+1) - c(3,j+1)]/2\Delta z \qquad 3.35$$

$$\Delta c(N+1,j+1) = [3c(N+1,j+1) - 4c(N,j+1) + c(N-1,j+1)]/2\Delta z \qquad 3.36$$

are forward and backward finite difference approximations to $O(\Delta z)^2$ of $\partial c/\partial z$ at $z = 0$ and $z = -L$ respectively.

Equations 3.27 to 3.36 allow a direct solution for the unknown $c(i,j+1)$. Numerical dispersion, which results from the truncation of the higher order terms in the Taylor Series is virtually eliminated when the second order terms are included in the analysis (Chaudhari, 1971, Lantz, 1971, Bresler, 1973).

3.6 Conclusion

The implicit finite difference model of Chapter 2 is unconditionally stable. That is, there are no restrictions placed on the magnitude of either Δz or Δt for a convergent, non-oscillating solution. These may be chosen solely on the basis of required accuracy which is of order $\{(\Delta t)^2 + (\Delta z)^2\}$. However, the explicit model above *is* subject to restrictions on the size of both Δt and Δz for a convergent and non-oscillatory solution. Stability considerations relevant to the explicit solute model are detailed in the following chapter.

4 NUMERICAL STABILITY OF THE SOLUTE ANALYSIS

4.1 Introduction

For any finite difference approximation to a partial differential equation to be reasonably accurate, two different, albeit interrelated conditions need to be satisfied. Firstly, the approximate solution must converge to the exact solution as the discretization by time and space steps approaches zero, and secondly any errors in the approximate solution must not propagate but decay as the solution process proceeds.

4.2 Combined Convection - Diffusion Equation

The finite difference form of the solute transport equation developed previously was

$$c(i,j+1) = c(i,j) + \Delta t\, F(i,j)[c(i+1,j) - 2c(i,j) + c(i-1,j)]/(\Delta z)^2 - \Delta t\, G(i,j)[c(i+1,j) - c(i-1,j)]/2\Delta z \qquad (3.27)$$

If it can be assumed that F(i,j) and G(i,j) are constant, or at least that they vary very slowly, a von Neumann stability analysis of equation 3.27 is applicable. If the stability criteria derived assuming constant F and G are applied locally for the case where the coefficients are variable, then it is reasonable to expect that the equation will be stable, provided that these criteria are satisfied at every point of the field (see for example, Roache 1976 and Fromm 1964). There is considerable numerical evidence to support this contention. For two-level difference schemes with one dependent variable and any number of independent variables, the von Neumann condition is sufficient as well as necessary for stability.

The following substitutions are made

$$d = \Delta t\, F(i,j)/(\Delta z)^2 \qquad 4.1$$

$$c = \Delta t\, G(i,j)/(\Delta z) \qquad 4.2$$

where d is termed the 'diffusion number', and c the 'Courant number'. A von Neumann stability analysis applies a finite Fourier series expansion of the solution to the model equation and then studies the amplification or decay of each mode separately to determine instability or stability.

Each Fourier component of the solution is written

$$c(i,j) = V(j)\exp(ik i\Delta z) \qquad 4.3$$

where V(j) is the amplification function at time j of the particular component whose wavenumber is k, and where $i = \sqrt{-1}$.

Similarly

$$c(i\pm1,j) = V(j)\exp\{ik(i\pm1)\Delta z\} \qquad 4.4$$

$$c(i,j+1) = V(j+1)\exp(ik i\Delta z) \qquad 4.5$$

Substituting equations 4.3 to 4.5 into equation 3.27 gives

$$V(j+1)\exp(ik\mathrm{i}\Delta z) = V(j)\exp(ik\mathrm{i}\Delta z) + d\,V(j)\exp(ik\mathrm{i}\Delta z)[\exp(ik\Delta z) - 2 + \exp(-ik\Delta z)] - \frac{c}{2}V(j)\exp(ik\mathrm{i}\Delta z)[\exp(ik\Delta z) - \exp(-ik\Delta z)] \quad 4.6$$

Cancelling the term $\exp(ik\mathrm{i}\Delta z)$ in equation 4.6, and defining the phase angle as $\phi = k\Delta z$, equation 4.6 reduces to

$$V(j+1) = V(j)[1 + d\,\{\exp(i\phi) - 2 + \exp(-i\phi)\} - \frac{c}{2}\{\exp(i\phi) - \exp(-i\phi)\}] \quad 4.7$$

The amplification factor of the function V(j) is defined as A where $V(j+1) = A\,V(j)$. If the identities

$$\{\exp(i\phi) + \exp(-i\phi)\} = 2\cos\phi \quad 4.8$$

$$\{\exp(i\phi) - \exp(-i\phi)\} = 2i\sin\phi \quad 4.9$$

are substituted into equation 4.7, an expression for the amplification factor is obtained which, on rearranging is

$$A = (1 - 2d) + 2d\cos\phi - ic\sin\phi \quad 4.10$$

Note that $A = A(\phi)$, ie the amplification factor varies for each Fourier component. Equation 4.10 can be recognised as the equation of an ellipse, centred on $(1 - 2d)$ on the real axis, with axis half-lengths of $2d$ on the real axis and c on the imaginary axis.

Clearly for stability $|A| \leq 1$ which, in terms of Fig 4.1 requires that the ellipse must lie entirely within the unit circle. By inspection $c \leq 1$, $d \leq \frac{1}{2}$ and $c^2 \leq 2d$. The most general restriction is found by solving for the modulus of A (with the complex conjugate denoted by $\bar{A}$).

$$|A|^2 = A\bar{A} = [(1 - 2d) + 2d\cos\phi]^2 + c^2\sin^2\phi \leq 1 \quad 4.11$$

A maximum is sought for $|A|^2$ in terms of $\cos\phi$. Thus

$$\frac{\partial|A|^2}{\partial(\cos\phi)} = (4d - 8d^2) + (8d^2 - 2c^2)\cos\phi \quad 4.12$$

$$\frac{\partial^2|A|^2}{\partial(\cos\phi)^2} = (8d^2 - 2c^2) \quad 4.13$$

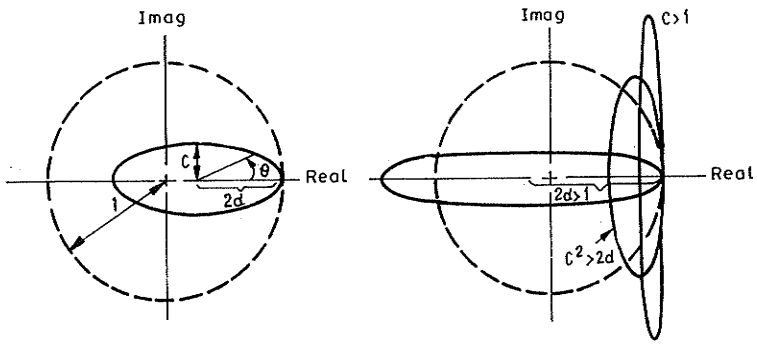

Fig 4.1 Polar diagram of the amplification factor 'A' from equation 4.10. For stability, the ellipse must fall within the unit circle

Note that a maximum only occurs if the second derivative (equation 4.13) is less than zero, ie $2d < c$. From equation 4.12 the maximum (or minimum) occurs for

$$\cos\phi = 2d(1 - 2d)/(c^2 - 4d^2) \qquad 4.14$$

Substituting equation 4.14 into equation 4.11 and expanding

$$|A|^2 = c^2(c^2 - 4d + 1)/(c^2 - 4d^2) \leq 1 \qquad 4.15$$

Equation 4.15 implies $(c^2 - 2d)^2 \leq 0$, but for a maximum equation 4.13 required $2d < c$. As the latter condition cannot be met, the conclusion is that no maximum can occur for $|A|^2 \leq 1$. Thus

$$\frac{c}{d} \leq 2 \qquad \text{or} \quad \Delta z \leq 2F(i,j)/G(i,j) \qquad 4.16$$

This criterion is called the cell Reynolds number restriction ($R_c = c/d \leq 2$) and ensures zero overshoot. Whilst no maximum occurs if equation 4.16 is satisfied, the extreme values of cos ϕ must still be considered. If cos ϕ = -1, equation 4.11 gives

$$d \leq \tfrac{1}{2} \qquad \text{or} \quad \Delta t \leq (\Delta z)^2/2F(i,j) \qquad 4.17$$

and if cos ϕ = +1 equation 4.11 merely gives $|A|^2 = 1$ implying stability.

The above analysis indicates two conditions, equations 4.16 and 4.17, which are both necessary and together sufficient to ensure stability for

equation 3.27 in the case where both F(i,j) and G(i,j) are constant. The effects of spatially varying F(i,j) and G(i,j) cannot be ascertained by this method.

Equation 4.16 is independent of the timestep, and implies a severe restriction on the maximum space step when flow is convection dominated. Equation 4.17 represents a very stringent requirement in terms of calculation time for the solute transport equation.

The numerical model used in this study readily copes with a variable timestep, but not a variable space step. If equations 4.16 and 4.17 are combined, a second necessary timestep restriction results

$$\Delta t \leq 2F(i,j)/G^2(i,j) \qquad 4.18$$

Although equations 4.17 and 4.18 are necessary conditions they do not include equation 4.16 and so are not sufficient to guarantee stability. It has been found that applying these two criteria, determined using the most critical values of F(i,j) and G(i,j), gives acceptable results when the space step used is small. Some overshoot, which appears as oscillations behind the solute front, indicates failure to meet the R_c restriction. The location of the solute front appears to be almost unaffected by this failure.

It is readily shown that if flow is purely diffusive, stability is guaranteed by satisfying equation 4.17 only. No space step restriction is required.

4.3 Alternative Expressions for the First Space Derivative

If the central difference expression for the first space derivative in equation 3.27 is replaced by a forward or backward finite difference approximation also of accuracy $O(\Delta z)^2$, then a second derivative component is introduced which effectively increases the dispersion term. For example,

$$\frac{\partial c(i,j)}{\partial z} = \frac{c(i+1,j) - c(i,j)}{\Delta z} + \frac{\Delta z}{2}\frac{\partial^2 c(i,j)}{\partial z^2} + O(\Delta z)^2 \qquad 4.19$$

By choosing the appropriate form for $\partial c/\partial z$, the total hydrodynamic dispersion coefficient will be increased in magnitude by the absolute value of $\frac{1}{2}\Delta z\, G(i,j)$. This means a favourable move in the ratio $F(i,j)/G(i,j)$, the basis of the severe cell Reynolds number restriction. Unfortunately, a stability analysis similar to that above indicates that the stability limits are now

$$\Delta t \leq (\Delta z)^2/[2F^*(i,j) \pm G(i,j)\,\Delta z] \qquad 4.20$$

$$\Delta z \leq F^*(i,j)/\pm G(i,j) \qquad 4.21$$

where $F^*(i,j)$ includes the additional $\frac{1}{2}\Delta z\, G(i,j)$ term. If equations 4.20 and 4.21 are compared with equations 4.16 and 4.17, with $F^*(i,j)$ expressed as $\{F(i,j) + \frac{1}{2}\Delta t\, G(i,j)\}$, it is clear that the restrictions on both Δz and Δt are unchanged.

5 VERIFICATION OF SOLUTE MODEL

5.1 Introduction

Before the numerical model described in Chapter 3 can be applied with confidence in simulating non-reactive solute movement for a range of flow conditions and soil types, it is necessary to test a set of results against a known solution. Ideally such a solution should be analytical in nature. It should be noted that the computer program is written so that the solute model is linked to, and solved simultaneously with the water flow model. The solution technique assumes that whilst solute flow is dependent on the water flow (via the soil water flux and volumetric water content) the latter is not affected by the presence of the solute and can thus be evaluated independently. The accuracy of the water flow model has already been established through comparisons with both theoretical and experimental results (Watson et al. 1973, Ayers and Watson 1977, Watson and You 1980).

Smiles et al. (1978) have developed a convenient quasi-analytical solution for non-reactive solute flow during unsteady horizontal absorption under constant concentration boundary conditions. This approach has been discussed by Watson and Jones (1981*a*) particularly in relation to assessing the performance of the solute model. In this chapter the quasi-analytical solution is discussed and an alternative integral solution presented. This solution is then used with a constant-valued dispersion coefficient for verification purposes.

5.2 Quasi-Analytical Approach

The hydrodynamic dispersion of solute during horizontal absorption was represented by equation 3.1 which is repeated here for convenience. All terms are defined as previously.

$$\frac{\partial(\theta c)}{\partial t} = \frac{\partial}{\partial x}\left[D_e(\theta,v)\,\frac{\partial c}{\partial x}\right] - \frac{\partial}{\partial x}(qc) \qquad 5.1$$

Smiles et al. (1978) showed that if the velocity dependence of D_e were neglected, as seems appropriate for many natural systems exhibiting small Péclet numbers, then equation 5.1 with $D_e(\theta)$ replacing $D_e(\theta,v)$ would lend itself to a convenient similarity solution using the transformation $\lambda = xt^{-\frac{1}{2}}$. The similarity solution is valid for the case of constant concentration boundary conditions. These conditions for water and solute, together with the initial conditions, may be written as follows:

$$\left.\begin{array}{lll} \theta = \theta_n & x > 0 & t = 0 \\ \theta = \theta_o & x = 0 & t \geq 0 \end{array}\right) \qquad 5.2$$

and

$$\left.\begin{array}{lll} c = c_n & x > 0 & t = 0 \\ c = c_o & x = 0 & t \geq 0 \end{array}\right) \qquad 5.3$$

The flow of water in a rigid horizontal system may be described by the well known equation

$$\frac{\partial \theta}{\partial t} = \frac{\partial}{\partial x}\left[D(\theta)\,\frac{\partial \theta}{\partial x}\right] \qquad 5.4$$

where $D(\theta)$ is the soil water diffusivity. Since

$$q = -D(\theta)\,\frac{\partial \theta}{\partial x} \qquad 5.5$$

following Smiles et al. (1978) equation 5.1 may be written in terms of $D_e(\theta)$ as

$$\theta\,\frac{\partial c}{\partial t} = \frac{\partial}{\partial x}\left[D_e(\theta)\,\frac{\partial c}{\partial x}\right] + D(\theta)\,\frac{\partial \theta}{\partial x}\,\frac{\partial c}{\partial x} \qquad 5.6$$

Making the substitution $\lambda = xt^{-\frac{1}{2}}$ in equations 5.2 to 5.6 the following are obtained

$$\frac{d}{d\lambda}\left[D(\theta)\,\frac{d\theta}{d\lambda}\right] + \frac{\lambda}{2}\,\frac{d\theta}{d\lambda} = 0 \qquad 5.7$$

$$\frac{d}{d\lambda}\left[D_e(\theta)\,\frac{dc}{d\lambda}\right] + \frac{g}{2}\,\frac{dc}{d\lambda} = 0 \qquad 5.8$$

$$\left.\begin{aligned} \theta &= \theta_n \qquad \lambda \to \infty \\ \theta &= \theta_o \qquad \lambda = 0 \end{aligned}\right\} \qquad 5.9$$

and

$$\left.\begin{aligned} c &= c_n \qquad \lambda \to \infty \\ c &= c_o \qquad \lambda = 0 \end{aligned}\right\} \qquad 5.10$$

where

$$g = \theta\lambda + 2D(\theta)\,\frac{d\theta}{d\lambda} = \theta\lambda - \int_{\theta_n}^{\theta} \lambda\, d\theta \qquad 5.11$$

Since $\theta(\lambda)$ is unique, equation 5.8 may be written as

$$\frac{d}{d\lambda}\left[D_e(\lambda)\,\frac{dc}{d\lambda}\right] + \frac{g}{2}\,\frac{dc}{d\lambda} = 0 \qquad 5.12$$

Smiles et al. (1978) give the solution of equation 5.12 subject to equations 5.9 and 5.10 as

$$\bar{c} = \frac{c - c_o}{c_n - c_o} = \frac{M(\lambda)}{M(\infty)} \qquad \text{when} \quad c_n > c_o \qquad 5.13$$

where

$$M(\lambda) = \int_0^{\lambda} \left\{\frac{1}{D_e(\lambda)}\,\exp\left[-\tfrac{1}{2}\int_0^{\lambda} \frac{g(\lambda)}{D_e(\lambda)}\,d\lambda\right]\right\} d\lambda \qquad 5.14$$

The integration in equation 5.14 is carried out from zero to λ. This contrasts with the more closely defined integration limits of Watson and Jones (1981*a*) who take advantage of the linearity of $g(\lambda)$ in the vicinity of the solute front as discussed in the next section.

In summary, the quasi-analytical approach first determines $\theta(\lambda)$ (Philip, 1955) which allows $g(\lambda)$ to be calculated. This is used in equations 5.13 and 5.14 to find the normalized relationship $\bar{c}(\lambda)$ and hence $c(\lambda)$. The above similarity solution postulates uniqueness not only in $\theta(\lambda)$ but also in $c(\lambda)$. Smiles and Philip (1978) and Smiles et al. (1978) describe a comprehensive set of experiments using a fine sand-kaolinite mixture as the porous material and show the uniqueness of $c(\lambda)$ for a range of initial water contents and for different solute concentration conditions.

An Alternative Integral Solution

Defining λ_* as the value of λ at which $g(\lambda) = 0$, and assuming $D_e(\theta)$ to be constant in the region of the solute front, equation 5.12 may be written as

$$\frac{d^2c}{d\lambda^2} = -\frac{g(\lambda)}{2D_e}\frac{dc}{d\lambda} \qquad 5.15$$

The $g(\lambda)$ relationship for Bungendore fine sand in the region of interest is shown in Fig 5.1. For $\lambda > \lambda_*$ let the angle between $g(\lambda)$ and the horizontal (λ) axis be α_U, and for $\lambda < \lambda_*$ let it be α_L. Defining λ_U as the value of λ where $c = c_o$, λ_L as the value where $c = c_n$, and c_* as the c value at λ_* then the integration of equation 5.15 for $\lambda_U > \lambda > \lambda_*$ gives

$$(c - c_*) = \left(\frac{dc}{d\lambda}\right)_* \int_{\lambda_*}^{\lambda} \exp\left\{\frac{-\tan\alpha_U}{4D_e}(\lambda - \lambda_*)^2\right\} d\lambda \qquad 5.16$$

Similarly for $\lambda_L < \lambda < \lambda_*$

$$(c_* - c) = \left(\frac{dc}{d\lambda}\right)_* \int_{\lambda}^{\lambda_*} \exp\left\{\frac{-\tan\alpha_L}{4D_e}(\lambda_* - \lambda)^2\right\} d\lambda \qquad 5.17$$

From equations 5.16 and 5.17

$$\left(\frac{dc}{d\lambda}\right)_* = (c_n - c_*)\Big/\int_{\lambda_*}^{\lambda_U} \exp\left\{\frac{-\tan\alpha_U}{4D_e}(\lambda - \lambda_*)^2\right\} d\lambda$$

$$= (c_* - c_o)\Big/\int_{\lambda_L}^{\lambda_*} \exp\left\{\frac{-\tan\alpha_L}{4D_e}(\lambda_* - \lambda)^2\right\} d\lambda \qquad 5.18$$

If c_o and c_n are both known in equation 5.18, then c_* can be found, thence $(dc/d\lambda)_*$. This is substituted in equations 5.16 and 5.17 to find the two 'parts' of $c(\lambda)$. The integration is quickly carried out for any value of D_e once α_U and α_L are known from the solution of equation 5.11.

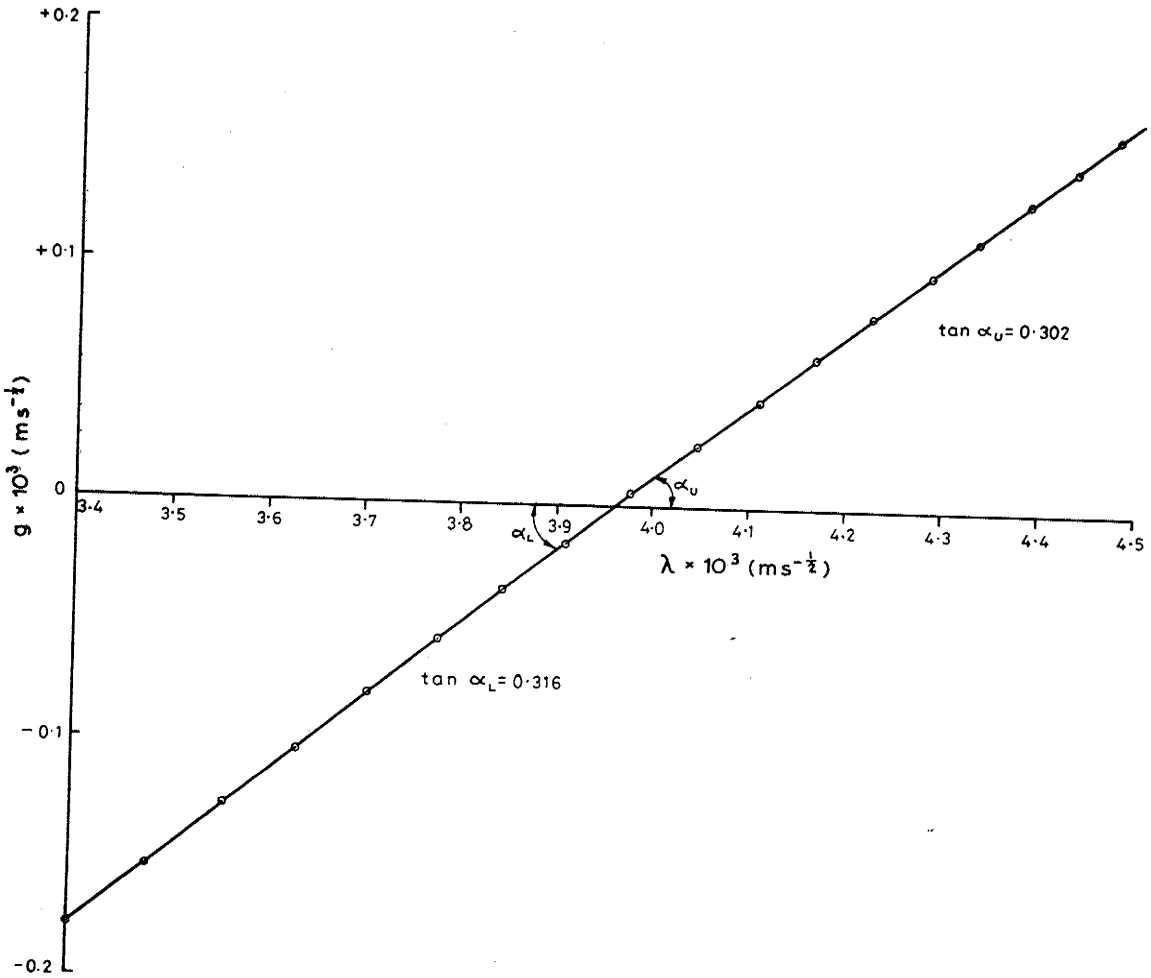

Fig 5.1 $g(\lambda)$ relationship for Bungendore fine sand in the region $3.4 \times 10^{-3} \leq \lambda \leq 4.5 \times 10^{-3} ms^{-\frac{1}{2}}$

5.3 Comparison Between Numerical Analysis and Quasi-Analytical Solution

In the next chapter, detailed comparisons between numerical and experimental results are presented for a sand locally known as Bungendore fine sand. The hydrologic characteristics of that sand are used in this chapter in carrying out the model verification.

Figure 5.2 shows the mean $D(\theta)$ relationship for a series of four experiments obtained using the Bruce and Klute (1956) method. The value of the saturated conductivity (K_{sat}) was determined as 1.48×10^{-5} ms^{-1} with a standard deviation of 0.27×10^{-5} ms^{-1}, and the saturated volumetric water content (θ_{sat}) as 0.34 m^3m^{-3}. Using this K_{sat} value, an appropriate function for $K(\theta)$ was chosen as

$$K(\theta) = K_{sat} \, (\theta/\theta_{sat})^{4.35} \qquad 5.19$$

The definition of the soil water diffusivity

$$D(\theta) = K(\theta) \frac{\partial h}{\partial \theta} \qquad 5.20$$

is used in conjunction with equation 5.19 to give a first approximation for $h(\theta)$. Spline techniques (see Appendix C) were then used to develop a satisfactory $h(\theta)$ relationship. The spline method has several advantages, one being the ready calculation of the specific water capacity ($\partial h/\partial \theta$) which is required in the solution process. The resulting $K(\theta)$ and $h(\theta)$ relationships are given in Fig 5.3.

The $\theta(\lambda)$ relationship for Bungendore fine sand was calculated using $\theta(x,t)$ data obtained from the numerical simulation of horizontal absorption subject to constant concentration boundary conditions. Similarity was shown to be preserved exactly, with the $\theta(x,t)$ profiles 'collapsing' onto the one $\theta(\lambda)$ curve. This is another indication of the accuracy of the water flow model. The $g(\lambda)$ relationship shown in Fig 5.4 was calculated from this $\theta(\lambda)$ relationship, and gave the following: $\lambda_* = 3.96 \times 10^{-3}$ $ms^{-\frac{1}{2}}$, $\tan \alpha_U = 0.302$ and $\tan \alpha_L = 0.316$. The $\bar{c}(\lambda)$ relationship for a constant hydrodynamic dispersion coefficient of 10^{-8} m^2s^{-1} was then calculated using the alternative integration technique of section 5.2. It is shown by the continuous line of Fig 5.5.

The explicit solute program was used with a very fine grid spacing of 1 mm to minimize 'overshoot' immediately behind the solute front (due to R_c instability) and the numerical $c(x,t)$ results transformed to $\bar{c}(\lambda)$ form for the simulation time $t = 2{,}500$ s. These results, plotted as circles in Fig 5.5, indicate the excellent correspondence with the analytical solution. Although not included in Fig 5.5, when the $c(x,t)$ numerical data for other times were transformed to $\bar{c}(\lambda)$, they also 'collapsed' onto the same $\bar{c}(\lambda)$ curve. This confirms that the solute program is correctly simulating the similarity hypothesis. The trivial exception occurs at very early times when the number of nodes affected by the solute movement process are insufficient for accurate λ representation.

The good agreement between numerical and analytical results indicates that the numerical approach is accurate and generally stable. On this basis, the use of the numerical program in simulating equation 5.1 can be approached with confidence. It is necessary however to compare the numerical solutions with experimental data to ensure that the physics of the processes involved

Fig 5.1 $g(\lambda)$ relationship for Bungendore fine sand in the region $3.4 \times 10^{-3} \leq \lambda \leq 4.5 \times 10^{-3}$ $ms^{-\frac{1}{2}}$

-0.2

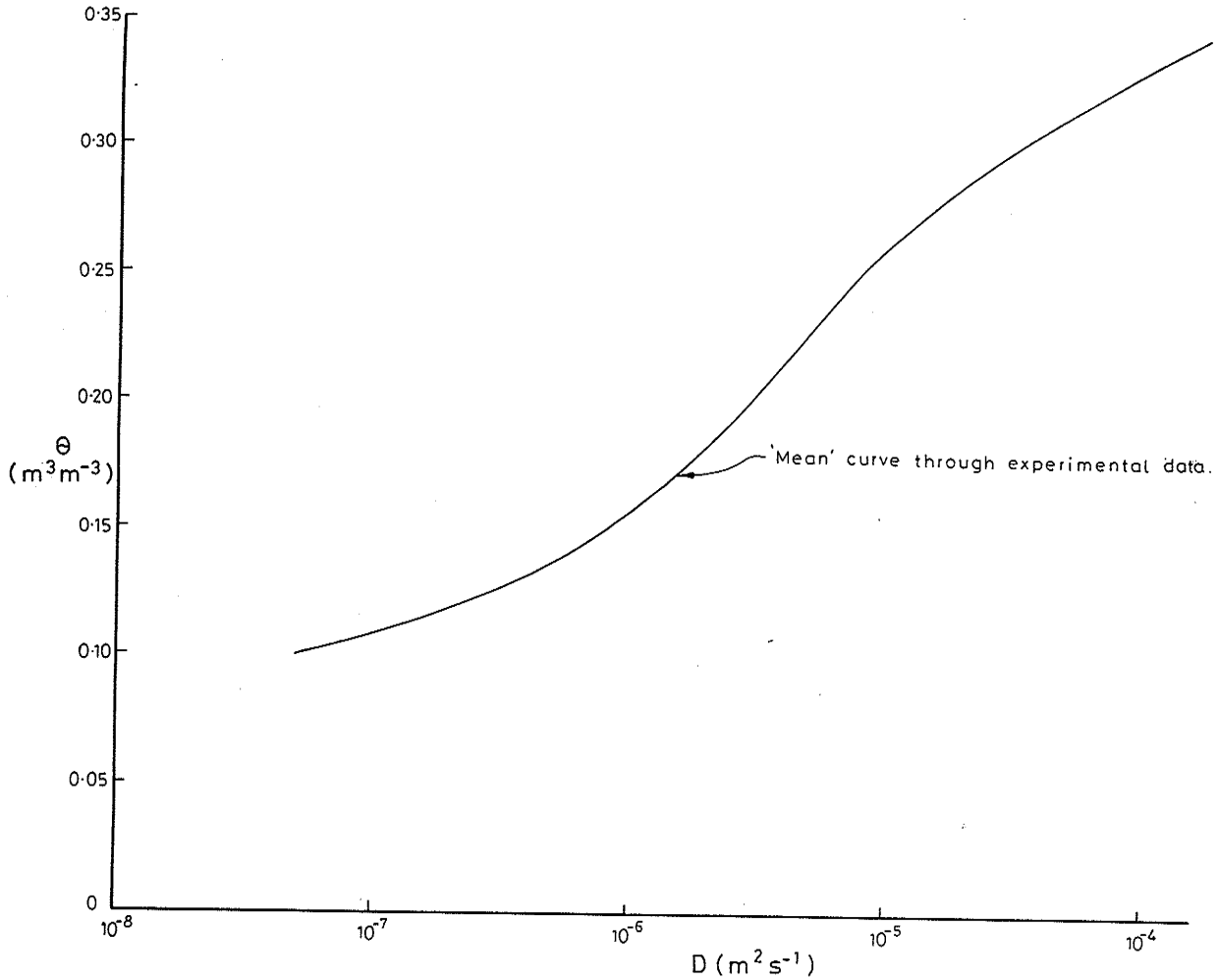

Fig 5.2 Soil water diffusivity [D(θ)] relationship for Bungendore fine sand

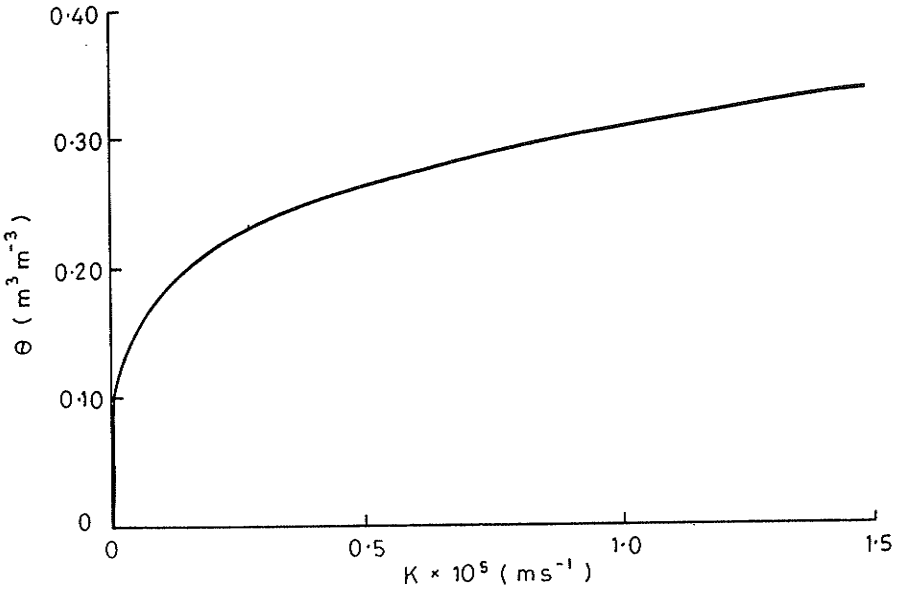

Fig 5.2 Soil water diffusivity [D(θ)] relationship for Bungendore fine sand

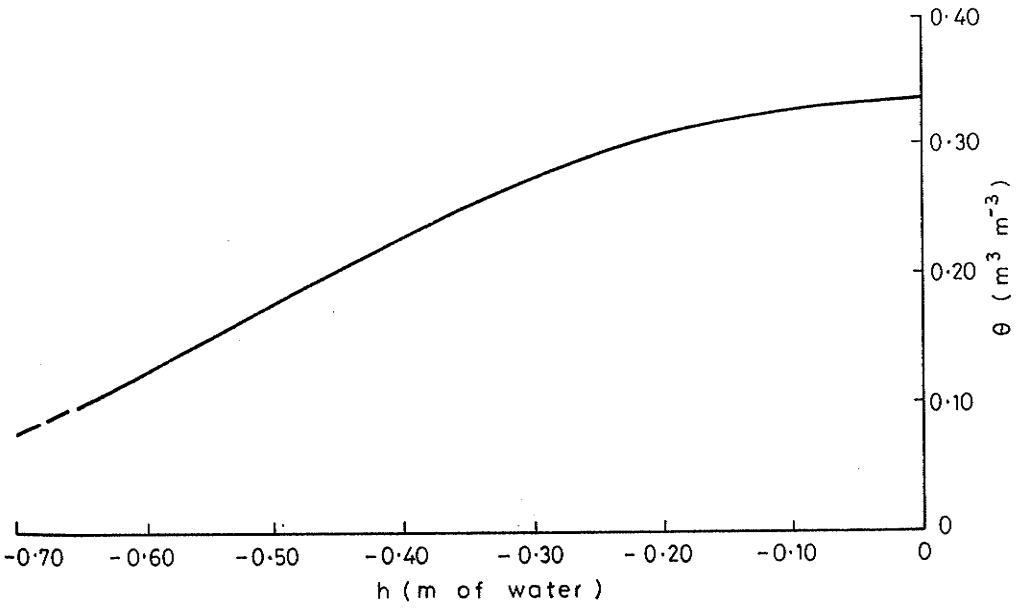

Fig 5.3 K(θ) and h(θ) relationships for Bungendore fine sand used in the numerical analysis

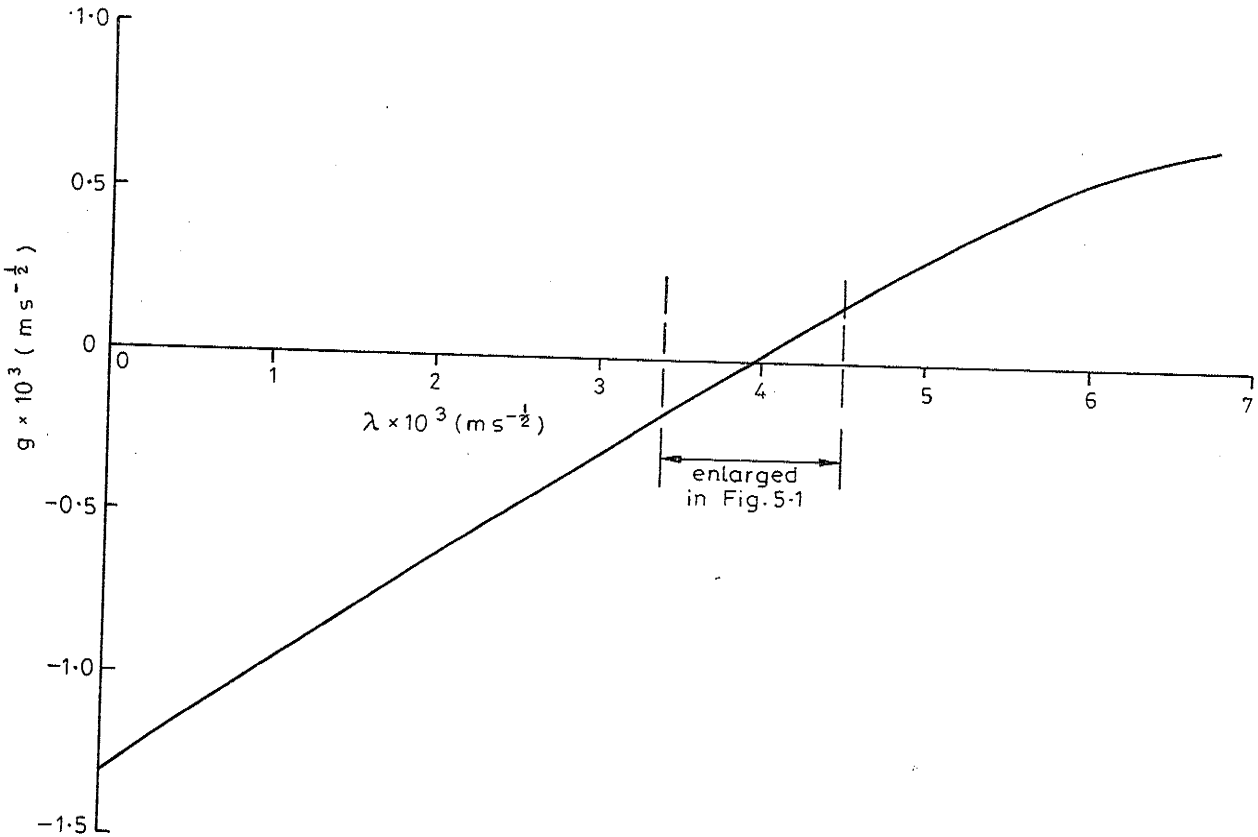

Fig 5.4 g(λ) relationship for Bungendore fine sand

Fig 5.4 g(λ) relationship for Bungendore fine sand

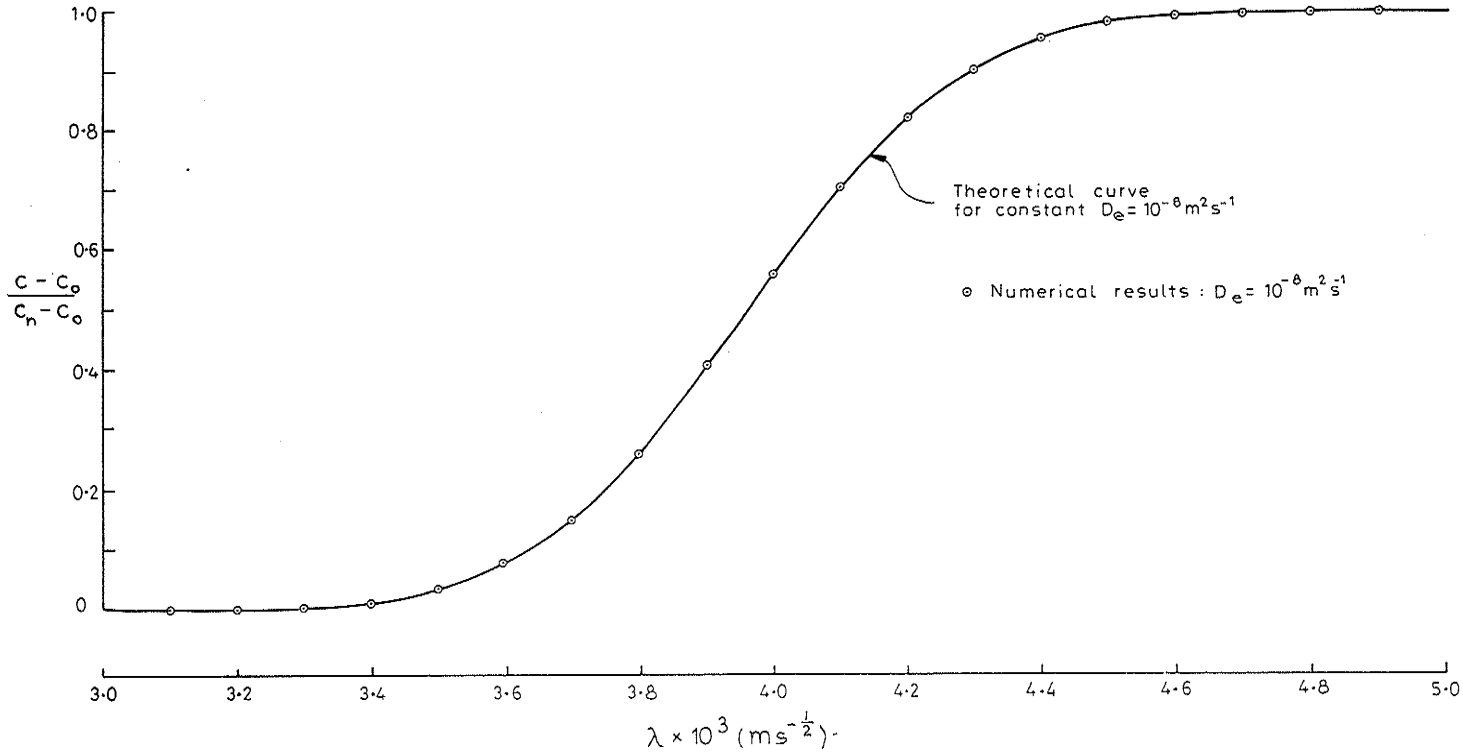

Fig 5.5 Normalized concentration profile for a constant D_e value of $10^{-8} m^2 s^{-1}$ compared with the numerical results for constant concentration absorption

are being correctly simulated, for example, the velocity dependence of the dispersion coefficient, and the mechanisms of solute transport during redistribution. Experimental data on such aspects are examined in the following chapters.

6 SOLUTE MOVEMENT DURING CONSTANT CONCENTRATION ABSORPTION

6.1 Introduction

The quasi-analytical solution for the hydrodynamic dispersion of non-reactive solute during unsteady, horizontal absorption under a constant concentration boundary condition is by nature limited due to the simplifying assumptions concerning D_e involved in its derivation. However, it forms a useful 'departure point' for the assessment of experimental results and the development of more realistic predictive procedures for the fine sand.

In this chapter the general significance of the parameter λ_* is discussed in detail, together with the effect on the concentration profiles of varying the constant dispersion coefficient. The existence and magnitude or otherwise of a velocity-dependent hydrodynamic dispersion coefficient is then considered using numerical and experimental data.

6.2 The General Significance of λ_*

The integral solution developed in Chapter 5 for a constant D_e involved the specification of λ at the point where $g(\lambda) = 0$. This was defined as λ_*. Both $g(\lambda)$ and λ_* were derived from the numerical $\theta(\lambda)$ relationship. Use of the transformation $\lambda = xt^{-\frac{1}{2}}$ can be used to give valuable information about the position of the solute front without any restriction having to be placed on the general nature of D_e as assumed in the earlier analysis.

As previously,

$$\frac{\partial(c\theta)}{\partial t} = \frac{\partial}{\partial x}\left[D_e(\theta,v)\,\frac{\partial c}{\partial x}\right] - \frac{\partial}{\partial x}[qc] \qquad 6.1$$

If the transformation $\lambda = xt^{-\frac{1}{2}}$ is applied to equation 6.1, then

$$\frac{d}{d\lambda}\left[D_e(\theta,v)\,\frac{dc}{d\lambda}\right] + \frac{g(\lambda)}{2}\,\frac{dc}{d\lambda} = 0 \qquad 6.2$$

If it is assumed that $D_e(\theta,v) = 0$, inferring piston-like solute movement, then

$$\frac{g(\lambda)}{2}\,\frac{dc}{d\lambda} = 0 \qquad 6.3$$

and since $dc/d\lambda \neq 0$, the equality $g(\lambda) = 0$ must hold. Hence the sharp solute front must occur at λ_*.

If $D_e(\theta,v) \neq 0$, it is necessary to assess the relationship between some recognisable position on a $c(\lambda)$ profile such as the point of maximum slope (the point of contraflexure) and λ_*. Assume that a particular $c(x,t)$ curve has been transformed to a λ scale and, due to $D_e(\theta,v)$ effects, the point of contraflexure is positioned at a λ value other than λ_*, as shown in Fig 6.1. Point A (Fig 6.1) now represents the position on $c(\lambda)$ where the ordinate is λ_* and hence $g(\lambda) = 0$. At point A then,

$$\frac{d}{d\lambda}\left[D_e(\theta,v)\,\frac{dc}{d\lambda}\right] = 0 \qquad 6.4$$

For the left hand side of equation 6.2 to be zero, $\left[D_e(\theta,v)\,\frac{dc}{d\lambda}\right]$ must be a maximum at point A. Numerical results indicate that for a given $c(x,t)$

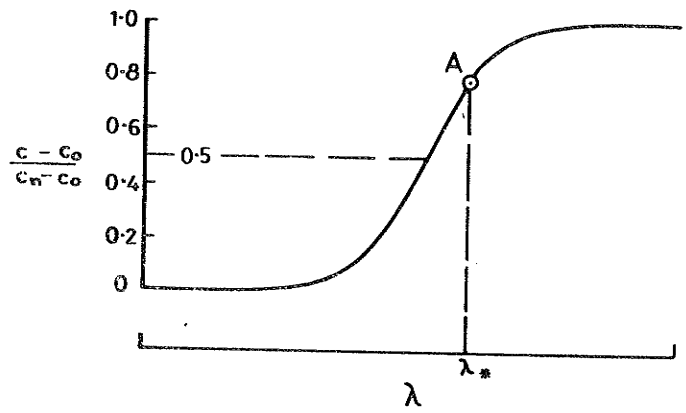

Fig 6.1 Normalized concentration profile used in showing the coincidence of point A and the point of contraflexure

curve, $D_e(\theta,v)$ is sensibly constant across the solute front and hence the maximum of the product will be governed by the maximum of $dc/d\lambda$ (Watson and Jones 1981*a*). Since $dc/d\lambda$ is a maximum at the point of contraflexure, it can be concluded that, to a very close approximation, point A and the point of contraflexure are coincident.

If the 'mean' position of a solute front is defined in terms of the point of contraflexure, its location can be safely assumed to be at λ_* for constant concentration horizontal absorption, and this location is dependent upon the soil water system only. The above applies also for constant concentration vertical infiltration at early times, when the gravity effect is very small.

6.3 The Significance of the Hydrodynamic Dispersion Coefficient

The alternative integral scheme of Chapter 5 was used with values of $\lambda_* = 3.96 \times 10^{-3} ms^{-\frac{1}{2}}$, $\tan \alpha_U = 0.302$ and $\tan \alpha_L = 0.316$ as before to calculate the normalized solute concentration ($\bar{c}$) for a range of constant D_e values. Fig 6.2 gives the resulting $\bar{c}(\lambda)$ profiles, using a large λ scale for clarity. The profile for $D_e = 10^{-8}\ m^2s^{-1}$ is included because it coincides closely with the experimental data which is plotted in Fig 6.3. The 'mean' $\bar{c}(\lambda)$ profile for the experimental results (full line in Fig 6.3) shows that at a $\bar{c}$ value of 0.5 the corresponding λ value is $4.07 \times 10^{-3}\ ms^{-\frac{1}{2}}$. This compares with the value of $3.96 \times 10^{-3}\ ms^{-\frac{1}{2}}$ used in the quasi-analytical and numerical work, and determined from the $\theta(\lambda)$ relationship of Fig 6.3 (dashed line). This in turn was obtained by transforming the $\theta(x,t)$ data of the numerical simulation. The comparison between the experimental data points and numerical $\theta(\lambda)$ curve of Fig 6.3 is good, with the main differences occurring where the curve 'steepens' as $\theta \to \theta_n$. This variation leads to a slightly smaller λ_* value when calculated from the dashed curve compared with the value given by the experimental data. This is consistent with the values given above.

To enable comparisons to be made between the 'shape' of the experimental data and the theoretical and numerical predictions, the experimental $\bar{c}(\lambda)$ curve of Fig 6.3 was horizontally transposed so that at $\bar{c} = 0.5$ the λ value was $3.96 \times 10^{-3}\ ms^{-\frac{1}{2}}$. The comparison is given in Fig 6.4 and reveals excellent agreement between experimental, numerical and theoretical results for a constant D_e of $10^{-8}\ m^2s^{-1}$. Certainly the value of D_e of $5 \times 10^{-10}\ m^2s^{-1}$ which Smiles et al (1978) found applicable to the sand-kaolinite mixture is not applicable to the coarser Bungendore fine sand.

6.4 The Velocity Dependence of the Dispersion Coefficient

Although Fig 6.4 shows that the $\bar{c}(\lambda)$ result for $D_e = 10^{-8}\ m^2s^{-1}$ matches the mean experimental curve well, it cannot necessarily be concluded from this that the hydrodynamic dispersion coefficient is velocity *independent*.

The hydrodynamic dispersion coefficient may be represented as

$$D_e = D_p + \beta|v| \qquad 6.5$$

where the dependence of $D_e(\theta,v)$ on θ and v is now effected solely through the pore water velocity. In this study, the constant term D_p was taken to be $5 \times 10^{-10} m^2s^{-1}$. The value of the parameter β was chosen so that the numerical results would match as closely as possible the experimental data and hence the theoretical $\bar{c}(\lambda)$ curve for $D_e = 10^{-8}\ m^2s^{-1}$. As the inclusion of the velocity dependence in D_e invalidates the similarity solution for $\bar{c}$, it was necessary to determine β from a data match at a specified time. This was taken at $t = 1220$ s which was the termination time of the first experiment. Using the

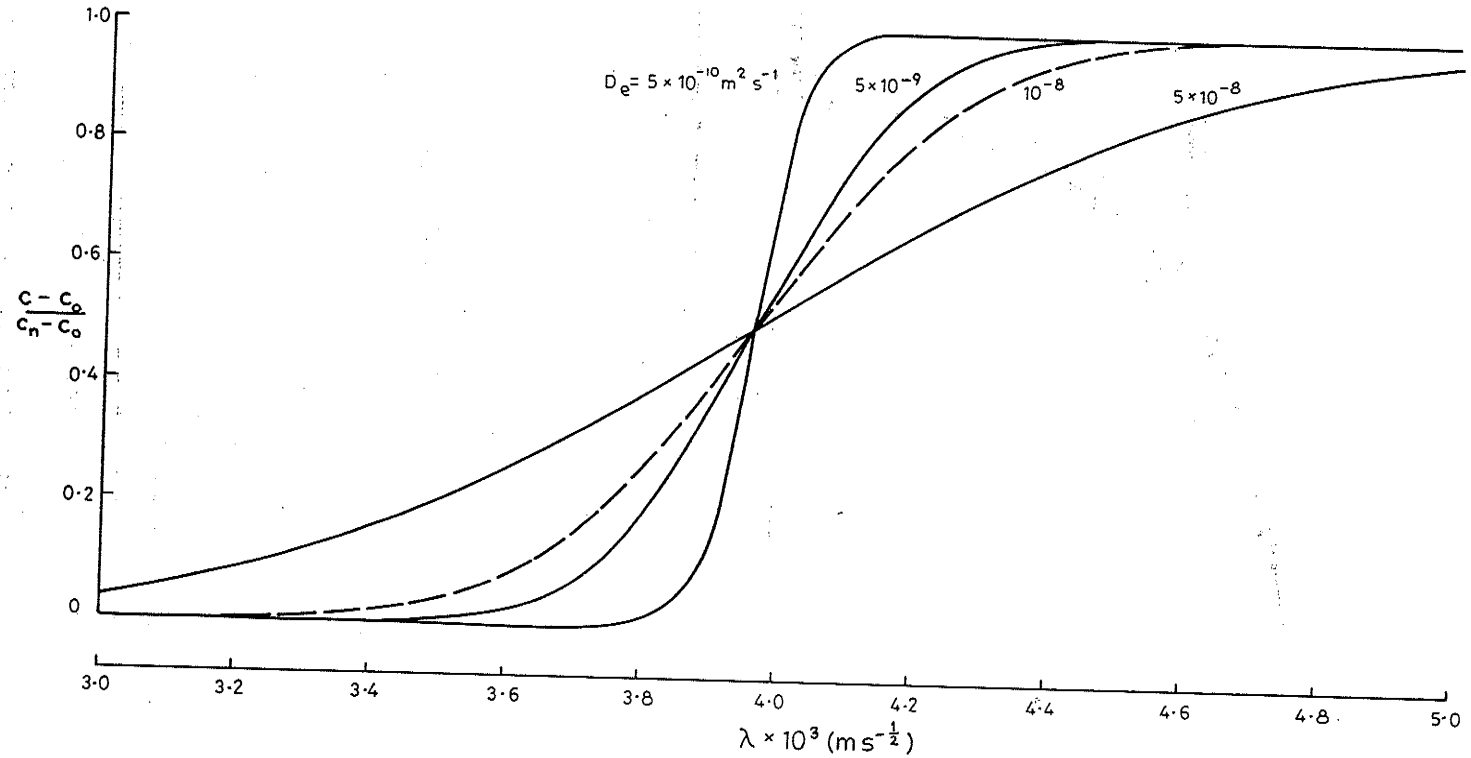

Fig 6.2 Normalized concentration profiles for constant D_e values of 5×10^{-10}, 5×10^{-9}, 10^{-8} and $5 \times 10^{-8} m^2 s^{-1}$ for constant concentration absorption (The profiles were calculated using the integral solution)

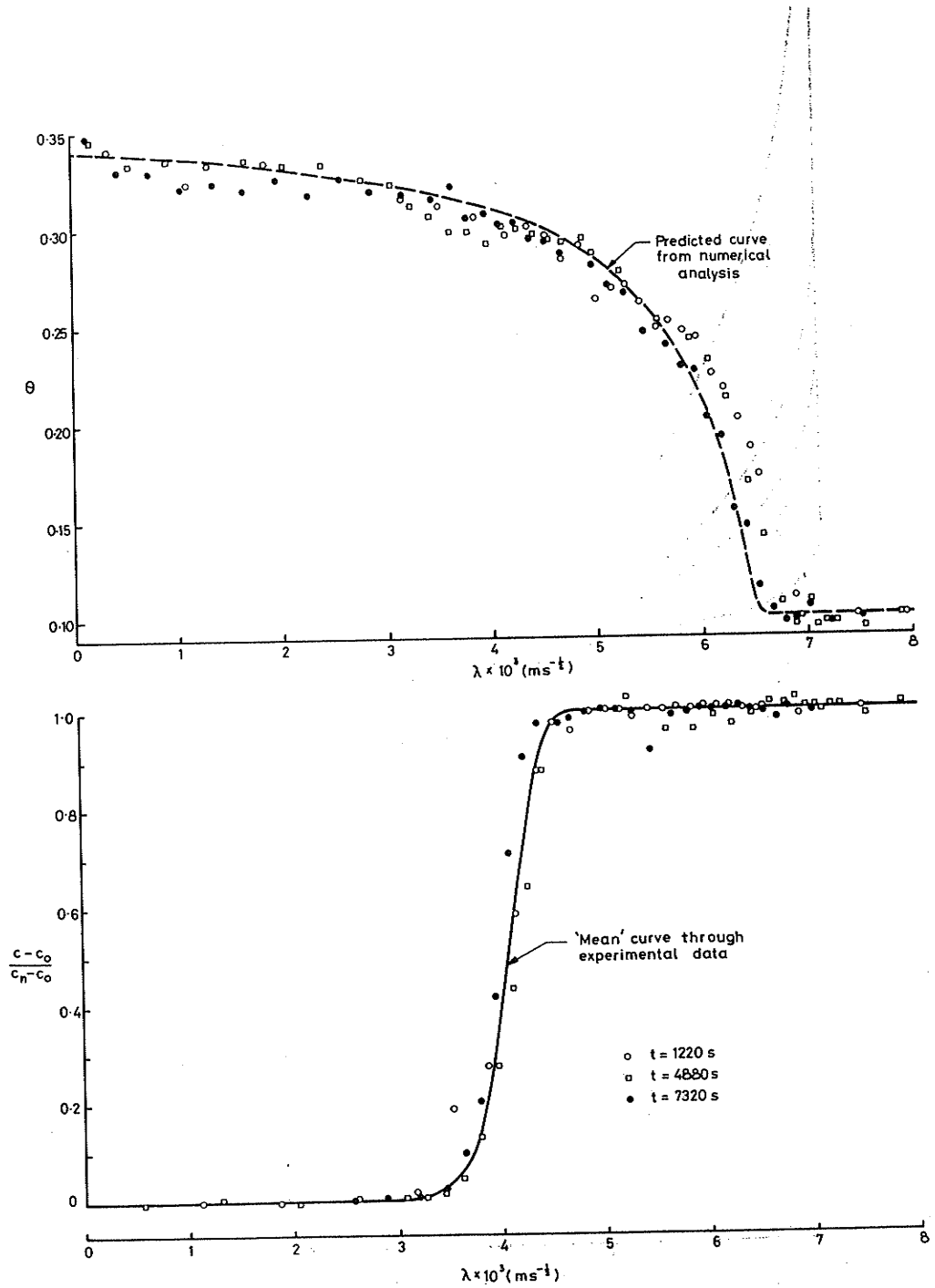

Fig 6.3 Experimental results plotted as $\theta(\lambda)$ and $\bar{c}(\lambda)$ for horizontal absorption in Bungendore fine sand under constant concentration conditions

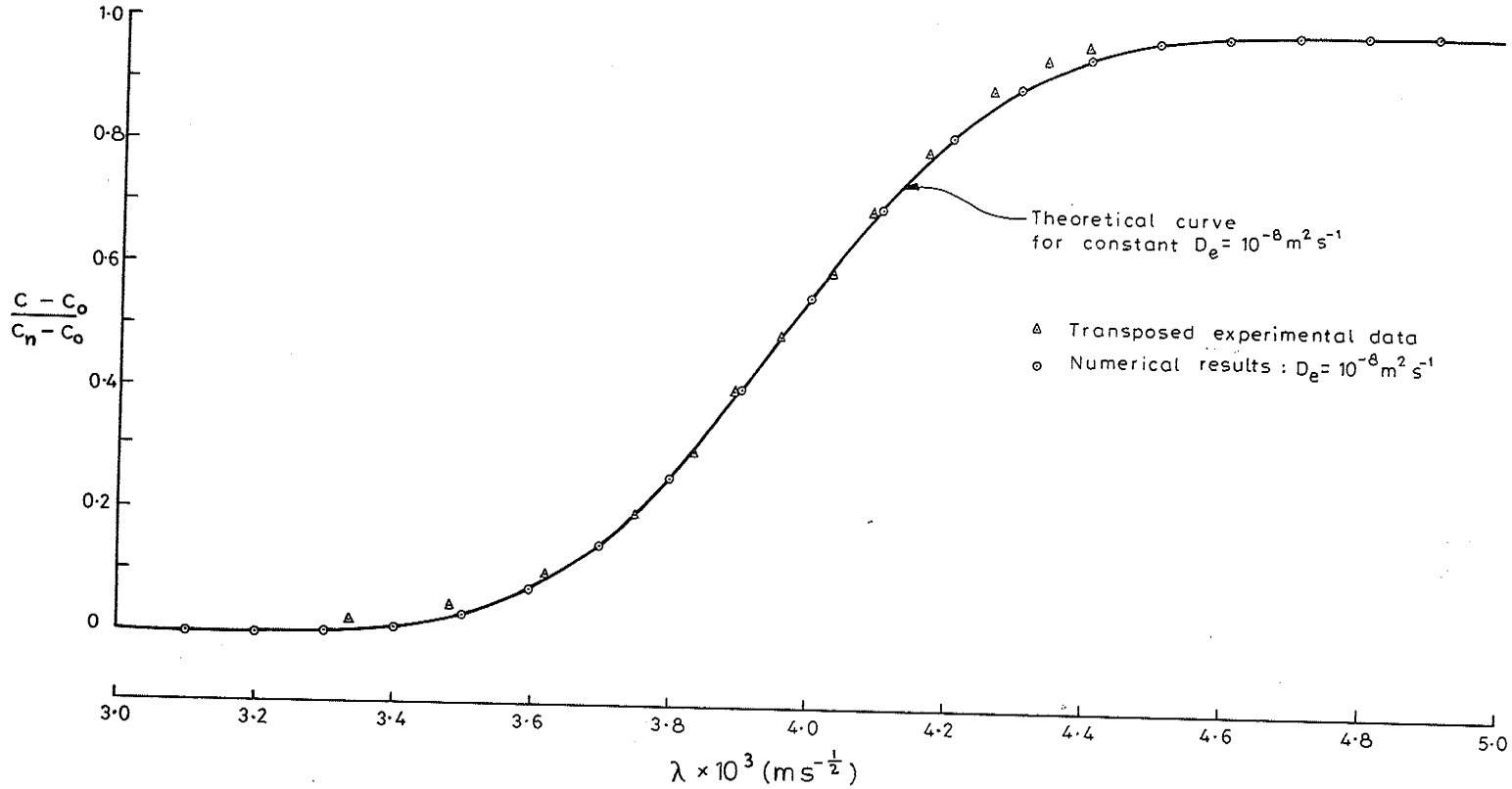

Fig 6.4 Normalized concentration profile for a constant D_e value of $10^{-8} m^2 s^{-1}$ compared with the transposed experimental data and the numerical results for constant concentration absorption

value of β so obtained (0.0001 m) the numerical results for $\bar{c}(\lambda)$ for times of 2500 s and 7225 s were determined. These results, together with those for t = 1220 s are plotted in Fig 6.5. The $\bar{c}(\lambda)$ curve for $D_e = 10^{-8}$ m^2s^{-1} is also included. The match at t = 1220 s is good. The effect of the velocity-dependent D_e on solute movement is shown as the gradual steepening of $\bar{c}(\lambda)$ with time. This follows logically since as v decreases with time, $D_e(\theta,v)$ also decreases with time which, on transformation, results in the steeper $\bar{c}(\lambda)$ relationship. Prior to transformation however, the $\bar{c}(x)$ relationship would be much 'flatter' (ie more dispersed) at 7225 s compared with 1220 s since the $t^{\frac{1}{2}}$ ratio is approximately 85:35.

Superimposed on Fig 6.5 are two dashed lines which represent the limits, after transformation, of the $\bar{c}(\lambda)$ experimental data points given in Fig 6.3. These limits are spaced approximately 0.1×10^{-3} $ms^{-\frac{1}{2}}$ on either side of the mean experimental data curve. Clearly, for the time range considered, the experimental scatter is larger than the spread of the $\bar{c}(\lambda)$ curves caused by the velocity-dependent effect. This suggests that the experimental data to hand is not sufficiently sensitive to allow the existence and magnitude (or otherwise) of a velocity-dependent effect in D_e to be determined, and that the use of an indirect non-destructive method rather than the destructive sampling technique used is probably necessary for such a study.

The possibility of the hydrodynamic dispersion coefficient being velocity dependent could also be considered by calculating the Péclet numbers (P_e) for the system. Smiles and Philip (1978) following Saffman (1959) and Pfannkuch (1963) suggest that the coefficient will be velocity independent for $P_e \leq 1$. This can be written as

$$\frac{S\ell t^{-\frac{1}{2}}}{2\theta_o D_m} \leq 1 \qquad 6.6$$

where for Bungendore fine sand S (sorptivity) = 1.3×10^{-3} $ms^{-\frac{1}{2}}$
ℓ (characteristic length) = 10^{-4} m
θ_o = 0.34
D_m (molecular diffusivity of KCl in solution) = 1.9×10^{-9} m^2s^{-1}

On substitution, t $\geq$ 10 000 s approximately if D_e is to be velocity independent. This time exceeds the longest experimental run of 7320 s.

The Péclet numbers were also calculated directly using numerical data for the velocity estimates, and were 5.1, 2.9 and 2.0 for the times 400 s, 1225 s and 2500 s respectively.

6.5 Conclusion

This part of the project has made use of theoretical, numerical and experimental results for a fine sand in order to examine in detail solute movement during horizontal absorption under constant concentration conditions. The function $g(\lambda)$, which is obtained directly from $\theta(\lambda)$ has linear characteristics in the vicinity of λ_* (defined as the λ value where $g(\lambda) = 0$) which enabled a simple integral solution to be used for calculating $\bar{c}(\lambda)$ profiles under conditions of constant D_e (see Chapter 5).

For purely convective-type solute movement, λ_* defines the position of the sharp solute front, whilst for constant D_e conditions it defines the location of the point of contraflexure of the $\bar{c}(\lambda)$ profile. To a very close approximation, λ_* locates the point of contraflexure for systems where the hydrodynamic dispersion coefficient is of the form $D_e(\theta,v)$.

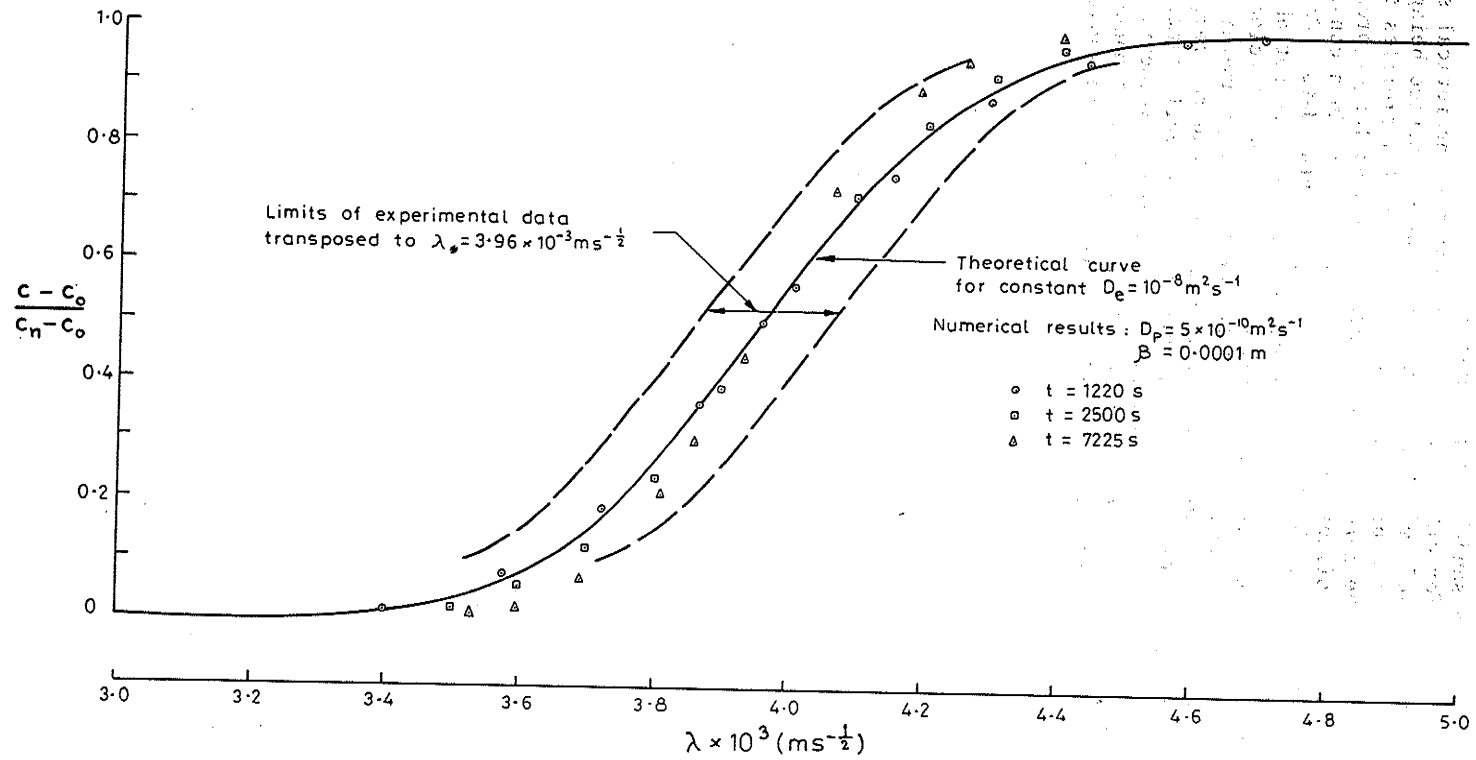

Fig 6.5 Normalized concentration profiles using a velocity-dependent dispersion coefficient, with $D_p = 5 \times 10^{-10} m^2 s^{-1}$ and $\beta = 0.0001$ m for constant concentration absorption

The experimental data for the fine sand can be well represented by the theoretical analysis when a constant D_e value of 10^{-8} m^2s^{-1} is used. This value is 20 times greater than the value of 5×10^{-10} m^2s^{-1} which Smiles et al (1978) found suitable for a sand-kaolonite mixture.

The numerical results for $\bar{c}(\lambda)$ were tested against the theoretical solution for a constant D_e of 10^{-8} m^2s^{-1} with excellent correspondence being obtained. When the numerical approach was used to obtain $\bar{c}(\lambda)$ profiles for a dispersion coefficient of the form $D_e(\theta,v)$, similarity was no longer preserved. However, the spread of the profiles for different times lay within a conservatively estimated bandwidth of the scatter of the experimental data. Consequently the experimental results for the Bungendore fine sand are not able to be used definitively to prove either the existence or otherwise of velocity-dependence effects. However, the magnitude of the constant D_e parameter required to achieve correspondence with the experimental data and the large values of the Péclet numbers for the system, particularly at early times, suggest that the hydrodynamic dispersion coefficient is indeed velocity dependent. Experimental verification of the magnitude of the effect under constant concentration conditions seems to require the use of more sophisticated equipment.

dispersion coefficient, with $D_p = 5 \times 10^{-10} m^2s^{-1}$ and $\beta = 0.0001$ m for constant concentration absorption

7 SOLUTE MOVEMENT DURING CONSTANT FLUX ABSORPTION

7.1 Introduction

The predictive behaviour of the numerical solution is tested further in this chapter using experimental data on solute movement in Bungendore fine sand under constant *flux* absorption. The experiments were again carried out by the staff of the C.S.I.R.O. Division of Environmental Mechanics. Smiles et al. (1981) have reported on the work and their paper should be consulted for discussion of the experimental details. Although the same data has been used in this chapter and in Smiles et al (1981) the interpretation of the experimental results does differ, particularly in relation to the velocity dependence of the dispersion coefficient.

7.2 Experimental Data

If v_o is the soil water flux at x = 0 it is possible (White et al., 1979) to describe constant flux absorption in a convenient manner using reduced variables T and X defined as

$$\left.\begin{aligned} T &= v_o^2 t \\ X &= v_o x \end{aligned}\right\} \qquad 7.1$$

For a given T value White et al. (1979) showed from theoretical grounds that the $X(\theta)$ curve would be unique. The numerical analysis of soil water movement has been tested against this requirement using a wide range of v_o values with a unique $X(\theta)$ relationship always being obtained for any given T value.

In the experimental work three T values were chosen, these being $10^{-8} m^2 s^{-1}$, $5.4 \times 10^{-8} m^2 s^{-1}$ and $3.98 \times 10^{-7} m^2 s^{-1}$. For each T value experiments using several v_o values were carried out and these are listed in Table 7.1.

Table 7.1 Summary of constant flux absorption and dispersion experiments

T ($m^2 s^{-1}$)	v_o (ms^{-1})	t (s)
1.00×10^{-8}	3.28×10^{-7}	9.348×10^4
	4.38×10^{-7}	5.232×10^4
	6.57×10^{-7}	2.322×10^4
	8.75×10^{-7}	1.308×10^4
5.40×10^{-8}	8.75×10^{-7}	7.050×10^4
	1.31×10^{-6}	3.132×10^4
	1.75×10^{-6}	1.758×10^4
	3.28×10^{-6}	5.010×10^4
3.98×10^{-7}	3.94×10^{-6}	2.556×10^4
	5.25×10^{-6}	1.440×10^4
	7.88×10^{-6}	6.420×10^3
	1.05×10^{-5}	3.600×10^3

Most experiments were duplicated and for each experiment the normal slicing technique was used to obtain samples for determining the θ and c profiles. The initial θ value approximated 0.10 $m^3 m^{-3}$ in each case and the uniform initial concentration of KCℓ was 1000 meq/litre. The solute concentration of the absorbing solution was 100 meq/litre. The experimental data in the

form $\theta(X)$ and $\bar{c}(X)$ is given for the T values in question in Figs 7.1, 7.2 and 7.3. In each figure the dashed line through the $\theta(X)$ data points represents the relationship as predicted by the constant flux numerical analysis using the $h(\theta)$ and $K(\theta)$ curves of Fig 5.3. However, the continuous line in the $\bar{c}(X)$ set in each figure, as with the constant concentration data, represents a 'mean' curve drawn through the experimental values.

7.3 Discussion

For a given T value, Smiles et al. (1981) showed that if the hydrodynamic dispersion coefficient was assumed to be velocity independent, then a unique $\bar{c}(X)$ relationship would result regardless of the v_o value used. It was considered that the 'collapse' of the $\bar{c}(X)$ data given in Figs 7.1, 7.2 and 7.3 was sufficiently definitive for velocity independence to be indicated. The hydrodynamic dispersion coefficient would thus consist only of the molecular diffusion component which can be expressed as

$$D_p = \theta_* D_m \qquad 7.2$$

where D_m is the diffusion coefficient for KCℓ in water ($1.9 \times 10^{-9} m^2 s^{-1}$) and θ_* is the θ value at X_* where X_* is defined as the value of X when

$$\theta X = \int_{\theta_n}^{\theta} X d\theta \qquad 7.3$$

The θ_* values for T values of 10^{-8}, 5.4×10^{-8} and $3.98 \times 10^{-7} m^2 s^{-1}$ are respectively 0.1868, 0.2231 and 0.2833 $m^3 m^{-3}$ giving D_p values of 3.5×10^{-10}, 4.3×10^{-10} and $5.4 \times 10^{-10} m^2 s^{-1}$. When these values were used by Smiles et al (1981) in an approximate analytical expression for constant D_e to obtain $\bar{c}(X)$ profiles the match with the experimental data seemed satisfactory. However, as will be detailed below, on the basis of this study and with the benefit of the numerical solutions, it seems that the experimental data supports the concept of the velocity dependence of the dispersion coefficient rather than velocity independence. It follows that if D_e is velocity dependent then a separate $\bar{c}(X)$ profile is obtained for each v_o value used. In this regard a detailed study of the experimental data in the solute front region indicates, in some instances, a trend in the positioning of the data points within the group which is consistent with the relative magnitude of the v_o value. The discussion which follows considers the determination of the constant D_e value giving the best match with the mean curve through the experimental points, the calculation of $\bar{c}(X)$ profiles assuming velocity dependence using a β value of 0.0001 m and an assessment of the validity of the velocity-dependent assumption by comparing the spread of the $\bar{c}(X)$ profiles for different v_o values with the bandwidth of the scatter of the experimental data in the solute front region.

In this study the effect on $\bar{c}(X)$ profiles of the velocity dependence in D_e increases as T increases due to the increasing v_o values (see Table 7.1); accordingly, the data for $T = 3.98 \times 10^{-7} m^2 s^{-1}$ will be analysed first. Fig 7.4 gives to an enlarged scale the mean curve through the experimental data and the $\bar{c}(X)$ profile for a constant D_e of $30 \times 10^{-10} m^2 s^{-1}$. Also included in the figure is $\bar{c}(X)$ for the D_e value of $5.4 \times 10^{-10} m^2 s^{-1}$ as used by Smiles et al. (1981). The comparison between the mean experimental curve and that for D_e of $30 \times 10^{-10} m^2 s^{-1}$ is good; however, the curve for D_e of $5.4 \times 10^{-10} m^2 s^{-1}$

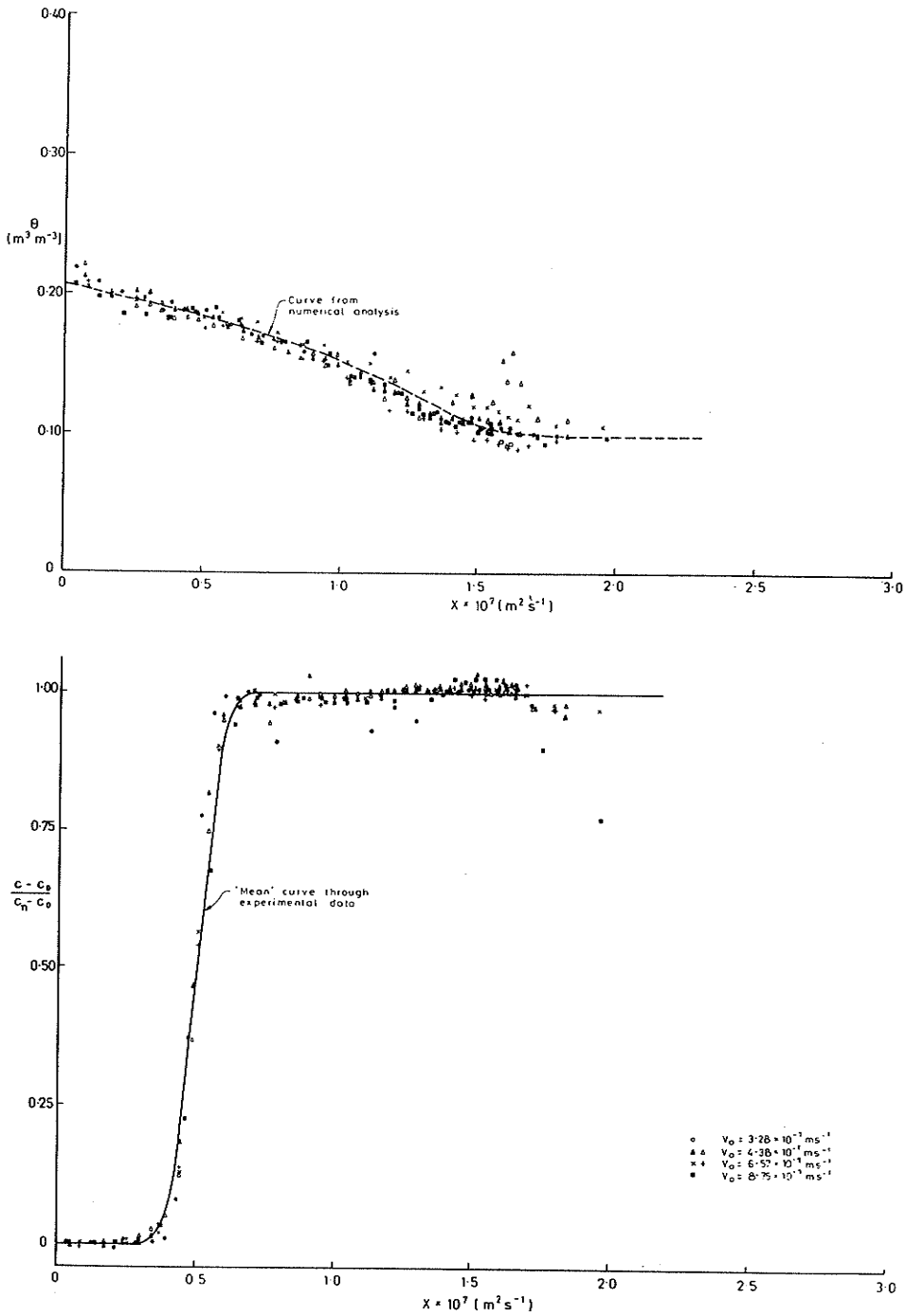

Fig 7.1 Experimental results plotted as $\theta(X)$ and $\bar{c}(X)$ for horizontal absorption in Bungendore fine sand under a constant flux boundary condition, for $T = 10^{-8} m^2 s^{-1}$

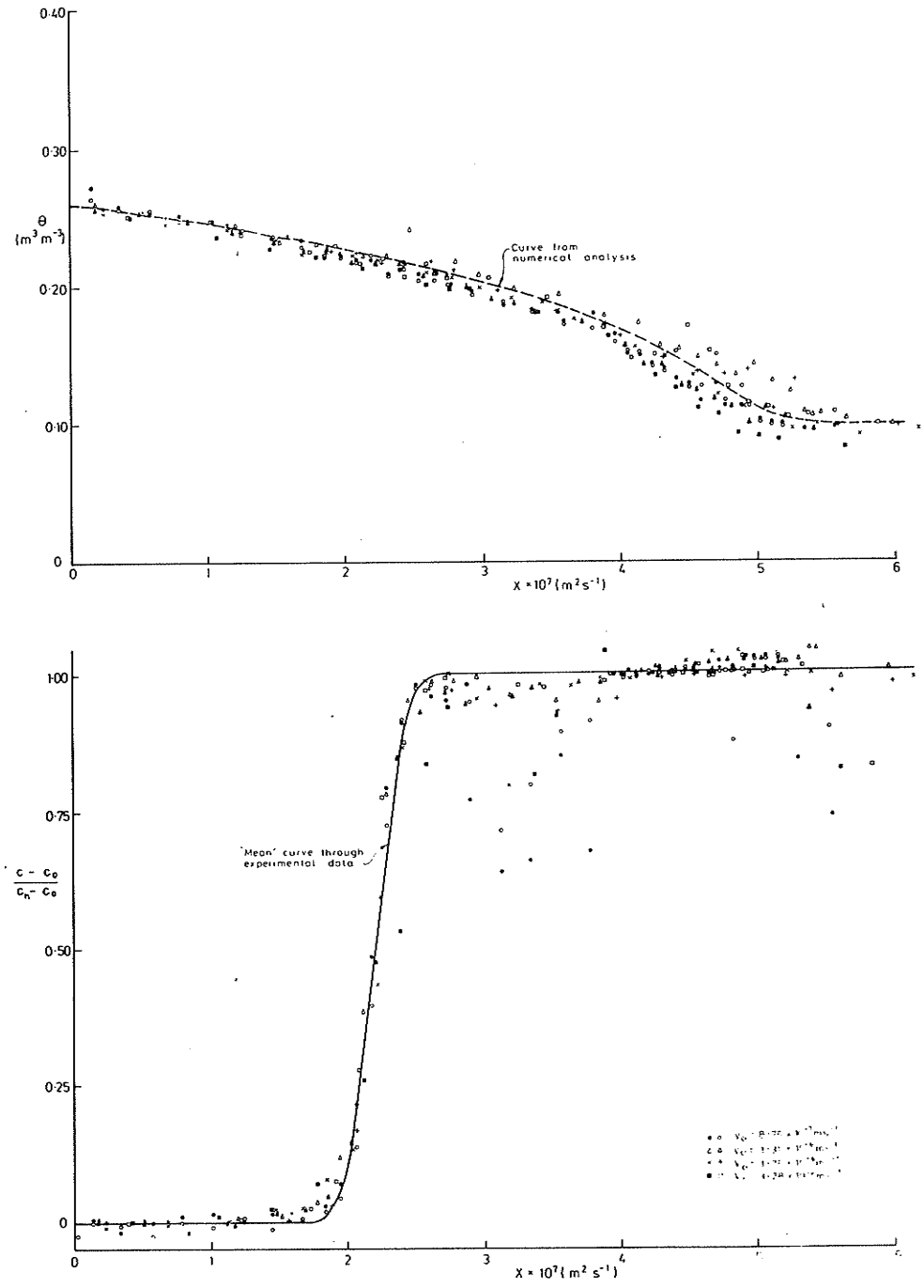

Fig 7.2 Experimental results plotted as $\theta(X)$ and $\bar{c}(X)$ for horizontal absorption in Bungendore fine sand under a constant flux boundary condition, for $T = 5.4 \times 10^{-8} m^2 s^{-1}$

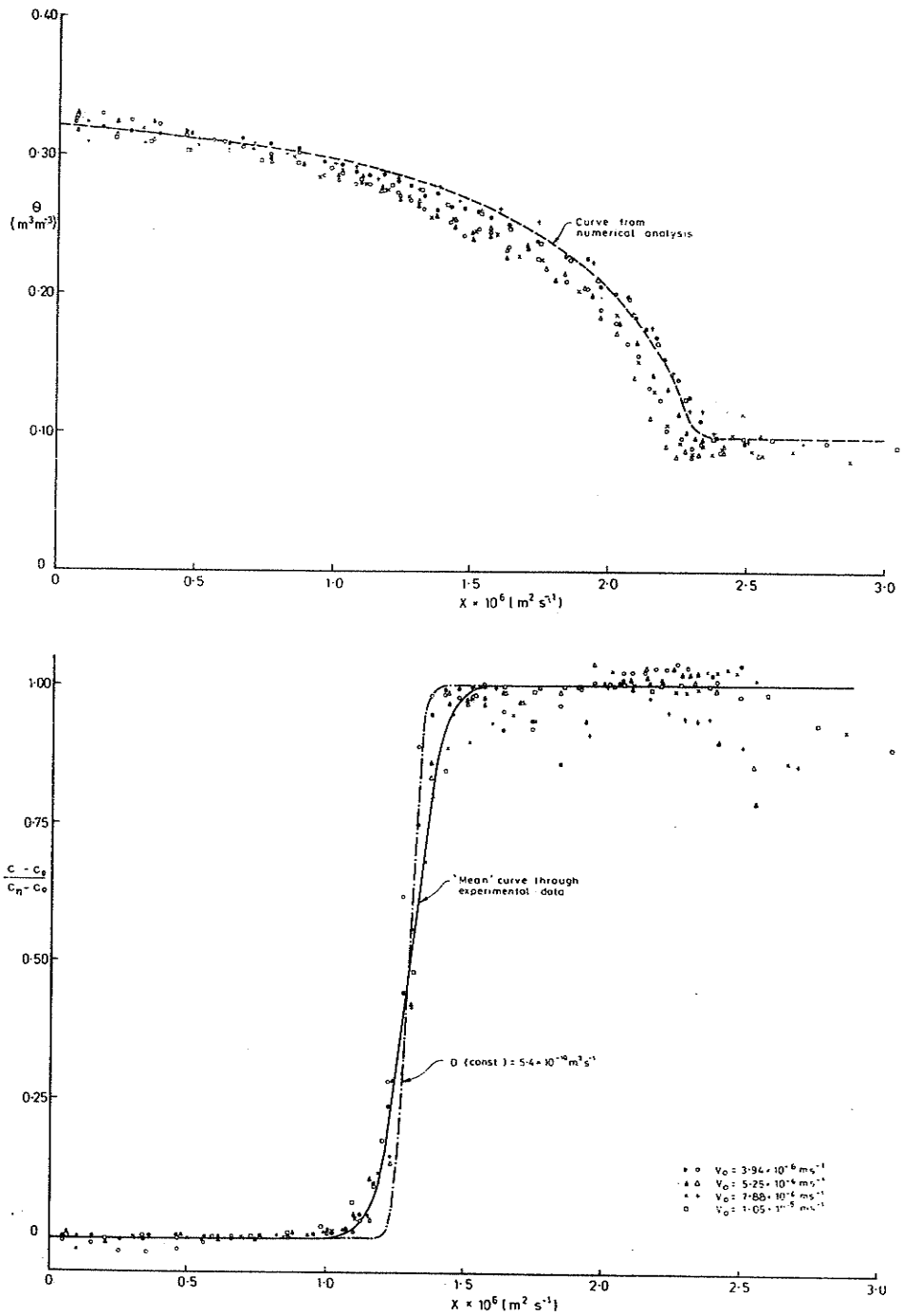

Fig 7.3 Experimental results plotted as $\theta(X)$ and $\bar{c}(X)$ for horizontal absorption in Bungendore fine sand under a constant flux boundary condition, for $T = 3.98 \times 10^{-7} m^2 s^{-1}$

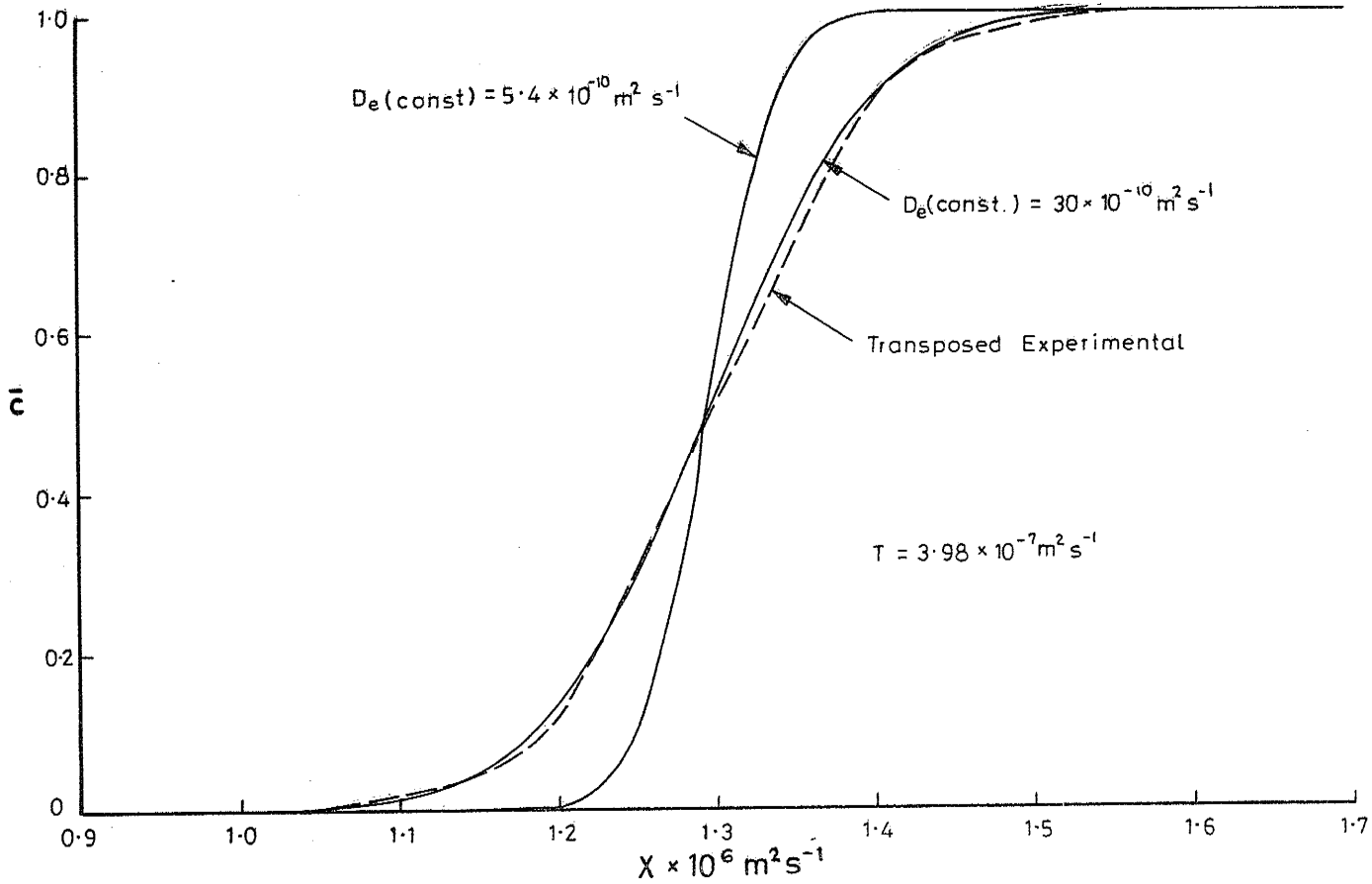

Fig 7.4 Normalized $\bar{c}(X)$ profiles for horizontal absorption in Bungendore fine sand under a constant flux boundary condition, for T = 3.98 x $10^{-7} m^2 s^{-1}$ (constant D_e)

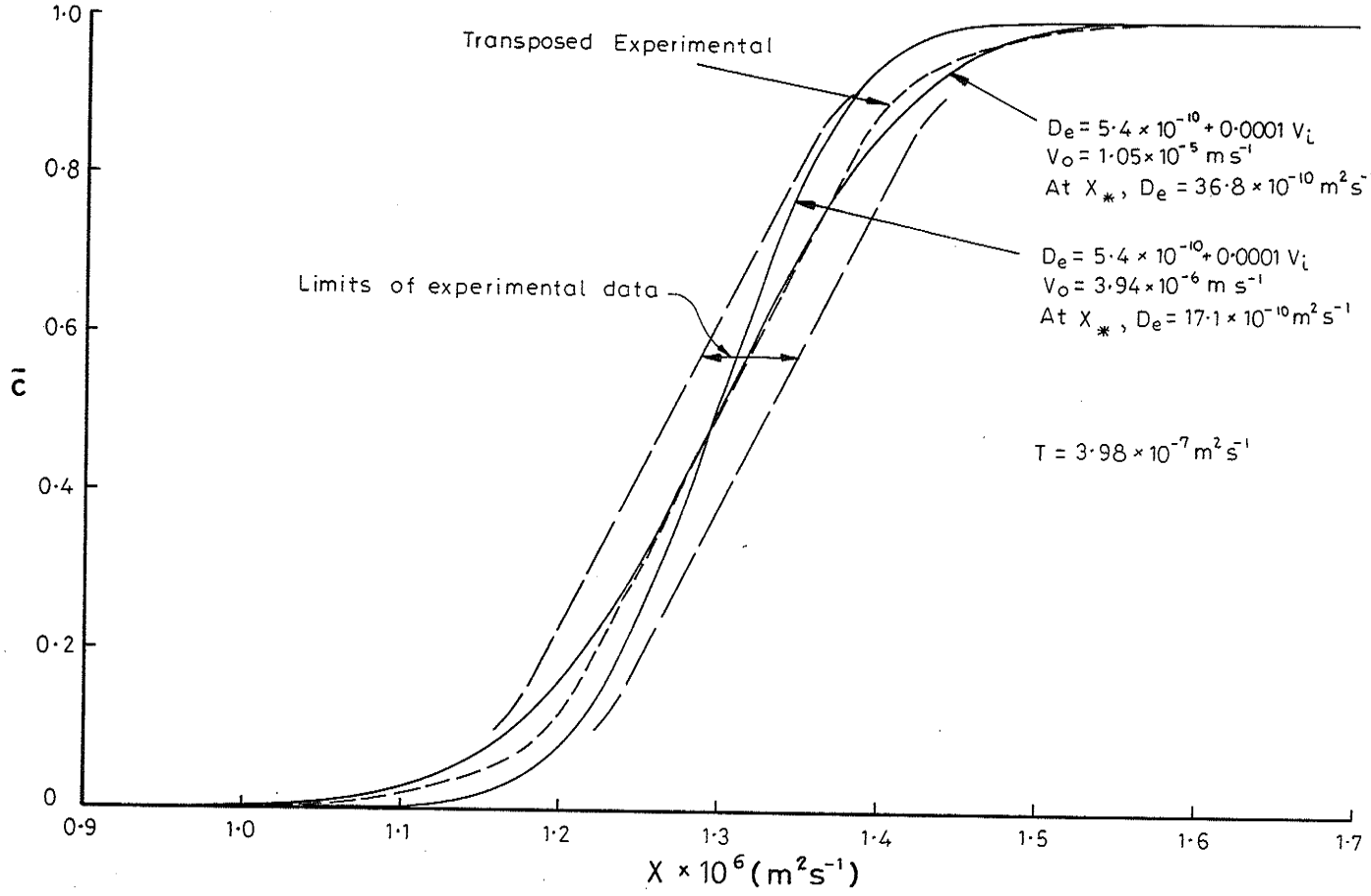

Fig 7.5 Normalized $\bar{c}(X)$ profiles for horizontal absorption in Bungendore fine sand under a constant flux boundary condition, for $T = 3.98 \times 10^{-7} m^2 s^{-1}$ (D_e velocity dependent)

agrees poorly with the other two curves. The $\bar{c}(X)$ relationship for D_e of $5.4 \times 10^{-10}\,m^2s^{-1}$ has also been included in Fig 7.3 to indicate its location with regard to the experimental data; it is clear that it represents a bounding curve to the data rather than a mean curve.

The mean curve is reproduced in Fig 7.5 together with the numerically-determined $\bar{c}(X)$ profiles for the smallest ($3.94 \times 10^{-6}\,ms^{-1}$) and largest ($1.05 \times 10^{-5}\,ms^{-1}$) of the v_o values listed in Table 7.1 for $T = 3.98 \times 10^{-7}\,m^2s^{-1}$. The dispersion coefficient was represented by the same equation as used previously namely

$$D_e = D_p + \beta|v| \qquad 7.4$$

with $D_p = 5.4 \times 10^{-10}\,m^2s^{-1}$ and $\beta = 0.0001\,m$.

The $\bar{c}(X)$ profile for $v_o = 1.05 \times 10^{-5}\,ms^{-1}$ matches the mean experimental curve closely whilst that for $v_o = 3.94 \times 10^{-6}\,ms^{-1}$ lies well within the bandwidth of the experimental scatter as shown in the figure. If D_e is determined by equation 7.4 using, for the pore water velocity, the value at X_* then the magnitude of D_e is $36.8 \times 10^{-10}\,m^2s^{-1}$ (ie $5.4 \times 10^{-10} + 31.4 \times 10^{-10}$) for $v_o = 1.05 \times 10^{-5}\,ms^{-1}$ and $17.1 \times 10^{-10}\,m^2s^{-1}$ (ie $5.4 \times 10^{-10} + 11.7 \times 10^{-10}$) for $v_o = 3.94 \times 10^{-6}\,ms^{-1}$. These results lend strong support to the conclusion that D_e is velocity dependent for the higher pore water velocity values during constant flux absorption in Bungendore fine sand. If the characteristic length (ℓ) for the sand is taken to be $10^{-4}\,m$ then the Péclet number for the case when v_o is $1.05 \times 10^{-5}\,ms^{-1}$ is 1.7. This further strengthens the conclusion regarding velocity dependence. It should be noted that a much smaller v_o value could be used for the same T value with the simulation being carried out for a much longer time and over a much longer column length. The mechanical dispersion component of D_e would then be considerably reduced and, if v_o were very small, the molecular diffusion component would become dominant.

For $T = 5.4 \times 10^{-8}\,m^2s^{-1}$ the best match with the mean experimental curve assuming D_e to be constant is obtained using a value of $8 \times 10^{-10}\,m^2s^{-1}$. These curves are shown in Fig 7.6. The experimental data requires slight horizontal transposition since for $\bar{c} = 0.50$ the value of X for the experimental curve is $2.22\,m^2s^{-1}$ compared with $2.23\,m^2s^{-1}$ for the numerical output. The constant D_e value of $8 \times 10^{-10}\,m^2s^{-1}$ is again larger than the $\theta_* D_m$ value of $4.3 \times 10^{-10}\,m^2s^{-1}$ applicable to this case. The $\bar{c}(X)$ curve for this value is also shown in Fig 7.6. Following the previous case, Fig 7.7 reproduces the mean curve and also gives $\bar{c}(X)$ profiles for the v_o bounding values (see Table 7.1) of $3.28 \times 10^{-6}\,ms^{-1}$ and $8.27 \times 10^{-7}\,ms^{-1}$. This latter curve matches the mean data curve very satisfactorily. The curve for $v_o = 3.28 \times 10^{-6}\,ms^{-1}$ extends beyond the bandwidth of the data scatter for $\bar{c} < 0.2$ and $\bar{c} > 0.8$. However, as Fig 7.2 indicates, in the vicinity of $\bar{c} = 0$ and $\bar{c} = 1.0$ the scatter of the experimental data is much greater than in the central region and, accordingly, it can be concluded that $\bar{c}(X)$ for $v_o = 3.28 \times 10^{-6}\,ms^{-1}$ is generally consistent with the experimental data. The D_e values at X_* for $T = 5.4 \times 10^{-8}\,m^2s^{-1}$ are $16.0 \times 10^{-10}\,m^2s^{-1}$ (ie $4.3 \times 10^{-10} + 11.7 \times 10^{-10}$) for $v_o = 3.28 \times 10^{-6}\,ms^{-1}$ and 7.4×10^{-10} (ie $4.3 \times 10^{-10} + 3.1 \times 10^{-10}$) for $v_o = 8.75 \times 10^{-7}\,ms^{-1}$. In the latter case the mechanical dispersion component of the coefficient is less than the molecular diffusion component.

The experimental v_o values for the smallest T value of $10^{-8}\,m^2s^{-1}$ range from $8.75 \times 10^{-7}\,ms^{-1}$ to $3.28 \times 10^{-7}\,ms^{-1}$ with a resultant decrease in the mechanical dispersion component of D_e. The mean experimental curve was well matched when a constant D_e value of $5 \times 10^{-10}\,m^2s^{-1}$ was used. A graphical comparison of these profiles has not been presented. Fig 7.8 gives $\bar{c}(X)$

Fig 7.5 Normalized c(X) profiles for horizontal absorption in Bungendore fine sand under a constant flux boundary condition, for $T = 3.98 \times 10^{-7}\,m^2s^{-1}$ (D_e velocity dependent)

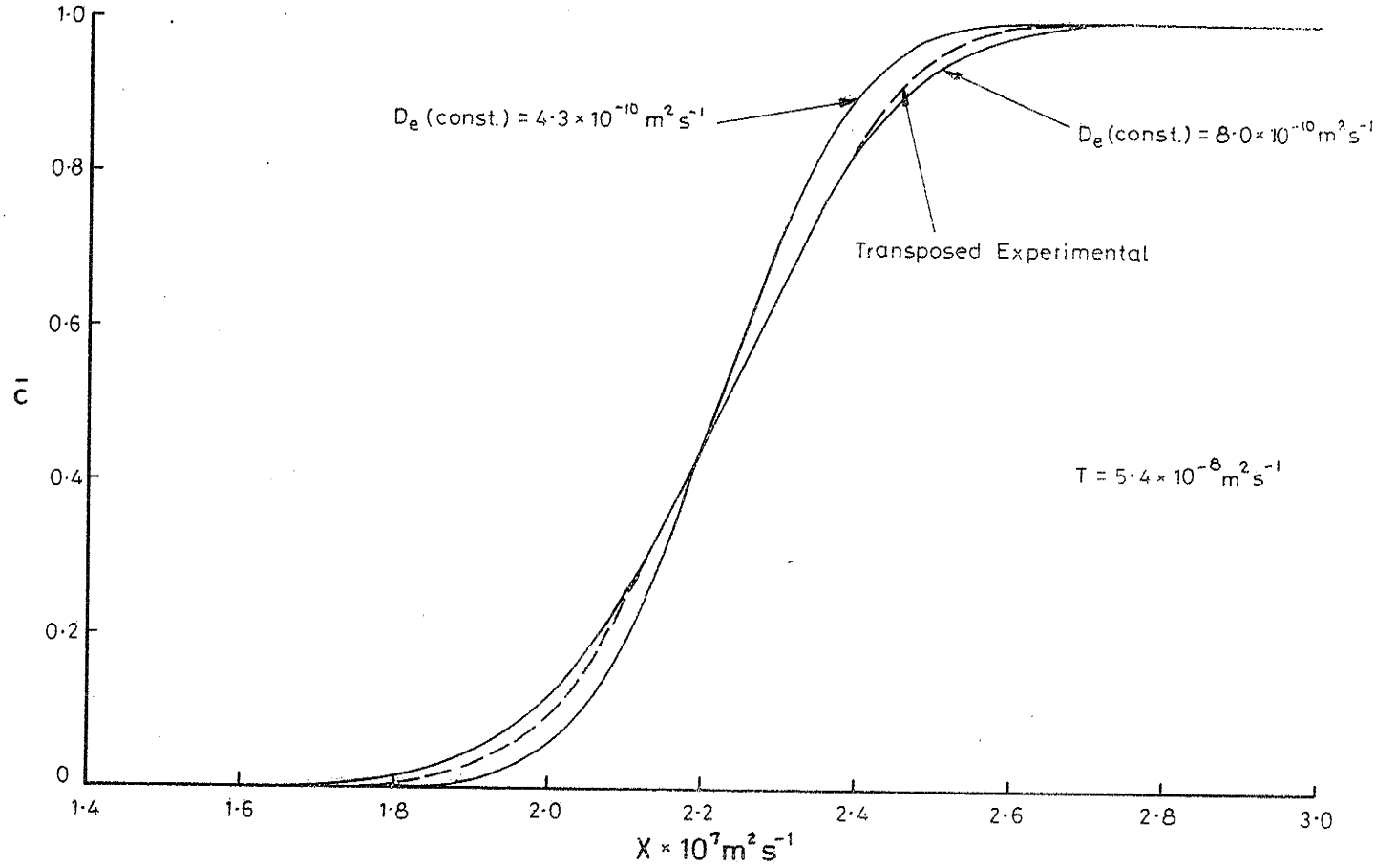

Fig 7.6 Normalized $\bar{c}(X)$ profiles for horizontal absorption in Bungendore fine sand under a constant flux boundary condition, for T = 5.4 x $10^{-8} m^2 s^{-1}$ (constant D_e)

Fig 7.6 Normalized $\bar{c}(X)$ profiles for horizontal absorption in Bungendore fine sand under a constant flux boundary condition, for T = 5.4 x $10^{-8} m^2 s^{-1}$ (constant D_e)

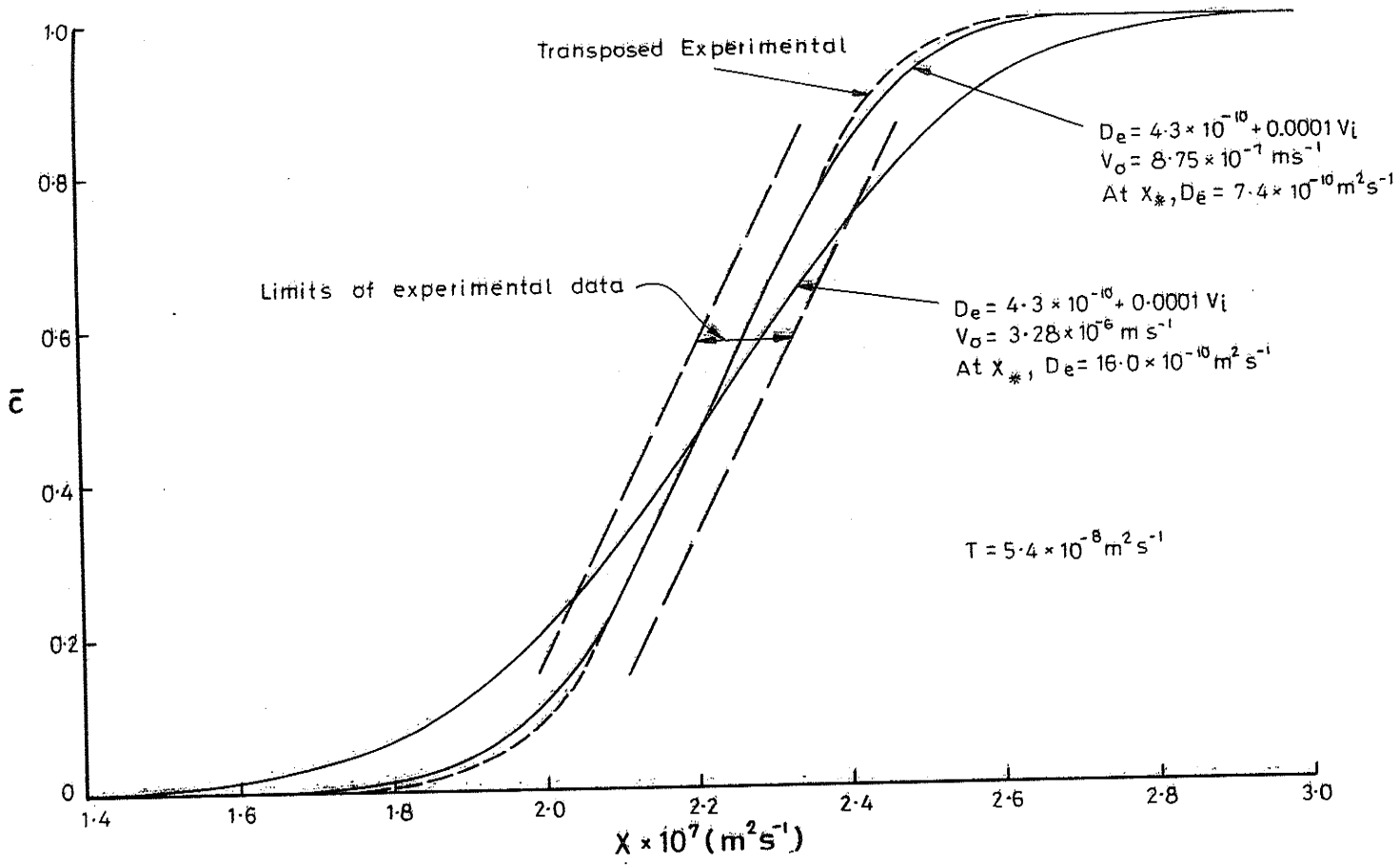

Fig 7.7 Normalized $\bar{c}(X)$ profiles for horizontal absorption in Bungendore fine sand under a constant flux boundary condition, for T = 5.4 x $10^{-8} m^2 s^{-1}$ (D_e velocity dependent)

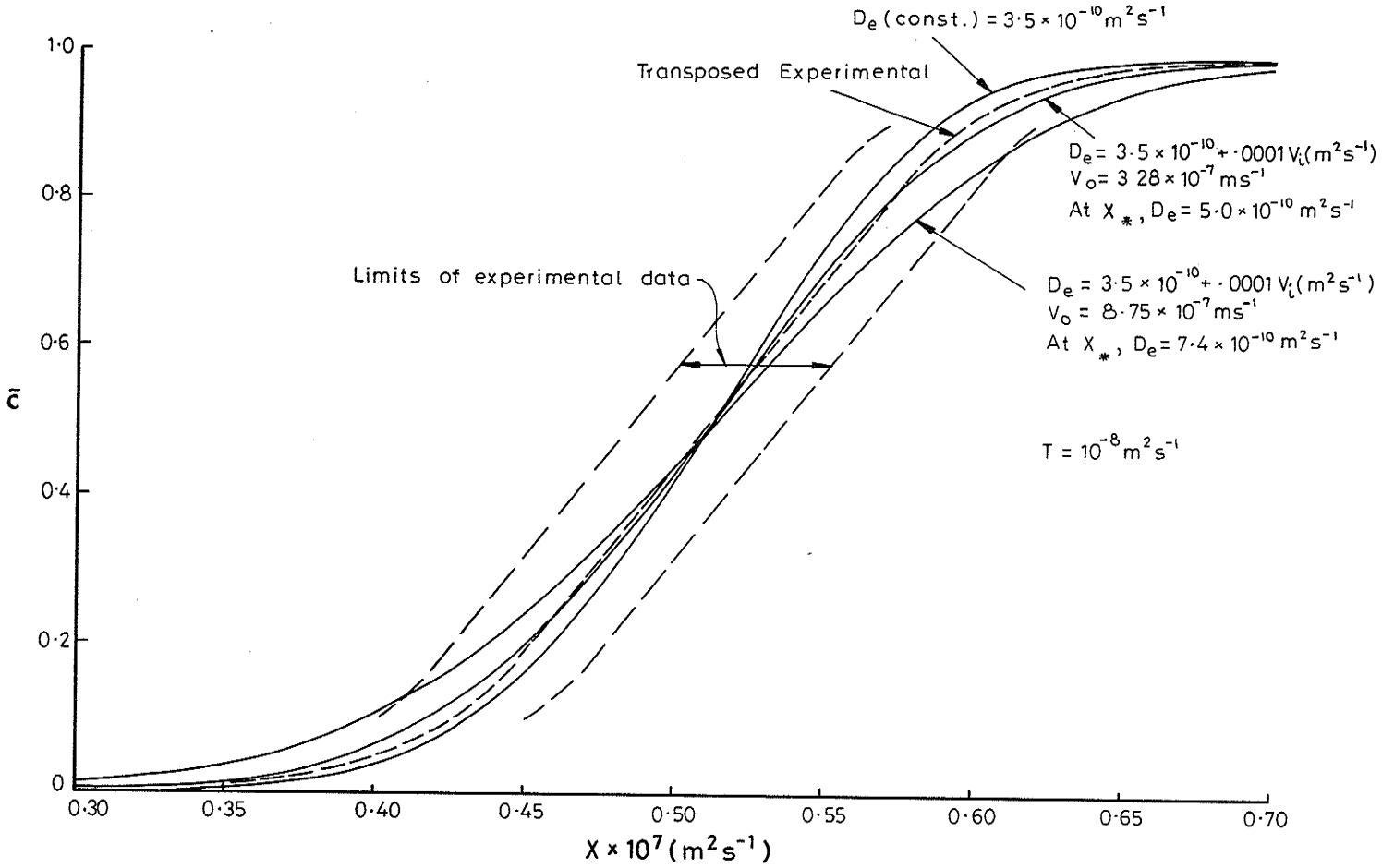

Fig 7.8 Normalized $\tilde{c}(X)$ profiles for horizontal absorption in Bungendore fine sand under a constant flux boundary condition, for $T = 10^{-8} m^2 s^{-1}$

profiles for the constant $\theta_* D_m$ value of $3.5 \times 10^{-10}\ m^2 s^{-1}$ and for the D_e values using the above v_o values. Also included is the mean curve through the experimental data transposed horizontally at $\bar{c} = 0.50$ from $0.50 \times 10^{-7}\ m^2 s^{-1}$ to $0.512 \times 10^{-7}\ m^2 s^{-1}$. As previously, the $\bar{c}(X)$ profiles calculated using the velocity dependent D_e values lie within the bandwidth of the scatter. The D_e values at X_* are respectively $7.4 \times 10^{-10}\ m^2 s^{-1}$ (ie $3.5 \times 10^{-10} + 3.9 \times 10^{-10}$) and $5.0 \times 10^{-10}\ m^2 s^{-1}$ (ie $3.5 \times 10^{-10} + 1.5 \times 10^{-10}$). Although, for this latter case, the mechanical dispersion component is very small it is apparent from Fig 7.8 that the use of a velocity dependent D_e with a β value of 0.0001 in no way gives results which are inconsistent with the experimental data.

For those cases where the mechanical dispersion is the dominant factor in the solute movement process Watson and Jones (1981*b*) have detailed an approximate analytical solution which agrees well with the numerical results.

7.4 Conclusion

The comparisons between the numerical predictions and experimental results in this and the previous chapter indicate the consistency of the numerical analysis in representing accurately hydrodynamic dispersion during absorption in Bungendore fine sand. In addition, it is apparent that the assumption of a constant D_e value equal to $\theta_* D_m$ underestimates the dispersion. However, the specification of a velocity dependent D_e with a β value of 0.0001m represents the experimental data satisfactorily with the $\bar{c}(X)$ profiles for the range of v_o values used lying within the limits of the scatter of the experimental data.

...Bungendore fine sand under a constant flux boundary condition, for T = $10^{-8} m^2 s^{-1}$

8 SOLUTE MOVEMENT DURING INFILTRATION AND REDISTRIBUTION

8.1 Introduction

The numerical model for non-reactive solute transport as presented in Chapter 3 has been subjected to a comprehensive testing program using experimental and quasi-analytical results for both constant concentration and constant flux absorption. This chapter extends the study to vertical flow systems involving both infiltration and redistribution processes. Since the solute model as presented utilizes only the flux and water content data from the soil water analysis in its solution, it can be applied without modification to the vertical flow conditions.

The physical validity of the soil water analysis under hysteretic conditions has already been discussed in section 2.4. Solute movement during infiltration and redistribution is now considered, and compared with experimental data provided by the C.S.I.R.O. Division of Environmental Mechanics.

8.2 Hysteresis Data for Bungendore Fine Sand

Comprehensive hysteresis data for the Bungendore fine sand sample used in the experimental program is not available. To enable comparisons to be made between the numerical results and a single infiltration-redistribution experimental sequence, the data of Talsma (1974) on Bungendore fine sand was used as the basis for developing a set of primary draining scanning curves for use with the interpolative hysteresis model. These are shown in Fig 8.1.

8.3 Solute Movement During Vertical Infiltration

A vertical column of Bungendore fine sand was set up with a uniform initial water content of approximately 0.10 m^3m^{-3} and a uniform initial concentration of KCℓ of 1000 meq/litre. A dilute KCℓ solution of concentration 100 meq/litre was supplied at the surface at a constant rate of $1.05 \times 10^{-5} ms^{-1}$ for 3600 s. Fig 8.2 shows the resultant experimental water content profile at the end of the infiltration period, and Fig 8.3 the normalized solute concentration profile. In both figures the continuous lines represent the results of the numerical analysis and the points denoted 'I' represent the experimental data.

Agreement between the numerical and experimental results is very good for both the water and solute profiles. Equally satisfactory correspondence was found for infiltration involving both a smaller constant surface flux of $5.25 \times 10^{-6} ms^{-1}$ and a constant concentration (surface ponding) boundary condition. The comparisons have not been included in this report.

8.4 Approximate Analytical Solution

An approximate analytical solution for a constant flux of water and a constant concentration of solute during vertical infiltration has been presented by Watson and Jones (1981*b*).

A parameter g_z is defined as

$$g_z = \theta z - \int_{\theta_n}^{\theta} z\,d\theta \qquad 8.1$$

with θ_{z_*} being the water content at z_* where $g_z = 0$. It then follows that

$$\frac{\partial \bar{c}}{\partial z_*} = \Omega_v \frac{\partial^2 \bar{c}}{\partial z^2} - \frac{\partial \bar{c}}{\partial z} \qquad 8.2$$

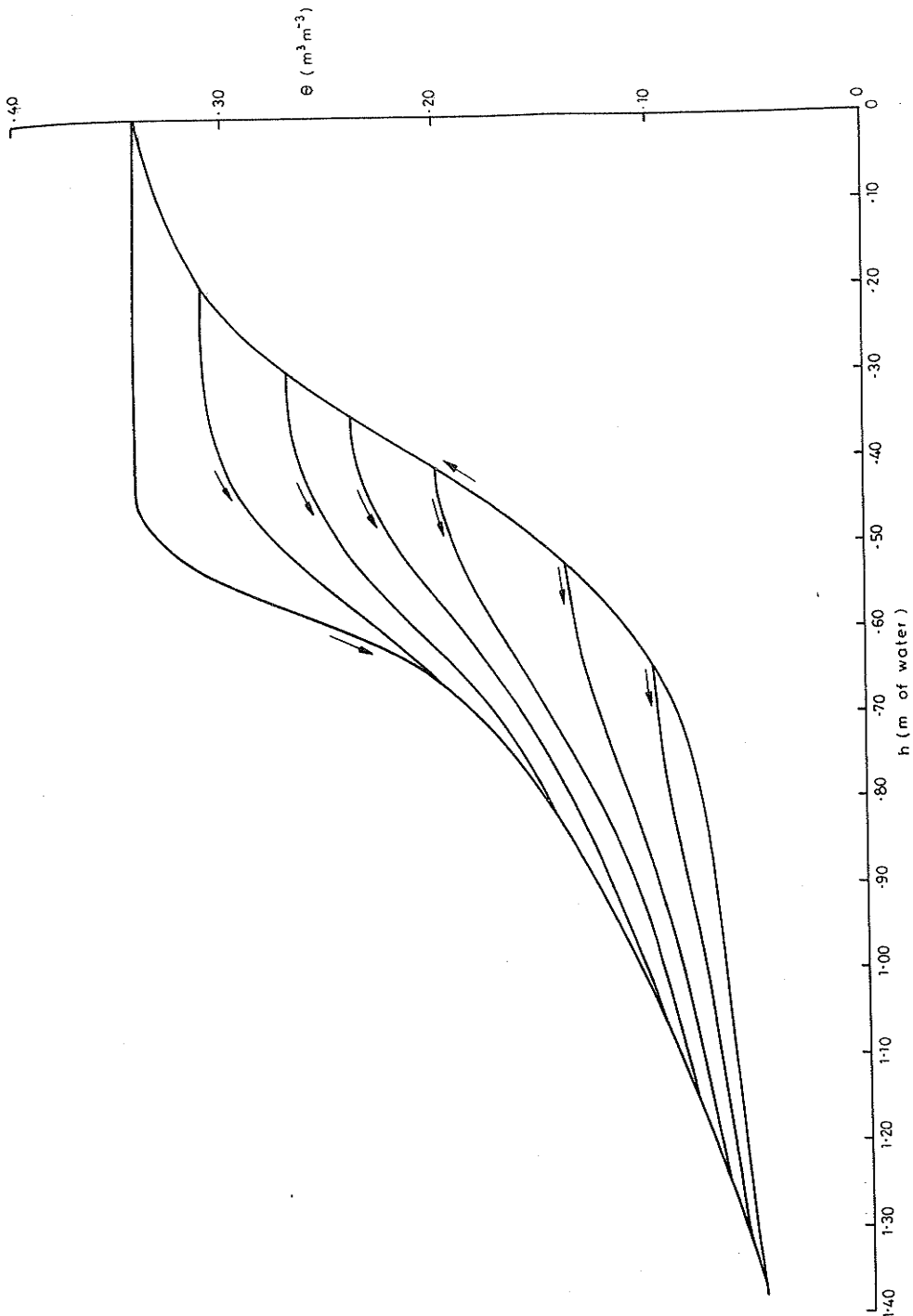

Fig 8.1 h(θ) relationship for Bungendore fine sand used in the redistribution studies

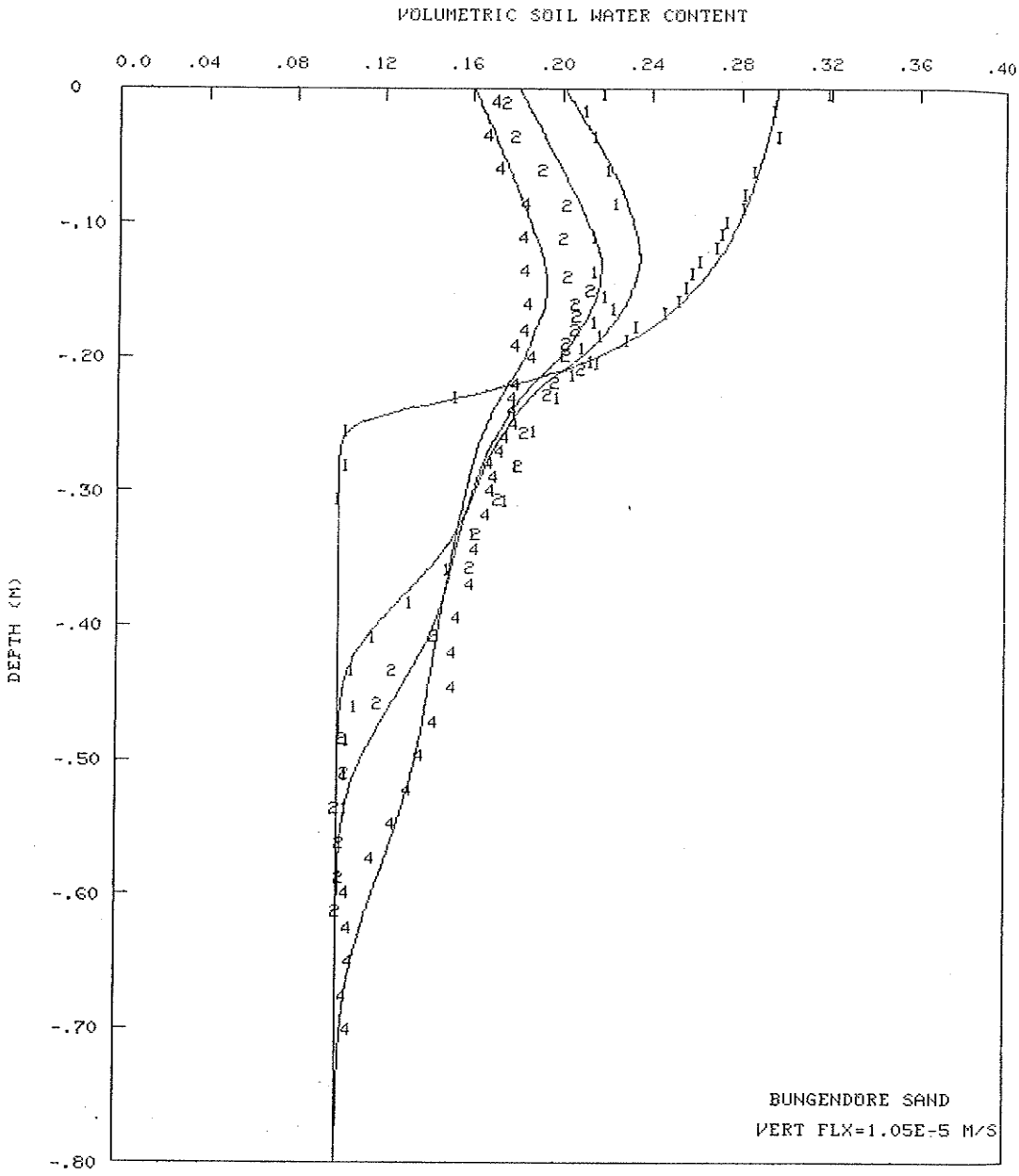

Fig 8.2 Experimental and numerical θ(z) profiles for constant flux vertical infiltration followed by redistribution in Bungendore fine sand (Symbols are defined in the text)

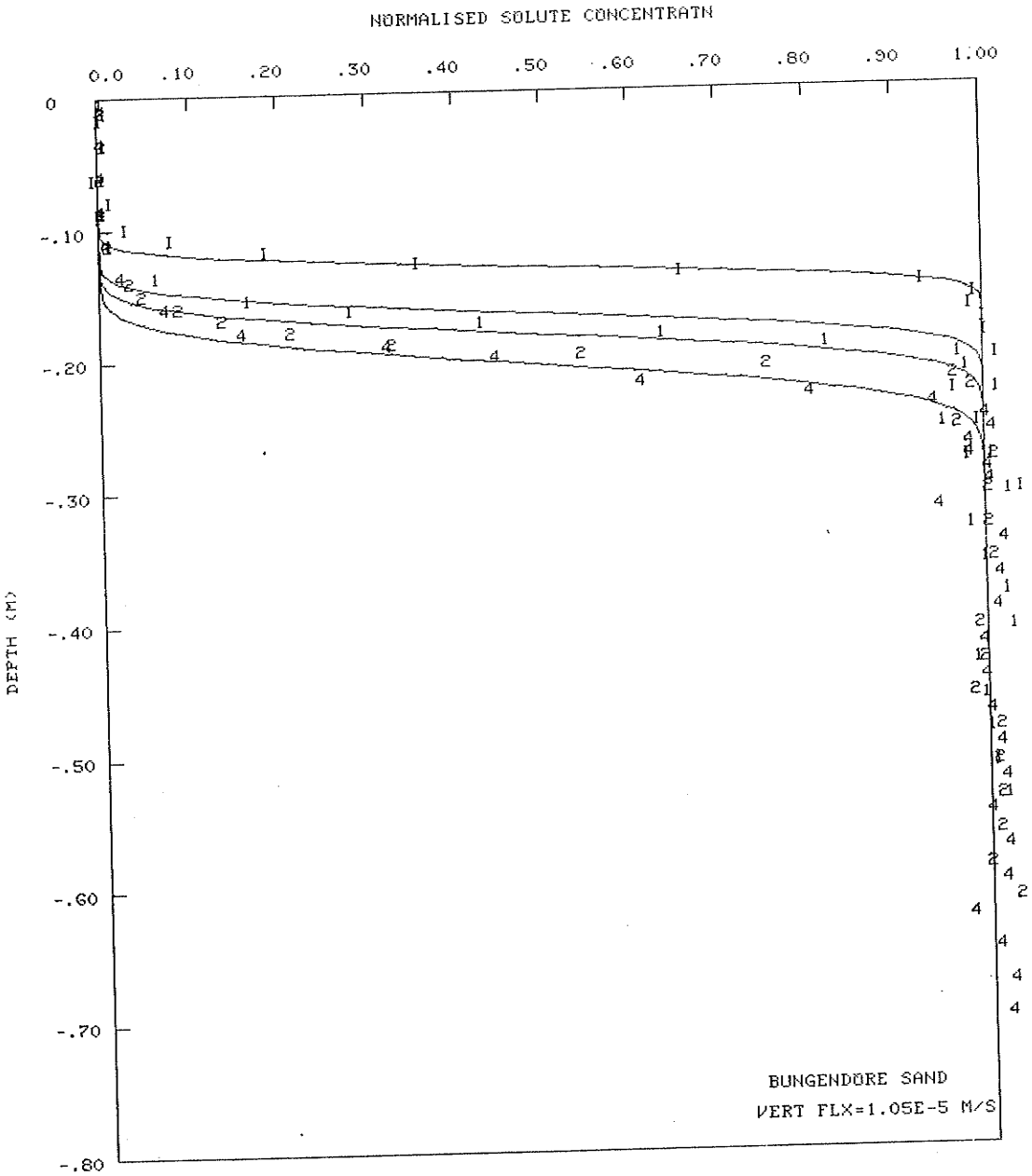

Fig 8.3 Experimental and numerical $\bar{c}(z)$ profiles for constant flux vertical infiltration followed by redistribution in Bungendore fine sand (Symbols are defined in the text)

subject to $\bar{c} = 1, \quad z > 0, \quad z_* = 0$

$\bar{c} = 0, \quad z = 0, \quad z_* > 0$ 8.3

where $\Omega_v = \beta/\theta_{z*}$

The solutions take the form

$$\bar{c} = 1 - \tfrac{1}{2}\text{erfc}\left[\frac{z - z_*}{2(\Omega_v z_*)^{\frac{1}{2}}}\right] \quad 8.4$$

and

$$\bar{c} = 1 - \tfrac{1}{2}\text{erfc}\left[\frac{z - z_*}{2(D_p t + \Omega_v z_*)^{\frac{1}{2}}}\right] \quad 8.5$$

Equation 8.5 is tested using the data from the previous section, namely:

$v_o = 1.05 \times 10^{-5}\,\text{ms}^{-1}$ $\quad D_p = 5.0 \times 10^{-10}\,\text{m}^2\text{s}^{-1}$

$t = 3600\,\text{s}$ $\quad \beta = 0.0001\,\text{m}$

From the numerical simulation z_* and θ_{z*} were found to be 0.133 m and 0.267 m^3m^{-3}. The continuous line in Fig 8.4 represents the numerical solution at t = 3600 s and the circled dots are selected values using equation 8.5. The agreement is very satisfactory.

8.5 Solute Movement During Vertical Redistribution

The experiment described earlier in section 8.3 was extended to study the disposition of solute during the redistribution phase. The experimentally determined water content and solute concentration profiles for three redistribution times are shown in Fig 8.2 and Fig 8.3. The experimental data is represented by numerals, with '1' representing 6000 s, '2' representing 12 000 s and '4' representing 24 000 s of redistribution respectively.

The hysteresis data of Fig 8.1 appears to describe the characteristics of the Bungendore fine sand satisfactorily; in particular the $\theta(z)$ comparisons of Fig 8.2 are reasonable. Unfortunately difficulties were experienced during this part of the experimental program. The supply of sand required replenishing and the new supply seems to have had slightly different soil water characteristics. This change occurred with the sand used in the 6000 s and 24 000 s redistribution experiments, and would account for the greater discrepancies between the numerical results and experimental data at these times. The general trend is however consistent. It should be noted that the numerical program only uses the soil characteristics determined from the original sand sample. D_p was taken to be $5 \times 10^{-10}\,\text{m}^2\text{s}^{-1}$ and $\beta = 0.0001$m throughout.

The corresponding solute profiles during redistribution are also shown in Fig 8.3. Although the paucity of experimental data does not allow any definitive statements to be made concerning solute redistribution, there is general consistency. The comparisons for redistribution times of 6000 s and 12 000 s are more variable that at 24 000 s; however, the discrepancies are

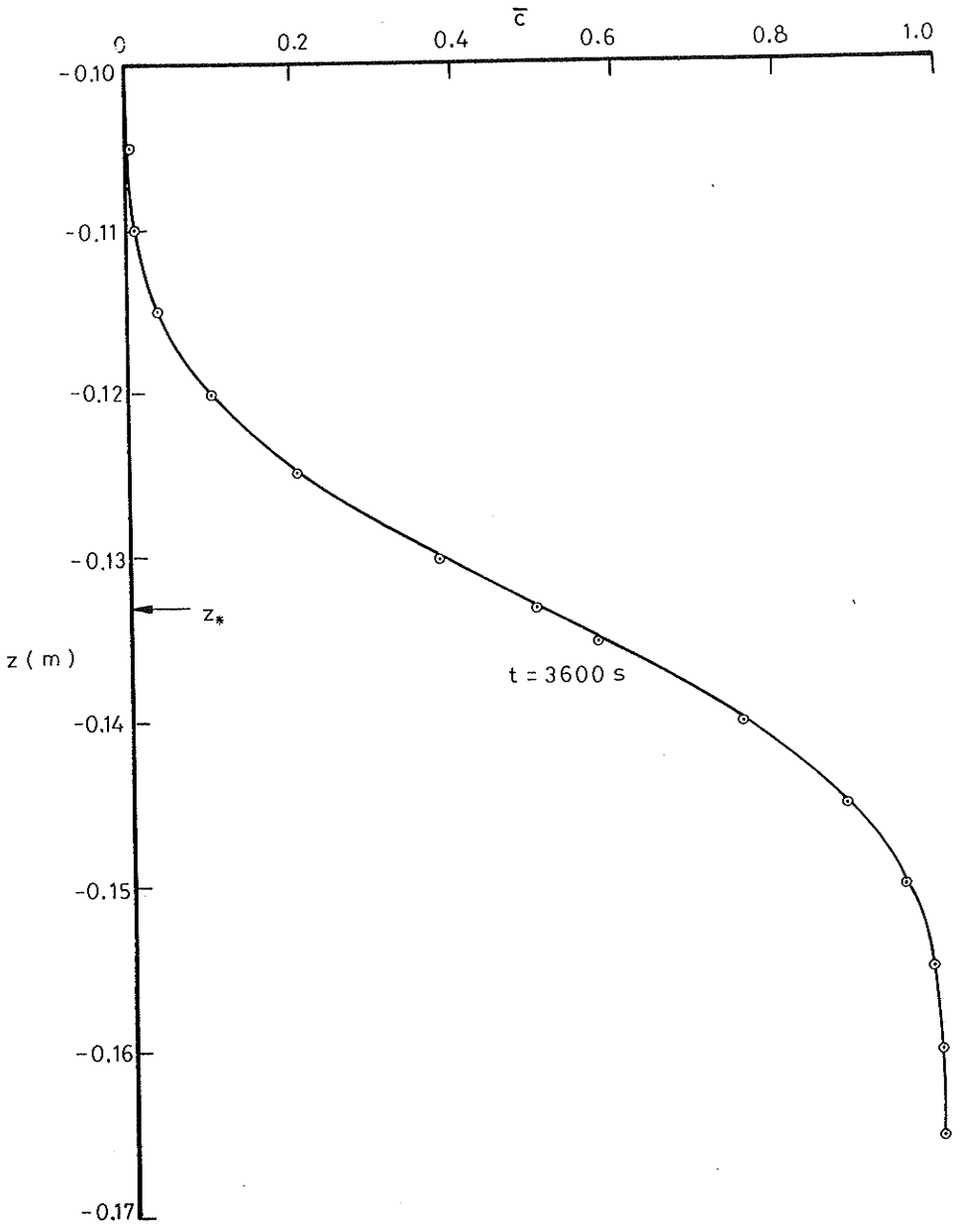

Fig 8.4 Comparison of numerical results (continuous line) and analytical solution (circled dots) for solute movement during constant flux vertical infiltration in Bungendore fine sand at t = 3600 s (D_p = 5 x $10^{-10}m^2s^{-1}$, β = 0.0001 m)

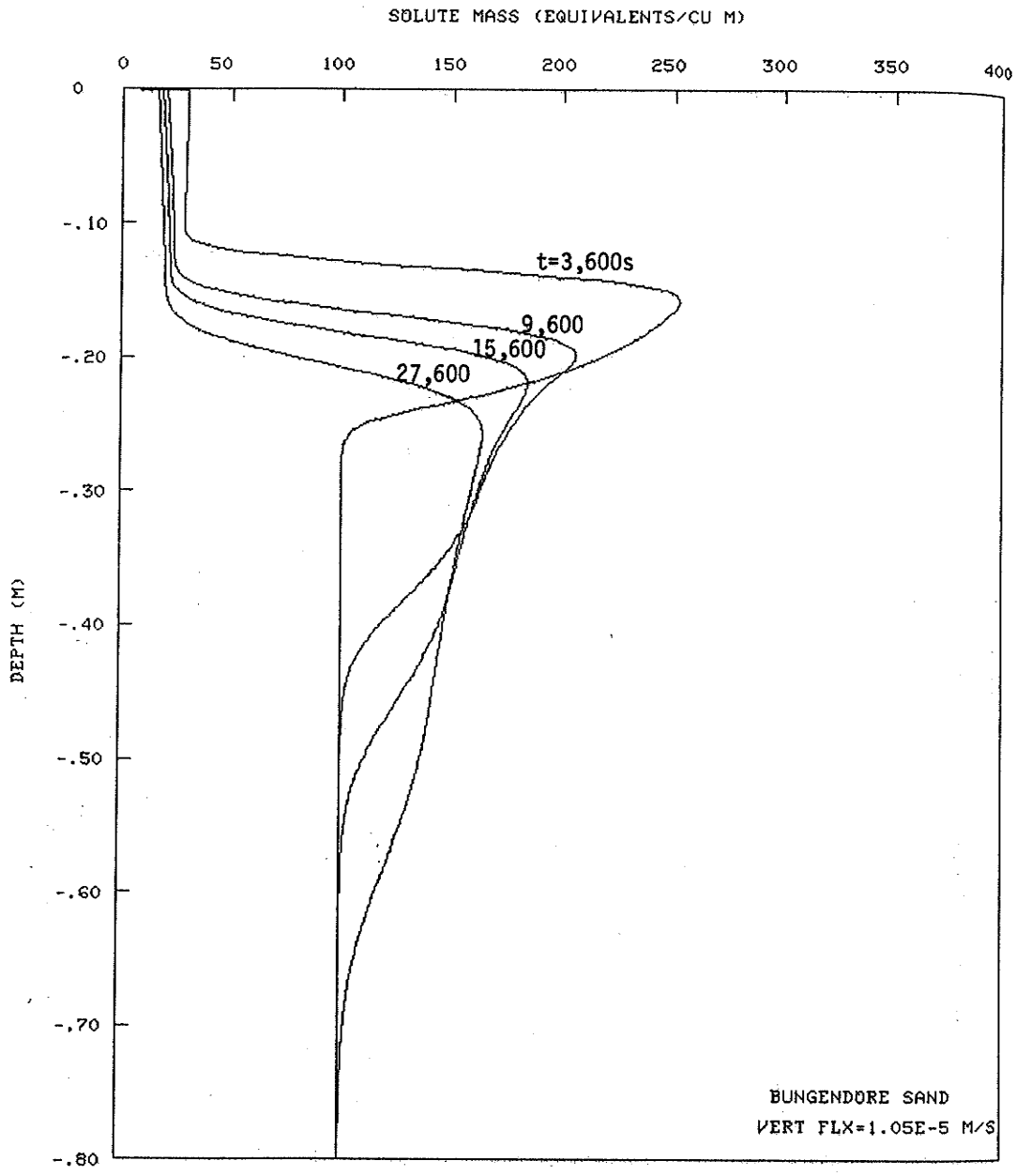

Fig 8.5 Numerical solute mass profiles for constant flux vertical infiltration followed by redistribution in Bungendore fine sand

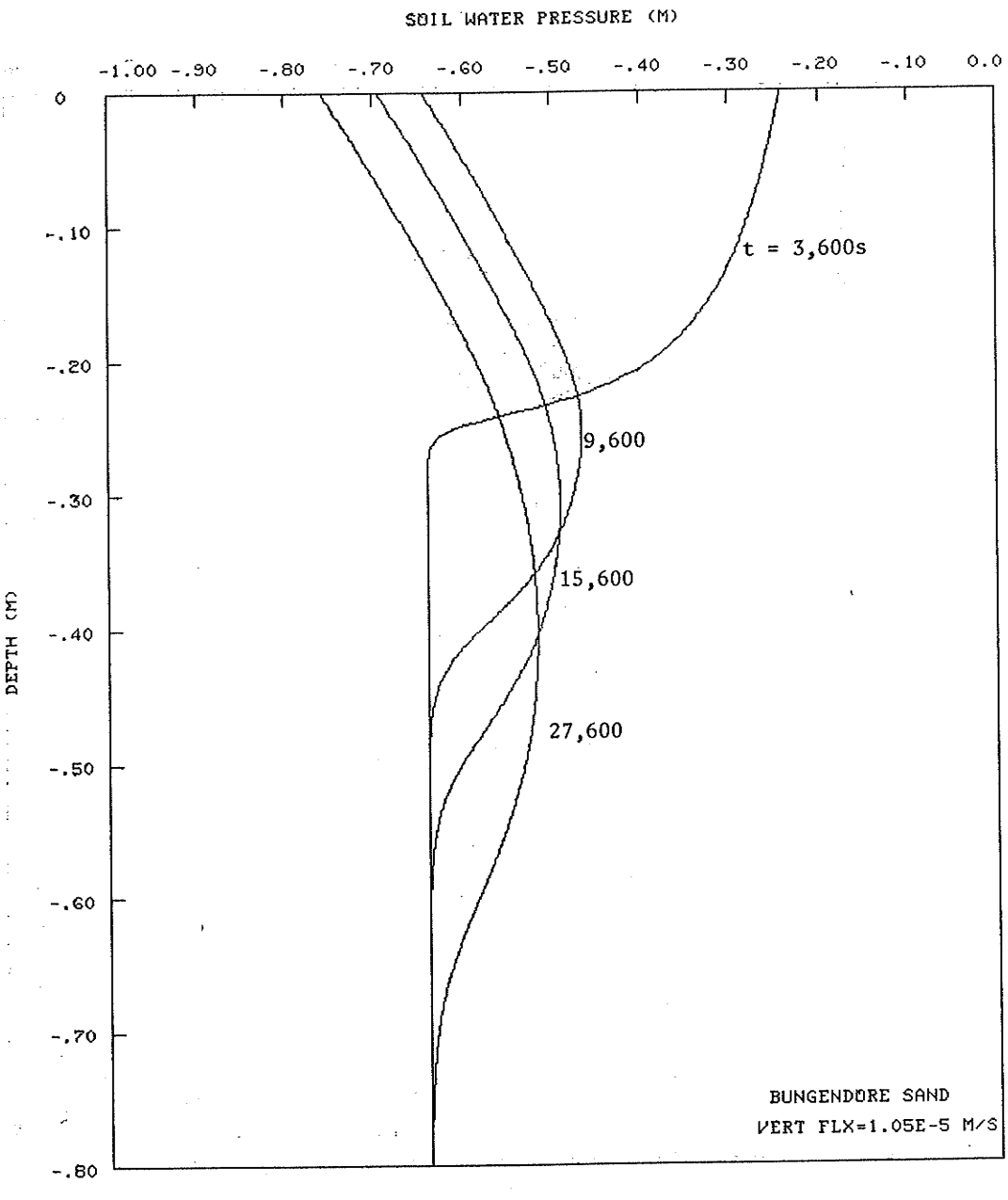

Fig 8.6 Numerical h(z) profiles for constant flux vertical infiltration followed by redistribution in Bungendore fine sand

consistent with the variations in the water content profiles at these intermediate times, and doubtless reflect the variation in soil properties discussed above.

The numerical model has been programmed to provide additional data on the transport processes involved. Figure 8.5 gives the solute mass profiles for infiltration-redistribution in Bungendore fine sand corresponding to the end of infiltration, and to 6000 s, 12 000 s and 24 000 s redistribution. This figure is most instructive in indicating salt disposition within the profile. Figure 8.6 provides the h(z) relationships and is included for completeness.

8.6 Solute Movement During Horizontal Redistribution

The experiments described in sections 8.3 and 8.5 were repeated using a horizontal column of Bungendore fine sand. The results are summarized in Fig 8.7 to Fig 8.10.

The comparisons are presented for redistribution times of 12 000 s and 24 000 s using the notation described previously. Figure 8.7 shows marked differences between the numerical and experimental water content profiles. The reason for this is not apparent, and suggests the need for additional experimentation.

The numerical and experimental solute concentration profiles for this case are given in Fig 8.8. The comparison is reasonable, with the discrepancies being consistent with those of the water content profiles of Fig 8.7 as discussed above.

8.7 Discussion

The problems experienced in obtaining the experimental data for the redistribution studies and the lack of a well-defined experimental base for determining the set of primary draining scanning curves (Fig 8.1) used in the predictive analyses have produced comparisons which are less definitive than those detailed in earlier chapters. In particular, it has not been possible to analyse accurately the significance of the velocity dependence of the dispersion coefficient during the redistribution phase. However, the overall consistency between the experimental and numerical results is good, indicating that the numerical approach may be used with confidence in redistribution studies.

The data presented in this chapter also highlights some characteristic differences between horizontal and vertical flow systems. At the end of the vertical infiltration period, Fig 8.2 indicates that the infiltrated water had penetrated 0.275m into the sand profile. The corresponding surface water content was $0.288\ m^3m^{-3}$. During horizontal absorption Fig 8.7 shows that, for the same volume of water inflow, the penetration was 0.25 m, with a correspondingly higher water content of $0.319\ m^3m^{-3}$ at the absorbing face. These differences reflect the influence of the gravity potential in the vertical system. During redistribution the differences are more pronounced and result in significantly different water content distributions. The vertical profile drains more rapidly in the surface region whereas for the horizontal system the water content decreases gradually over most of the wetted region, in a manner similar to that obtained with finer textured materials.

Figures 8.3 and 8.8 show the solute concentration profiles for the vertical and horizontal systems. The differences become more evident on comparing the corresponding solute mass profiles in Figs 8.5 and 8.9. The differences reflect the effect of the larger pore water velocities present in the vertical system in two ways. Firstly, the larger velocities result in greater convective transport, particularly during redistribution. Secondly, the dispersive

solute transport is increased, due to the velocity dependence of the mechanical dispersion component of the hydrodynamic dispersion coefficient.

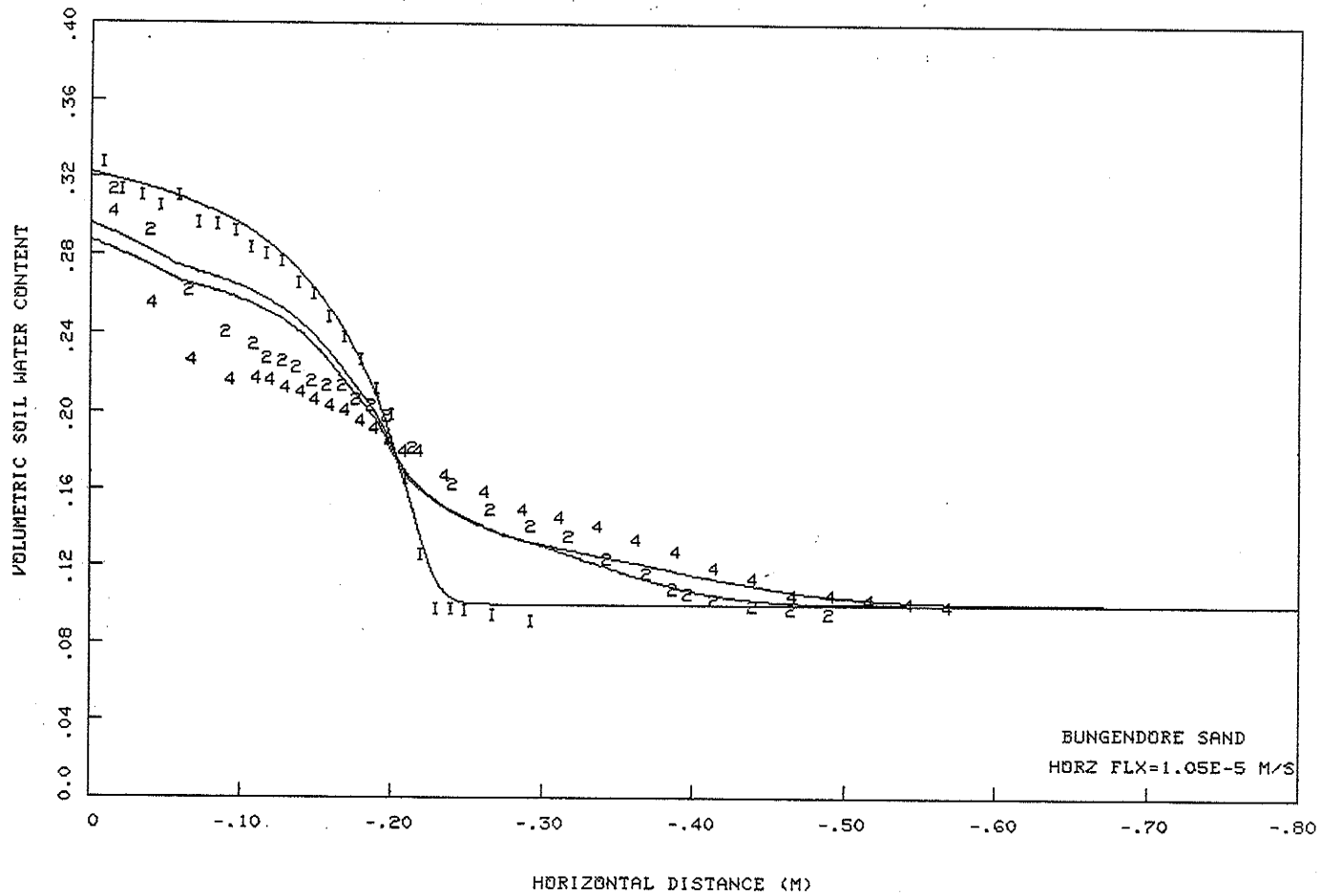

Fig 8.7 Experimental and numerical θ(x) profiles for constant flux horizontal absorption followed by redistribution in Bungendore fine sand (Symbols are defined in the text)

Horizontal absorption followed by redistribution in
Bungendore fine sand (Symbols are defined in the text)

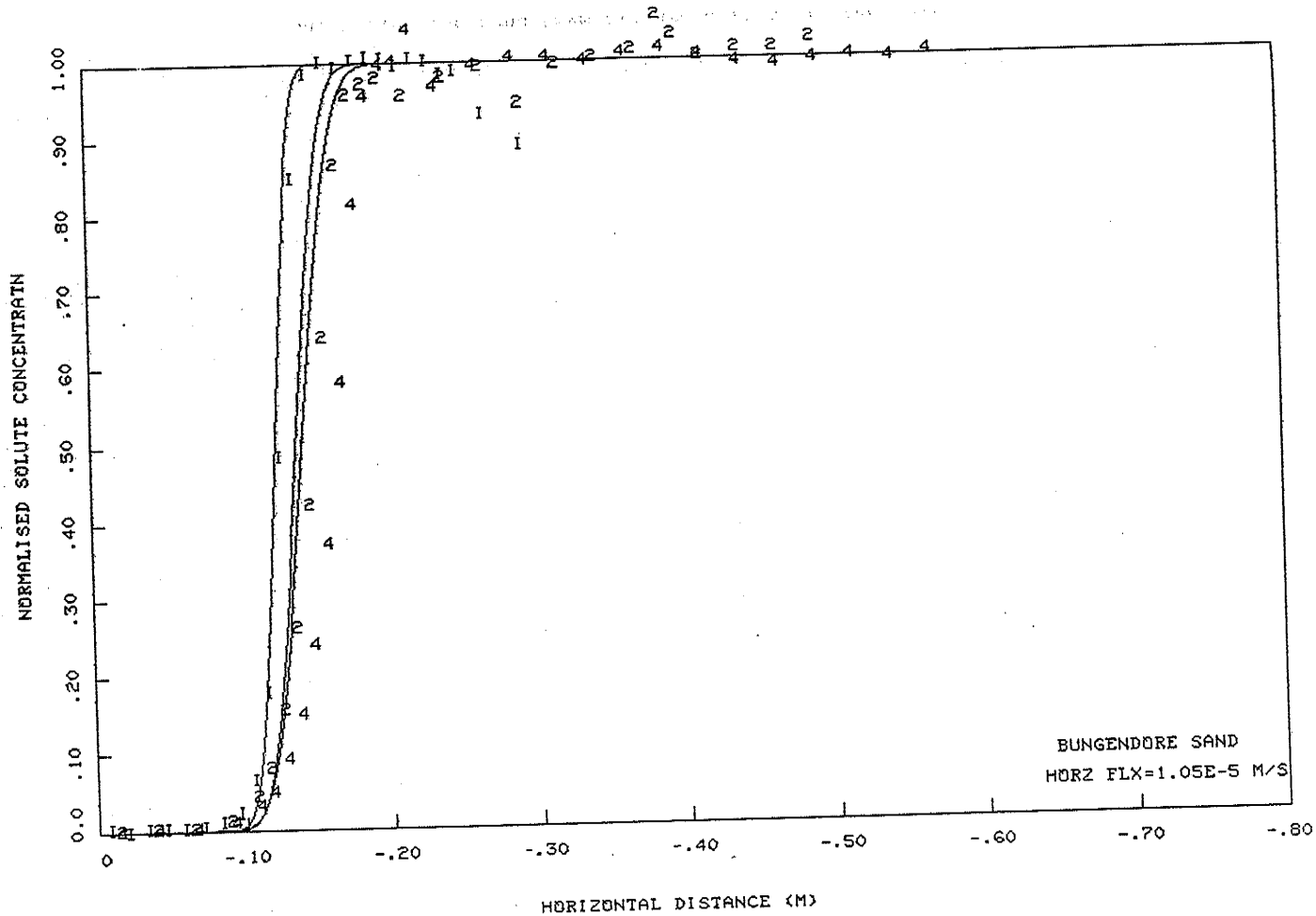

Fig 8.8 Experimental and numerical $\bar{c}(x)$ profiles for constant flux horizontal absorption followed by redistribution in Bungendore fine sand (Symbols are defined in the text)

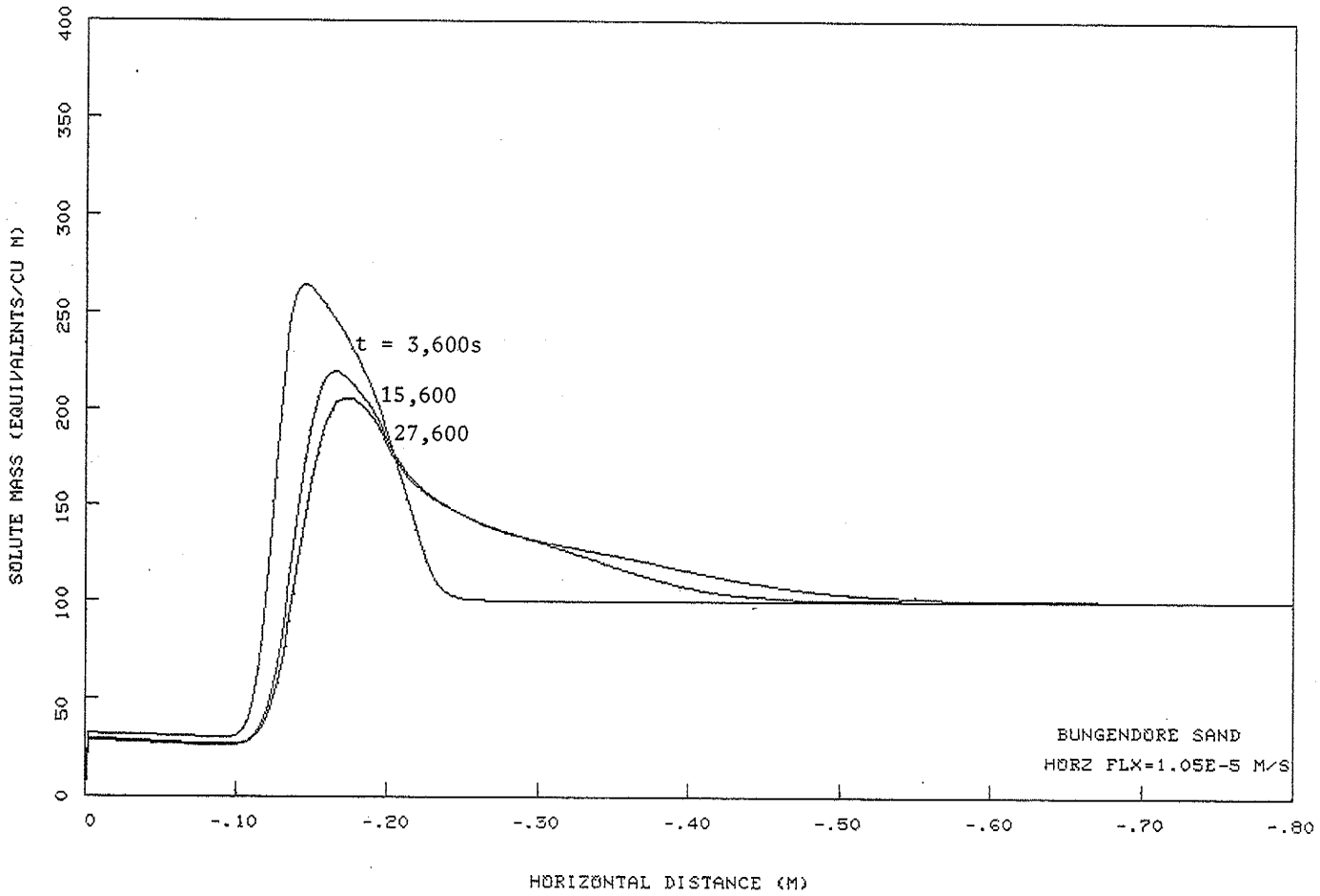

Fig 8.9 Numerical solute mass profiles for constant flux horizontal absorption followed by redistribution in Bungendore fine sand

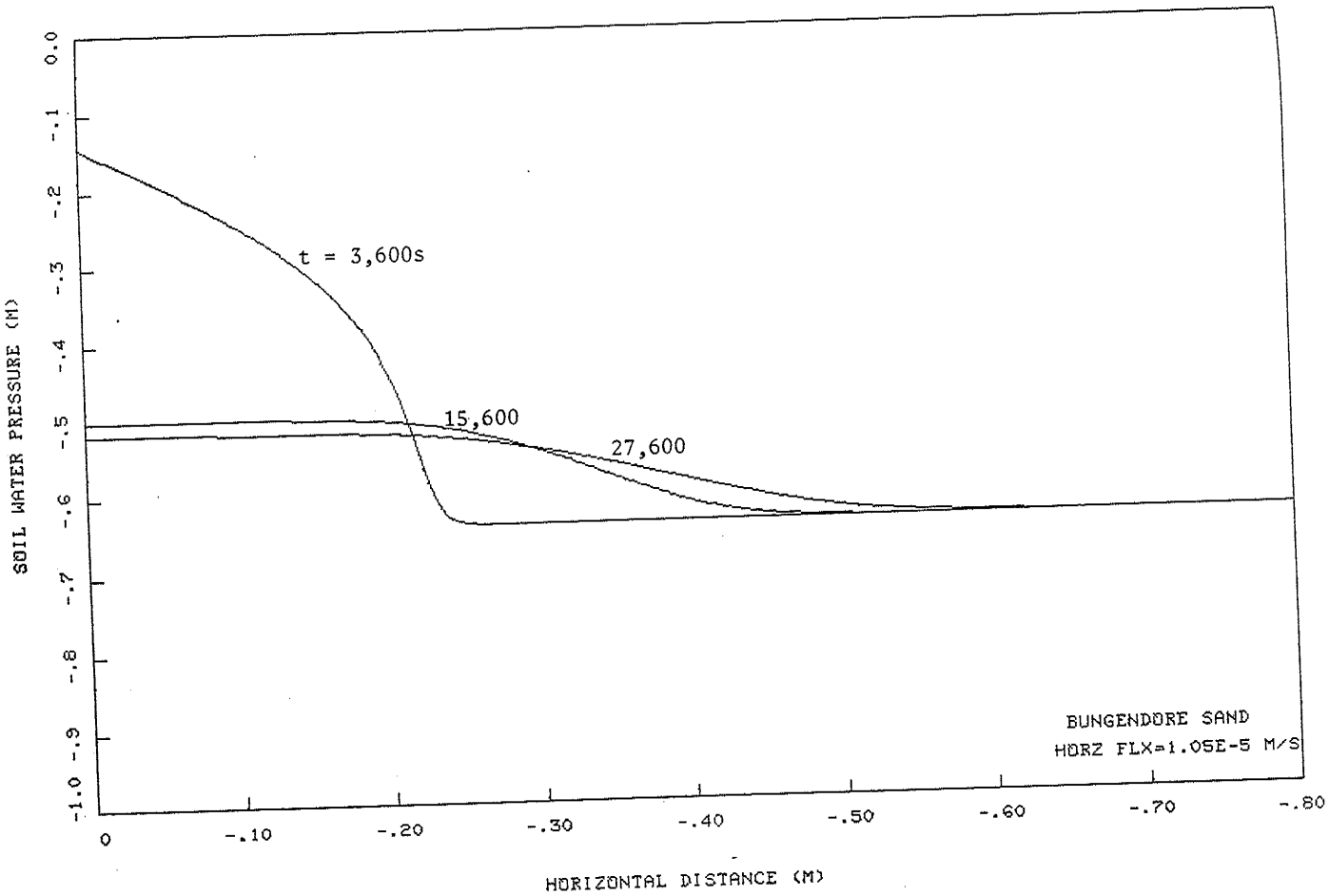

Fig 8.10 Numerical h(x) profiles for constant flux horizontal absorption followed by redistribution in Bungendore fine sand

9 SOLUTE MOVEMENT DURING INTERMITTENT INFILTRATION AND REDISTRIBUTION

9.1 Introduction

One of the principal aims of this project has been the development of a numerical model capable of simulating solute movement under an intermittent surface flux regime. On the basis of the results of the last chapter it is evident that the explicit finite difference approach can model such a system satisfactorily. As the final stage of this work, the model is used to study the disposition of solute within a profile of sandy loam subjected to a series of infiltration-redistribution sequences.

9.2 Results and Discussion

The soil material used in this chapter is Rubicon sandy loam, the characteristics of which were described by Topp (1969). These are presented in Fig 9.1 and Fig 9.2. The saturated hydraulic conductivity of the material is 5×10^{-6} ms^{-1} and its saturated water content is 0.38 m^{3}m^{-3}. A vertical 0.80 m profile of the sandy loam is used in the analysis, with a uniform initial water content of 0.164 m^{3}m^{-3} containing a uniform concentration of KCℓ equivalent to 1000 meq/litre. The dispersion characteristics of Rubicon sandy loam are not available. A search of published experimental data indicates that the mechanical dispersion parameter would be of the order 10^{-3}m. The molecular diffusion coefficient D_h was chosen to be 6×10^{-10} m^{2}s^{-1}. A grid spacing of 2 mm is required to satisfy the R_c stability constraint. A leaching regime applies, with a 0.1 N KCℓ solution (100 meq/litre) applied under constant concentration conditions according to the time sequence of Table 9.1.

Table 9.1 Time Sequence for Infiltration & Redistribution Events

Cycle	Total Elapsed Simulation Time	Event Time	
		Infiltration	Redistribution
1	900 s	900 s	
	4500 s		3600 s
	29700 s		28800 s
2	30600 s	900 s	
	34200 s		3600 s
	59400 s		28800 s
3	60300 s	900 s	
	63900 s		3600 s
	89100 s		28800 s

Although over 2200 water timesteps were used in the simulation, corresponding to some 2700 solute timesteps, profiles for nine elapsed times have been chosen to illustrate the effects of intermittency of water application on the distribution of water and solute in the soil profile. These times are given in Table 9.1 and relate to the end of each infiltration period (900 s duration) and two profiles during the redistribution phase, namely at 3600 s and 28 800 s after the start of the event.

Figure 9.3 gives the $\theta(z)$ profiles and shows that the wet front reached a depth of 0.15 m at the end of the first infiltration period. During the first 3600 s redistribution the front had moved to 0.26 m, and after 28 800 s (corresponding to a total simulation time of 29 700 s) the front had reached

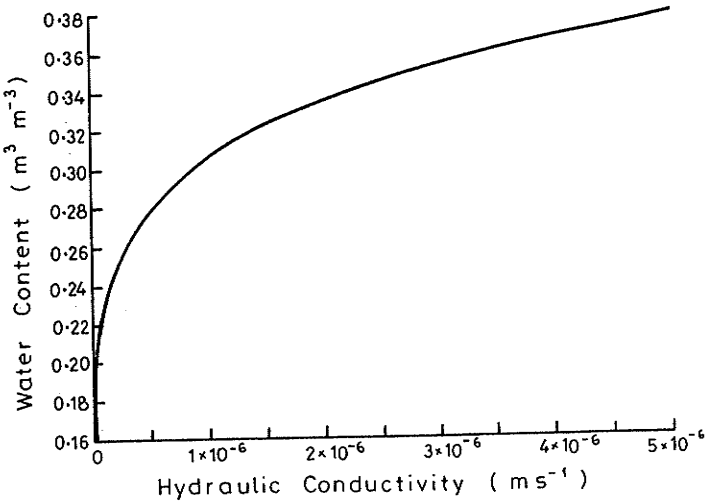

Fig 9.1 Water content vs hydraulic conductivity relationship for Rubicon sandy loam

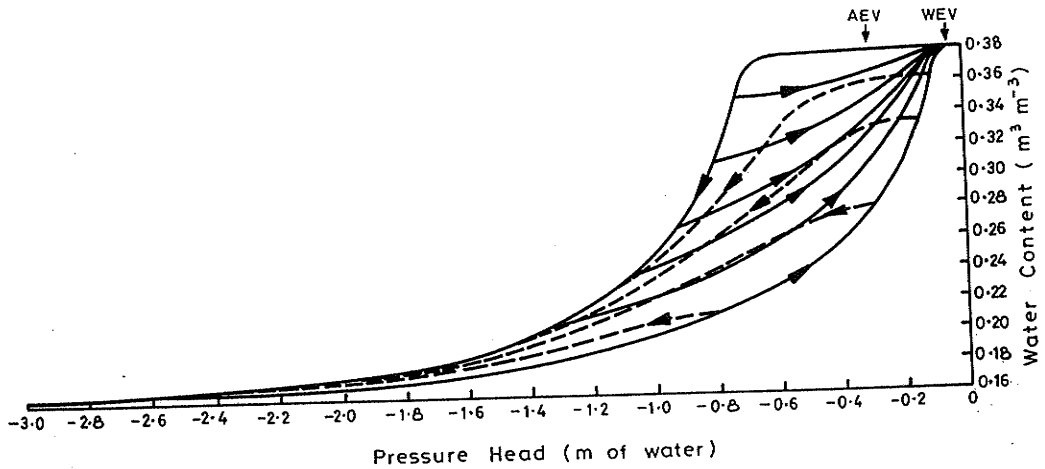

Fig 9.2 Hysteretic water content vs pressure head relationships for Rubicon sandy loam

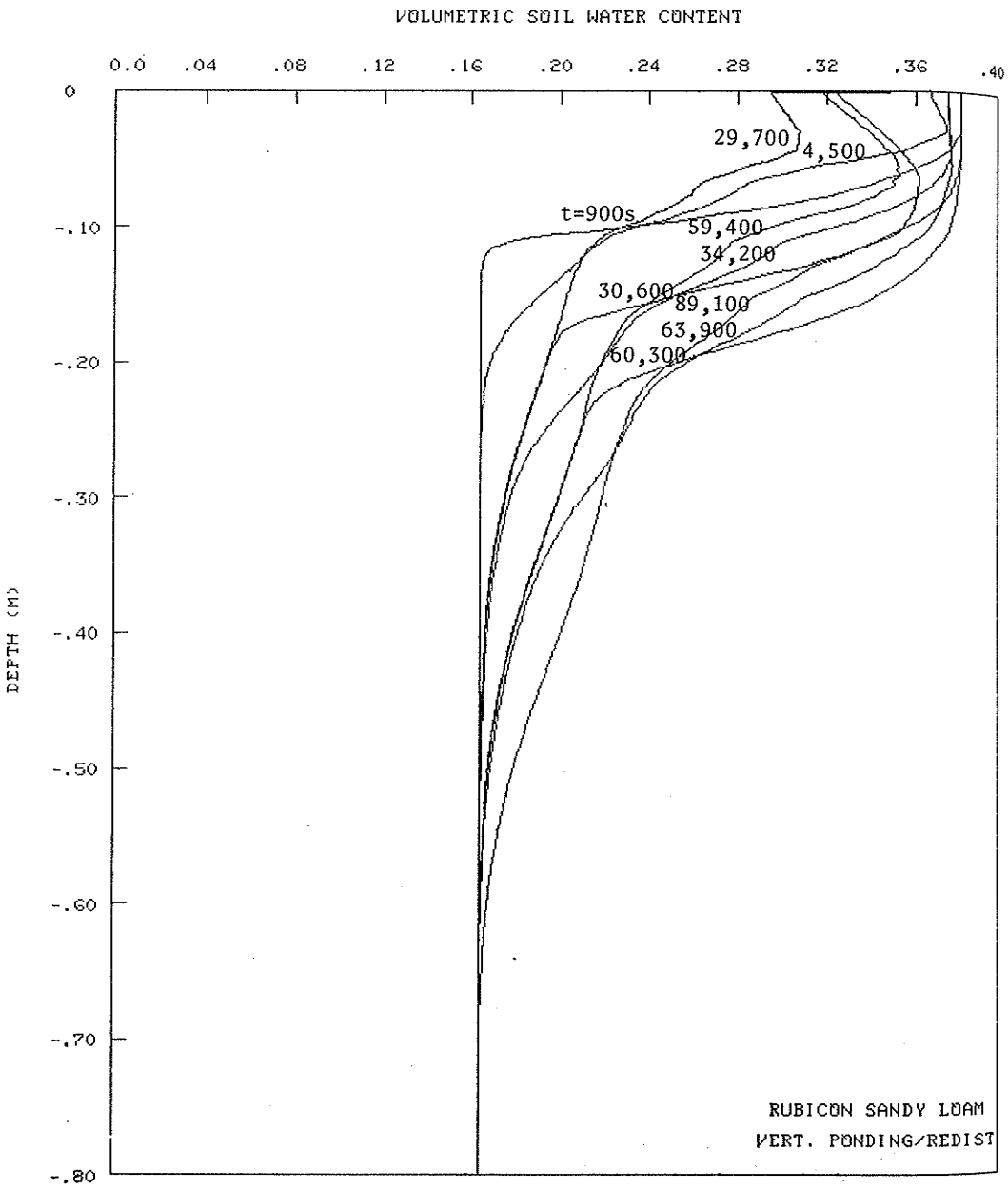

Fig 9.3 θ(z) profiles for three cycles of constant concentration vertical infiltration followed by redistribution in Rubicon sandy loam (hysteresis effects included)

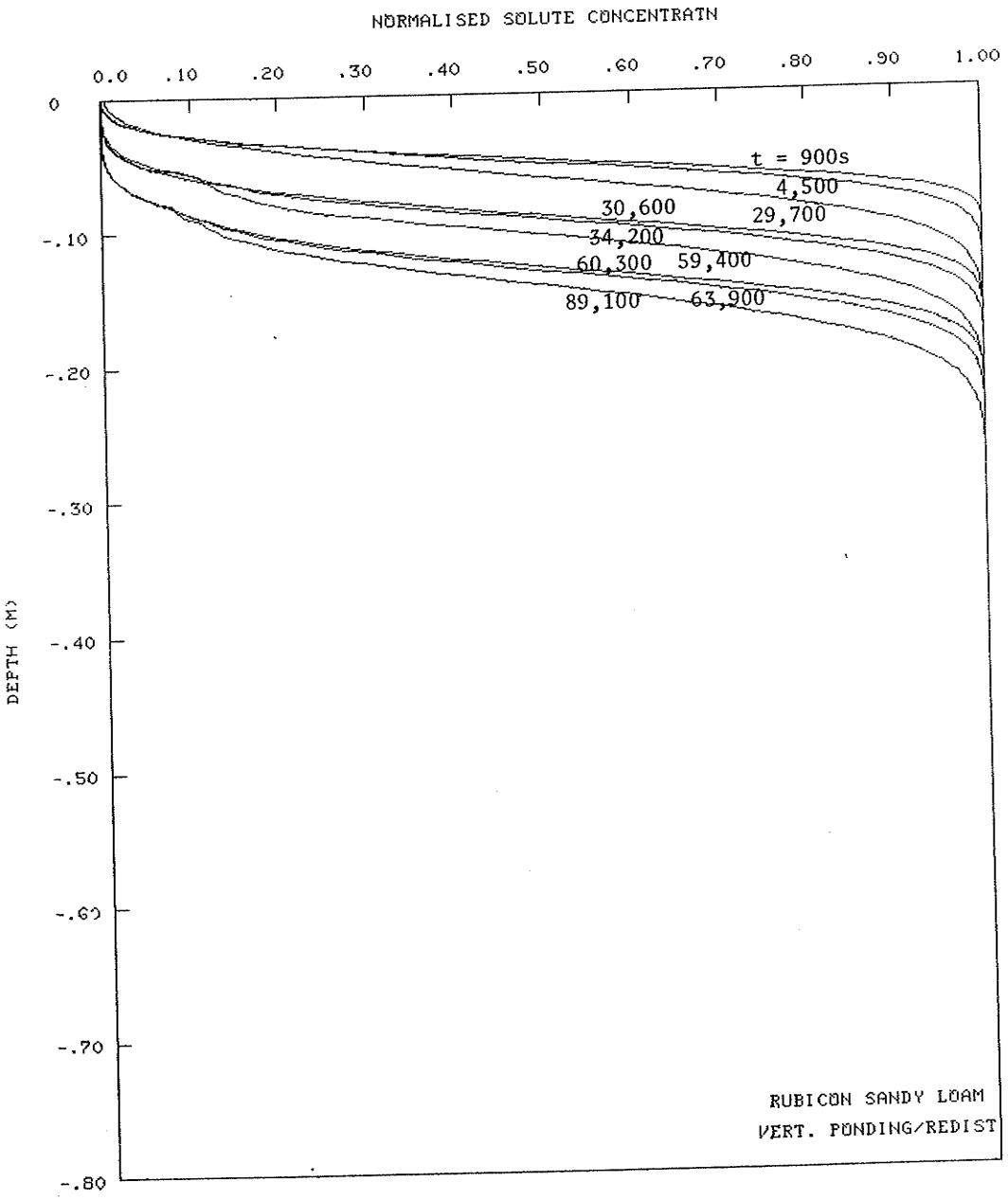

Fig 9.4 $\bar{c}(z)$ profiles for three cycles of constant concentration vertical infiltration followed by redistribution in Rubicon sandy loam (hysteresis effects included)

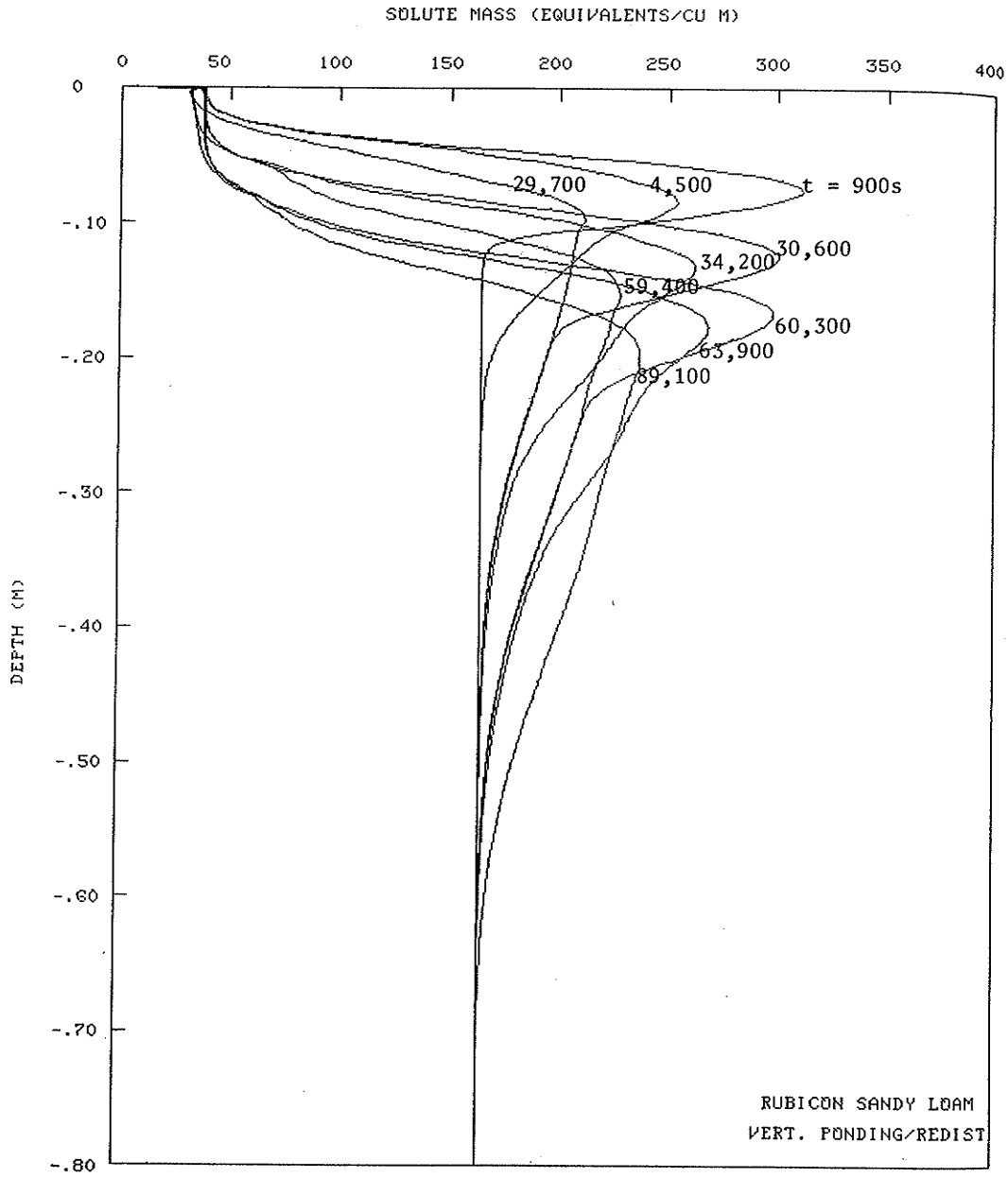

Fig 9.5 Solute mass profiles for three cycles of constant concentration vertical infiltration followed by redistribution in Rubicon sandy loam (hysteresis effects included)

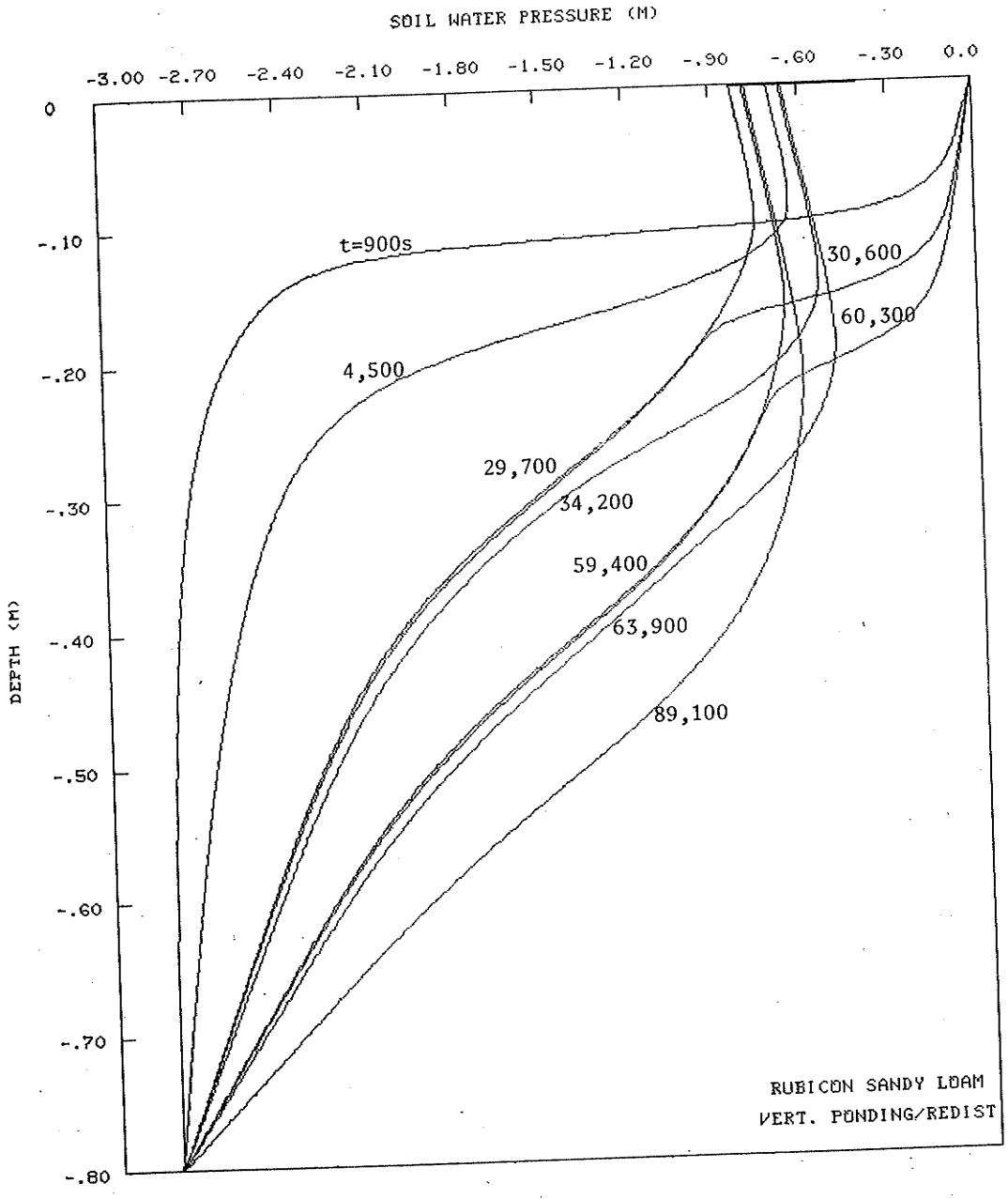

Fig 9.6 h(z) profiles for three cycles of constant concentration vertical infiltration followed by redistribution in Rubicon sandy loam (hysteresis effects included)

a depth of 0.56 m. During the second cycle the front moved more slowly, reaching 0.59 m after 3600 s and 0.65 m after 28 800 s of the second redistribution event. At time 89 100 s, the end of the third cycle, the wet front had reached a depth of 0.70 m.

Figure 9.4 contains the normalized solute concentration profiles at the same times. It is clear from this figure that the changes in the $\bar{c}(z)$ profiles during redistribution are small in comparison with the changes that take place during infiltration. The gradual 'steepening' of the profiles, more pronounced during the latter part of the redistribution sequences, is the effect of the hydrodynamic dispersion component of the mass transport equation. As the solution fluxes and hence the convective transport decreases, dispersion becomes increasingly significant. Although Fig 9.4 represents the output from the solution of the solute transport equation, it does not readily show the solute mass distribution. This can be seen in Fig 9.5.

At the end of the first infiltration period, Fig 9.3 shows that the KCℓ has been distributed in a 'bell' shape with a maximum of 311 meq/m^3 at a depth of 0.076 m. During the first redistribution period the mass peak is reduced to 212 meq/m^3 at a depth of 0.082 m. The distribution is now distinctly skewed, a result of increasing dispersion in the lower flux regions. Subsequent infiltration and redistribution sequences follow a similar trend, with bulk convective movement dominating during infiltration, and dispersion during redistribution. As the salt moves deeper into the soil profile the influence of the infiltration period is less pronounced, with increasingly smaller mass peaks and greater dispersion.

Figure 9.6 gives the h(z) profiles and completes the range of output from the program. These are the direct results from the solution of the water flow equation of Chapter 2. The maintenance of a constant soil water pressure head at the boundary z = -0.80 m results in pressure head changes above the boundary, and is thus not strictly modelling a semi-infinite column. However, from Fig 9.1 it is clear that no water content changes occur in the lower 0.10 m of the profile. This is a consequence of the shape of the $h(\theta)$ curve in the region of interest.

9.3 Significance of Hysteresis on Solute Movement

The numerical analysis presented in the previous section was repeated ignoring the hysteresis data. The boundary wetting curve was used as the hydrologic parameter $h(\theta)$ for both infiltration and redistribution.

The results presented in Fig 9.7 to Fig 9.10 correspond to the end of each 900 s infiltration event, and the end of each 28 800 s redistribution event. The intermediate profiles at redistribution times of 3600 s have been omitted for clarity.

The water content profiles of Fig 9.3 vary considerably from those of Fig 9.7. The absence of hysteresis effects results in quicker and more complete drainage, with the shapes of the profiles showing distinct differences.

The effect of the absence of hysteresis on solute disposition in the profile is appreciable. The concentration profiles of Fig 9.8 indicate an increase in both convection and dispersion of solute during redistribution compared with the corresponding profiles in Fig 9.4. This is a direct result of the higher pore water velocities and consequently higher mechanical dispersion coefficients for the case using the non-hysteretic data. The solute mass profiles (Fig 9.4 and Fig 9.9) show clearly the differences in salt movement, and indicate the development of a different leaching pattern.

A detailed study of the significance of hysteresis on solute movement is beyond the scope of this report. From the results of the comparisons above,

it is clear that caution must be exercised in omitting the hysteretic nature of the $h(\theta)$ data when considering redistribution processes. For Rubicon sandy loam, hysteresis has a significant effect on both water and solute disposition during intermittent infiltration and redistribution.

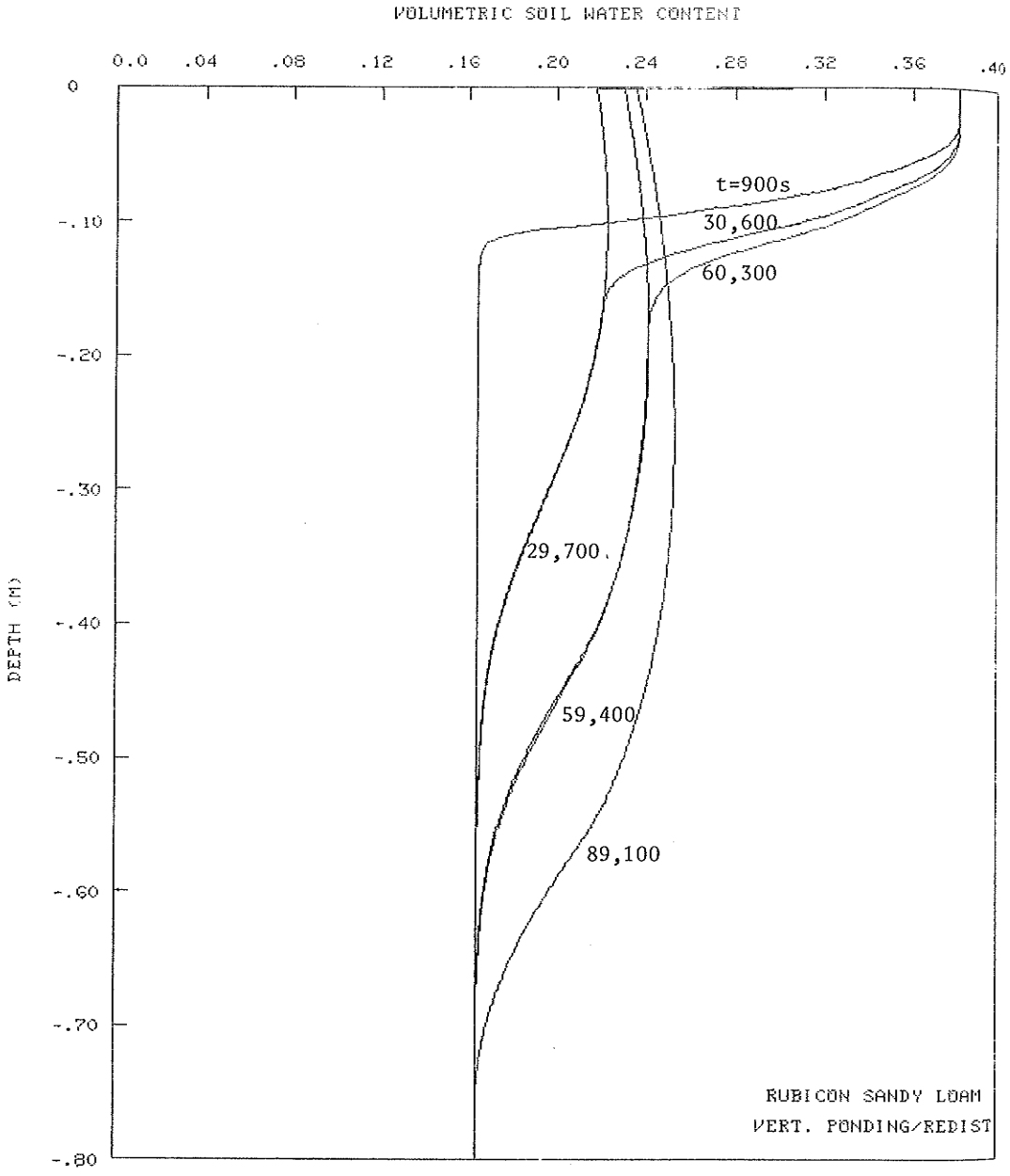

Fig 9.7 θ(z) profiles for three cycles of constant concentration vertical infiltration followed by redistribution in Rubicon sandy loam (hysteresis effects ignored)

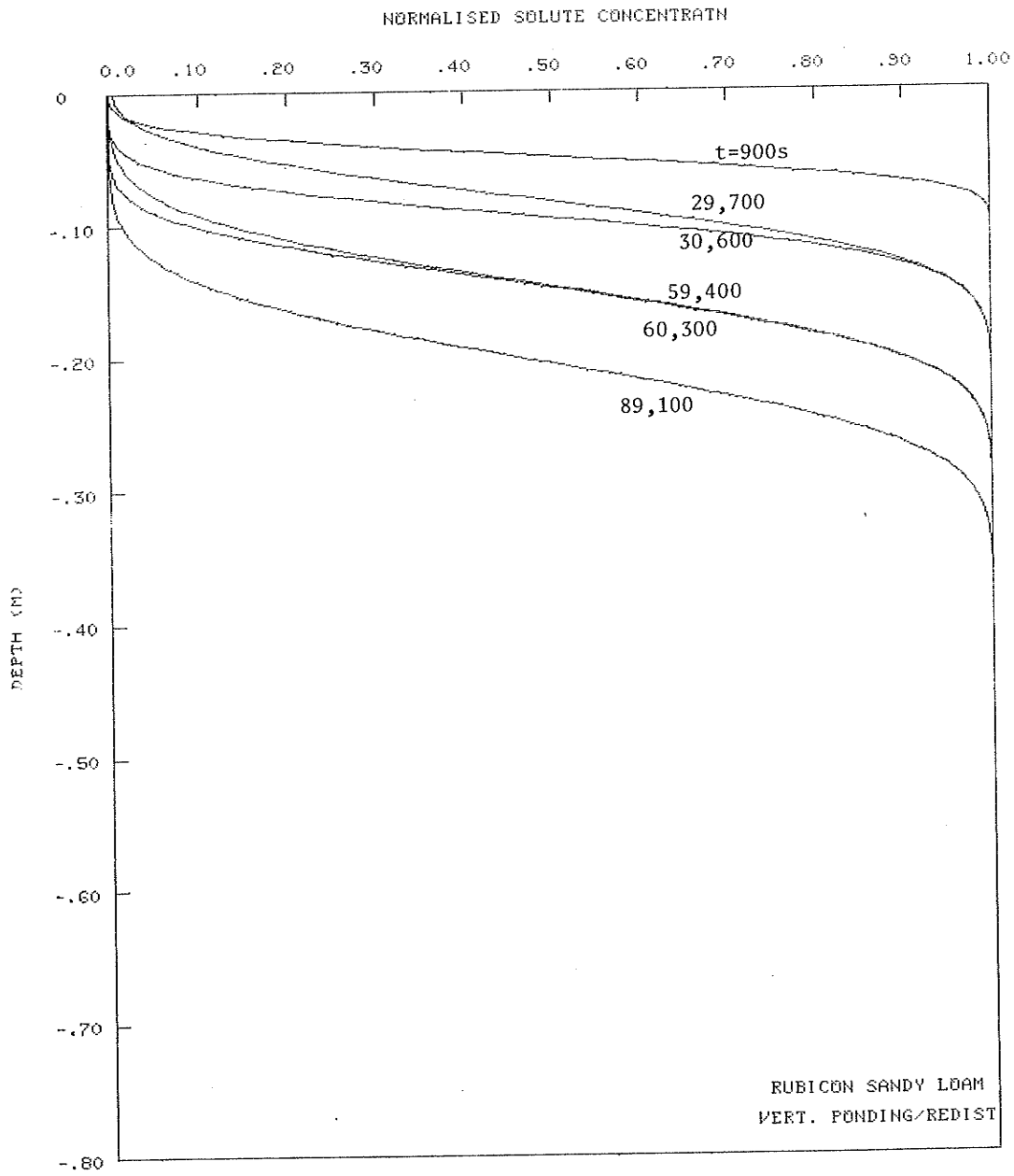

Fig 9.8 $\bar{c}(z)$ profiles for three cycles of constant concentration vertical infiltration followed by redistribution in Rubicon sandy loam (hysteresis effects ignored)

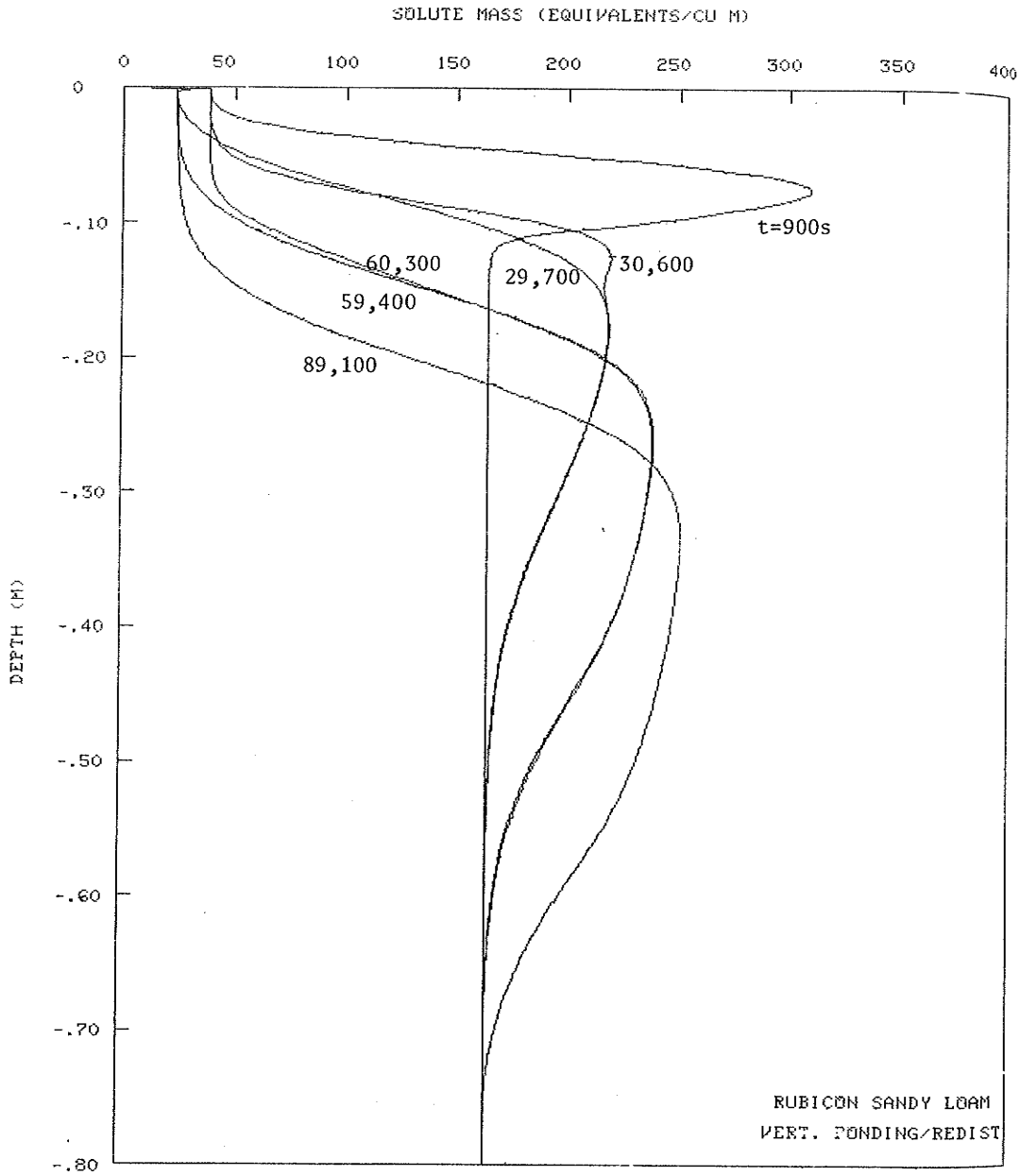

Fig 9.9 Solute mass profiles for three cycles of constant concentration vertical infiltration followed by redistribution in Rubicon sandy loam (hysteresis effects ignored)

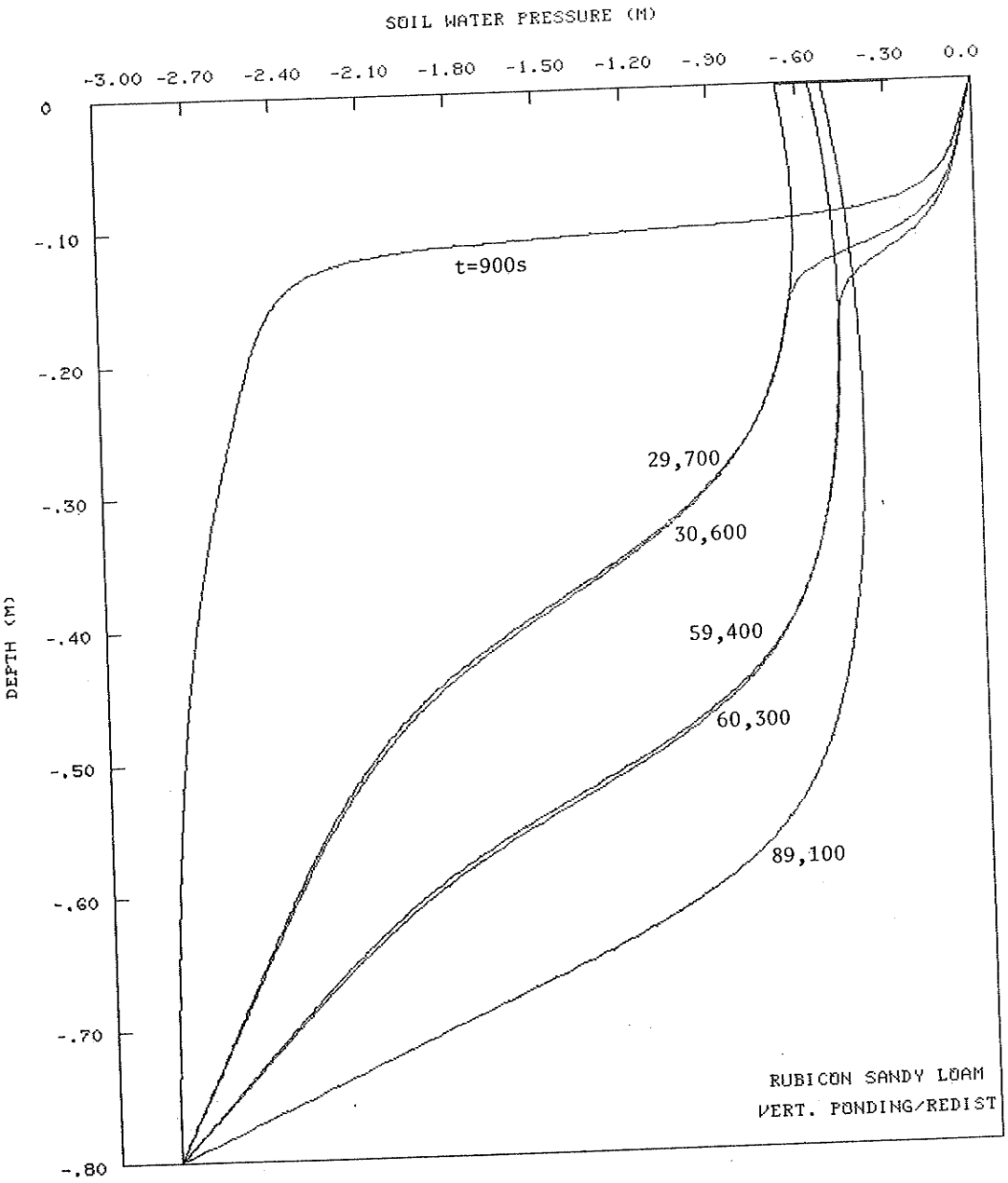

Fig 9.10 h(z) profiles for three cycles of constant concentration vertical infiltration followed by redistribution in Rubicon sandy loam (hysteresis effects ignored)

10 SUMMARY OF RESULTS

Throughout this report, each chapter has been relatively self-contained with regard to both the development of the research material and the results and conclusions derived from such material. This chapter provides a summary of the more significant results.

a. An explicit finite difference model for non-reactive solute transport in unsaturated porous materials under unsteady-state conditions is successfully developed using an established implicit finite difference model for the soil-water phase. The water and solute equations are solved simultaneously with the results being presented in terms of soil-water pressure, soil-water content, solute concentration and solute mass.

b. The numerical soil-water model is unconditionally stable. However, the numerical solute transport model is only conditionally stable. A stability analysis is presented which indicates that limitations on the magnitude of both the timestep and the space step are required for a stable and convergent numerical solution. These limitations are exacting when the solute movement is dominated by convection processes.

c. A quasi-analytical solution is presented for non-reactive solute transport during unsteady horizontal absorption under constant concentration boundary conditions and a constant hydrodynamic dispersion coefficient. This is used to assess the performance of the numerical model. Excellent correspondence is achieved between the analytical and numerical results, indicating that the numerical approach is both accurate and generally stable.

d. A detailed study of solute movement during unsteady horizontal absorption under constant concentration boundary conditions is presented for Bungendore fine sand. The comparisons between theoretical, numerical and experimental results are very good. The significance of the parameter λ_* is discussed and solute concentration profiles studied for a range of constant-valued dispersion coefficients.

e. Numerical and experimental results are compared to assess the existence and magnitude of the velocity dependence of the dispersion coefficient. The dispersion coefficient for Bungendore fine sand is shown to be velocity dependent, and well described using a value for β of 0.0001 m.

f. The predictive behaviour of the numerical model is tested using experimental data for solute movement during constant flux absorption. The numerical model accurately represents the solute movement. The dispersion coefficient for Bungendore fine sand is again shown to be velocity dependent.

g. An approximate analytical solution for solute movement during constant flux infiltration is presented. Good agreement is found between the analytical and numerical results when the mechanical dispersion component of the hydrodynamic dispersion coefficient is dominant.

h. The numerical model is used to study redistribution following both horizontal absorption and vertical infiltration. The model adequately simulates the experimental results. Difficulties experienced with the experimental work and the lack of definitive hysteresis data for the Bungendore fine sand produced results which are less satisfactory than the constant concentration and constant flux absorption results. It is

therefore not possible to analyse accurately the significance of the velocity dependence of the dispersion coefficient during redistribution. Further experimental work on this aspect is necessary.

i. The potential of the numerical model for simulating solute movement under intermittent water application is considered by studying the disposition of solute in a profile of Rubicon sandy loam under three infiltration-redistribution sequences. The solute mass profiles are particularly useful in assessing solute movement.

j. The significance of neglecting soil-water hysteresis in modelling solute movement during redistribution is studied briefly. From this work it appears that the shapes of the solute profiles are sensitive to the $h(\theta)$ data used, suggesting that physically realistic data should be used wherever possible.

REFERENCES

Ayers, R.N. and Watson, K.K. (1977), Experimental and numerical studies of soil water movement to a water table, 6th Aust. Conf. on Hydraulics & Fluid Mechanics, *I.E. Aust., Nat. Conf. Publn. 77/12*, 72-75

Bresler, E. (1973), Simultaneous transport of solutes and water under transient, unsaturated flow conditions, *Water Resour. Res., 9*, 975-986.

Bresler, E. and Hanks, R.J. (1969), Numerical method for estimating simultaneous flow of water and salt in unsaturated soils, *Soil Sci. Soc. Am. Proc., 33*, 827-832.

Biggar, J.W. and Nielsen, D.R. (1967), Miscible displacement and leaching phenomena, in *Irrigation of Agricultural Lands*, Agron. 11, ed. R.M. Hagen et al, Am. Soc. Agron. Madison, Wis., 254-274.

Bruce, R.R. and Klute, A. (1956), The measurement of soil water diffusivity, *Soil Sci. Soc. Am. Proc., 20*, 458-462.

Carslaw, H.S. and Jaeger, J.C. (1960), *Conduction of Heat in Solids*, Oxford Univ. Press, New York.

Chaudhari, N.M. (1971), An improved numerical technique for solving multi-dimensional miscible displacement equations, *Soc. Pet. Eng. J., 11*, 277-284.

Davidson, J.M., Brusewitz, G.H., Baker, D.R. and Wood, A.L. (1975), *Use of Soil Parameters for Describing Pesticide Movement Through Soils*, U.S. Environ. Protect. Agency, EPA-660/2-75-009 Report R-800364.

De Smedt, F. and Wierenga, P.J. (1978), Approximate analytical solution for solute flow during infiltration and redistribution, *Soil Sci. Soc. Am. J., 42*, 407-412.

Fried, J.J. and Combarnous, M.A. (1971), Dispersion in porous media, *Adv. Hydrosci., 7*, 170-282.

Fromm, J. (1964), The time dependent flow of an incompressible viscous fluid, in *Methods in Computational Physics, 3*, 345-382.

Jones, M.J. and Watson, K.K. (1980), Solute movement in soil under an intermittent water application regime, Hydrology & Water Resources Symp., *I.E. Aust., Nat. Conf. Publn. 80/9*, 1-5.

Lantz, R.B. (1971), Qualitative evaluation of numerical diffusion (truncation error), *Soc. Pet. Eng. J., 11*, 315-320.

Lees, S.J. and Watson, K.K. (1975), The use of a dependent domain model of hysteresis in numerical soil water studies, *Water Resour. Res., 11*, 943-948.

Ogata, A. (1970), Theory of dispersion in a granular medium, *U.S. Geol. Surv. Prof. Paper*, 411-I.

Olsen, S.R. and Kemper, W.D. (1968), Movement of nutrients to plant roots, in *Adv. Agronomy, 20*, 91-151.

Passioura, J.B. (1971), Hydrodynamic dispersion in aggregated media, 1 Theory, *Soil Sci., 111*, 339-344.

Pfannkuch, H.O. (1963), Contribution à l'étude des déplacements de fluides miscibles dans un milieu poreux, *Rev. Inst. Fr. Pet., 18*, 215-268.

Philip, J.R. (1955), Numerical solution of equations of the diffusion type with diffusivity concentration dependent, *Trans. Faraday Soc., 51,* 885-892.

Roache, P.J. (1976), *Computational Fluid Dynamics,* Hermosa, New Mexico.

Saffman, P.G. (1959), Dispersion due to molecular diffusion and macroscopic mixing in flow through a network of capillaries, *J. Fluid Mech., 7,* 194-208.

Smiles, D.E. and Gardiner, B.N. (1981), Hydrodynamic dispersion during unsteady, unsaturated water flow in a clay soil, *Soil Sci. Soc. Am. J.,* Submitted for publication.

Smiles, D.E., Perroux, K.M., Zegelin, S.J. and Raats, P.A.C. (1981), Hydrodynamic dispersion during constant rate absorption of water by soil, *Soil Sci. Soc. Am. J., 45,* 453-458.

Smiles, D.E. and Philip, J.R. (1978), Solute transport during absorption of water by soil: laboratory studies and their practical implications, *Soil Sci. Soc. Am. J., 42,* 537-544.

Smiles, D.E., Philip, J.R., Knight, J.H. and Elrick, D.E. (1978), Hydrodynamic dispersion of water by soil, *Soil Sci. Soc. Am. J., 42,* 229-236.

Talsma, T. (1974), The effect of initial moisture content and infiltration quantity on redistribution of soil water, *Aust. J. Soil Res., 12,* 15-26.

Topp, G.C. (1969), Soil water hysteresis measured in a sandy loam and compared with the hysteresis domain model, *Soil Sci. Soc. Am. Proc., 33,* 645-651.

Watson, K.K. and Curtis, A.A. (1975), Numerical analysis of vertical water movement in a bounded profile, *Aust. J. Soil Res., 13,* 1-11.

Watson, K.K. and Jones, M.J. (1981*a*), Hydrodynamic dispersion during absorption in a fine sand 1. The constant concentration case, In press, *Water Resour. Res.*

Watson, K.K. and Jones, M.J. (1981*b*), Estimation of hydrodynamic dispersion in a fine sand using an approximate analytical solution, In press, *Aust. J. Soil Res., 19(4).*

Watson, K.K. and Lees, S.J. (1975), Simulation of the rainfall - runoff process using a hysteretic infiltration - redistribution model, *Aust. J. Soil Res., 13,* 133-140.

Watson, K.K. and Perrens, S.J. (1973), Numerical analysis of intermittent infiltration - redistribution, Hydrology Symp., *I.E. Aust., Nat. Conf. Publn. 73/3,* 27-33.

Watson, K.K., Perrens, S.J. and Whisler, F.D. (1973), A limiting flux condition in infiltration into heterogeneous porous media, *Soil Sci. Soc. Am. Proc., 37,* 6-10.

Watson, K.K. and Whisler, F.D. (1976), Comparison of drainage equations for the gravity drainage of stratified profiles, *Soil Sci. Soc. Am. J., 40,* 631-635.

Watson, K.K. and You, S.K. (1980), Comparison of analytical and numerical solutions of water movement in unsaturated soils, Agricultural Engg. Conf., *I.E. Aust., Nat. Conf. Publn. 80/7,* 188-191.

Webb, S.N. and Watson, K.K. (1977), Gravity drainage of a sand profile under a time-dependent surface flux, *Aust. J. Soil Res., 15,* 9-16.

Whisler, F.D. and Watson, K.K. (1968), One dimensional gravity drainage of uniform columns of porous materials, *J. Hydrol.*, *61*, 277-296.

Whisler, F.D. and Watson, K.K. (1969), Analysis of infiltration into draining porous media, *J. Irr. & Drain. Div.*, *ASCE*, *95*, 481-491.

Whisler, F.D., Watson, K.K. and Perrens, S.J. (1972), The numerical analysis of infiltration into heterogeneous porous media, *Soil Sci. Soc. Am. Proc.*, *36*, 868-874.

White, I., Smiles, D.E. and Perroux, K.M. (1979), Absorption of water by soil: the constant flux boundary condition, *Soil Sci. Soc. Am. J.*, *43*, 659-664.

Wilson, J.L. and Gelhar, L.W. (1974), Dispersive mixing in a partially saturated porous medium, *Tech. Rep. 191*, Ralph M. Parsons Lab. for Water Resources and Hydrodynamics, Mass. Inst. Tech., Cambridge.

APPENDIX A

ANNOTATED BIBLIOGRAPHY OF SOLUTE MOVEMENT

1. Al-Niami, A.N.S. & Rushton, K.R. (1979), Dispersion in stratified porous media: analytical solutions, *Water Resour. Res., 15*, 1044-48.
   Analytical solutions are presented for dispersion in stratified porous media under saturated, steady flow conditions, allowing for interaction between layers. Flow parallel to the stratifications and flow perpendicular to the interfaces are considered.

2. Balasubramanian, V., Ahuja, L.R., Kanehiro, Y. & Green, R.E. (1976), Movement of water and nitrate in an unsaturated aggregated soil during nonsteady-infiltration - a simplified solution for solute flow, *Soil Sci., 122*, 245-55.
   Experimental studies of water and nitrate movement in unsaturated, highly aggregated soil under unsteady flow conditions, with different initial water content. A simplified analytical solution is presented for a slug of solute under a constant surface concentration flow condition.

3. Basak, P. & Murty, V.V.N. (1977), Nonlinear diffusion applied to groundwater contamination problems, *J. Hydrology, 35*, 357-363.
   An analytical solution for the concentration dependent diffusion of nonreactive solute under stationary, saturated water conditions with increasing solute concentration at the source.

4. Basak, P. & Murty, V.V.N. (1978), Concentration-dependent diffusion applied to groundwater contamination problems, *J. Hydrology, 37*, 333-337.
   An analytical solution for the concentration-dependent diffusion equation with decreasing contaminant concentration at the source. Solute is non reactive, and saturated, steady-state conditions prevail.

5. Batu, V. & Gardner, W.R. (1978), Steady-state solute convection in two dimensions with nonuniform infiltration, *Soil Sci. Soc. Am. J., 42*, 18-22.
   The unsaturated, steady-state soil-water equation is solved analytically for two dimensional flow conditions. The resulting flow network, described by streamlines, travel times and isochrones is used to predict the movement of solutes, assuming a convective transport mechanism. The effect of surface variations in infiltration on the pattern of solute transport is discussed.

6. Beese, F. & Wierenga, P.J. (1980), Solute transport through soil with adsorption and root water uptake computed with a transient and a constant-flux model, *Soil Sci., 129*, 245-52.
   A comparison of two numerical models simulating reactive solute transport during a sequence of infiltration-redistribution cycles. One model assumes steady water flow, the other unsteady flow, and in each the water and solute flow equations are solved simultaneously using explicit finite difference (CSMP) models. Adsorption and root water uptake (a sink) are included, and their significance studied.

7. Besbes, M., Ledoux, E. & de Marsily, G. (1976), Modelling of the salt transport in multilayered aquifers, *System Simulation in Water Resources*, ed. G.C. Vansteenkiste, North Holland, 229-245.
   Following a brief discussion on the theory of solute transport in

saturated, unsteady flow conditions, a simplification is made for multilayered aquifers and the model applied to two field problems.

8. Biggar, J.W. & Nielsen, D.R. (1960), Diffusion effects in miscible displacement occurring in saturated and unsaturated porous materials, *J. Geophys. Res.*, *65*, 2887-95.
An experimental study of miscible displacement in porous media under saturated and unsaturated steady flow conditions for various average flow velocities. Effluent concentration curves are compared, and variations due to soil type and flow conditions highlighted.

9. Biggar, J.W. & Nielsen, D.R. (1962), Miscible displacement. II. Behaviour of tracers, *Soil Sci. Soc. Proc.*, *26*, 125-28.
An experimental study of the effect of average flow velocity, initial water content and soil type on the spreading of an initially sharp front of a solute (tracer) moving under steady-state flow conditions. Solute distribution as measured in the effluent is explained in terms of the relative effects of pore geometry, diffusion rates, adsorption and exchange.

10. Biggar, J.W. & Nielsen, D.R. (1963), Miscible displacement. V. Exchange processes, *Soil Sci. Soc. Proc.*, *27*, 623-627.
Three mathematical models describing reactive solute transport are compared with experimental results for horizontal, steady-state flow in a sand. Saturated and unsaturated conditions are included, for a range of flow velocities.

11. Biggar, J.W. & Nielsen, D.R. (1967), Miscible displacement and leaching phenomenon, *Irrigation of Agricultural Lands*, ed. Hagan et al, Amer. Soc. Agron., 254-274.
A classic review of miscible displacement phenomena in porous media. Experimental breakthrough curves for both reactive and non-reactive solutes under saturated and unsaturated steady flow conditions and for a range of porous media are compared and discussed. Several theoretical models of dispersion are critically presented, and introductory comments made concerning leaching phenomena. Suggestions are given for future investigations.

12. Boast, C.W. (1973), Modelling the movement of chemicals in soils by water, *Soil Sci.*, *115*, 224-230.
A brief review of classical macroscopic continuum theories for describing movement of solutes through soil. Equations describing different mechanisms for solute movement are combined to form a general flow model. Component models are described, but initial and boundary conditions and solutions to the equations are not included.

13. Bresler, E.(1967), A model for tracing salt distribution in the soil profile and estimating the efficient combination of water quality and quantity under varying field conditions, *Soil Sci.*, *104*, 227-233.
A numerical model is presented for describing reactive solute movement during infiltration of water. The model, based on the conservation of solute mass, computes the disposition of solute in the profile following an infiltration event. Calculated results are compared with data obtained from field studies. The model is used to evaluate efficient combinations of quality and quantity of irrigation water subject to a desired salinity distribution within a field soil.

14. Bresler, E. & Hanks, R.J. (1969), Numerical method for estimating simultaneous flow of water and salt in unsaturated soils, *Soil Sci. Soc. Am. Proc.*, *33*, 827-832.
A numerical model is presented for describing simultaneous flow of water and nonreactive solute during unsteady-state conditions in unsaturated soils. The solute model only accounts for convective flow, and is based on the conservation of solute mass. Infiltration, redistribution and evaporation are simulated by the model, which computes the concentration profile as a function of time and depth. Comparisons between experimental and numerical results are given.

15. Bresler, E. (1973), Simultaneous transport of solutes and water under transient unsaturated flow conditions, *Water Resour. Res.*, *9*, 975-86.
Implicit finite difference models for both water and nonreactive solute flow are solved simultaneously for unsaturated, unsteady-state flow conditions. Numerical results are compared with analytical solutions for steady water flow, and with previously reported field data for unsteady infiltration. The model is used to study solute movement during infiltration, redistribution and evaporation.

16. Bresler, E. (1975), Two-dimensional transport of solutes during non-steady infiltration from a trickle source, *Soil Sci. Soc. Am. Proc.*, *39*, 604-613.
A simultaneous solution of the water and solute flow equations during unsteady, unsaturated flow in two dimensions, using noniterative alternating-direction-implicit finite difference models. Soil water hysteresis effects are ignored. Two different models are presented - one using cartesian, the second radial co-ordinates. Examples using the radial co-ordinate model are presented for trickle irrigation at different flow rates in different soils.

17. Bresler, E. & Dagan, G. (1979), Solute dispersion in unsaturated heterogeneous soil at field scale II. Applications, *Soil Sci. Soc. Am. J.*, *43*, 467-472.
A quasi-analytical solution for nonreactive solute transport under vertical, steady-state water flow in a heterogeneous porous media is applied to a real soil. Average solute concentration profiles as a function of depth and time are computed for various surface rates of infiltration, and the average concentration over a layer extending from the soil surface to a given depth is computed. These are compared to predictions using a conventional convective diffusive model in a homogeneous field.

18. Cameron, D.R., Kowalenko, C.G. & Campbell, C.A. (1975), Factors affecting nitrate nitrogen and chloride leaching variability in a field plot, *Soil Sci. Soc. Am. J.*, *43*, 455-460.
A field study aimed at identifying significant factors affecting differential leaching patterns. Spatial variability in soil properties (density, hydraulic conductivity, water desorption curves) and point differences in redistribution of runoff (due to differences in surface microrelief) are the major factors affecting differential leaching rates. Non-uniform fertilization application accounted for much of the sampling variability immediately after fertilization.

19. Cassel, D.K., Krueger, T.H., Schroer, F.W. & Norum, E.B. (1974), Solute movement through disturbed and undisturbed soil cores, *Soil Sci. Soc. Am. Proc.*, *38*, 36-40.

An experimental study to determine the effect of soil structure (ie disturbed vs undisturbed) on solute movement.

20. Carbonell, R.G. (1979), Effect of Pore Distribution and flow segregation on dispersion in porous media, *Chem. Eng. Sci.*, *34*, 1031-1039.
Equations are derived for the dispersion coefficient in laminar and turbulent flow to study the effect of pore size distribution and flow segregation on dispersion in porous media. Predictions using this theory are compared with cumulative experimental data.

21. Chhatwal, S.S., Cox, R.L., Green, D.W. & Ghandi, B. (1973), Experimental and mathematical modeling of liquid-liquid miscible displacement in porous media, *Water Resour. Res.*, *9*, 1369-1377.
A comparison of numerical models used to solve the water-solute equations in unsteady, saturated flow fields in both one and two space dimensions. An improved implicit finite difference scheme for solute transport is presented which significantly reduces the numerical oscillations and numerical dispersion. Results are compared with an analytical solution for one dimensional transport and with experimental data for two dimensional transport.

22. Coats, K.H. & Smith, B.D. (1964), Dead-end pore volume and dispersion in porous media, *Soc. Pet. Eng. J.*, *4*, 73-84.
A series of laboratory experiments on dispersion of nonreactive solutes under saturated, steady-state flow conditions over a range of materials and flow velocities are analysed using different mathematical models. The experimental and predicted results are compared to test the physical validity of the existence of a stagnant volume of soil-water. Note: see also the discussion and author's reply in the same reference, 282-284.

23. Couchat, P.H., Brissaud, F. & Gayraud, J.P. (1980), A study of strontium-90 movement in a sandy soil, *Soil Sci. Soc. Am. J.*, *44*, 7-13.
The adsorption-desorption of Sr is investigated in saturated columns of sandy soil under constant flux conditions, and kinetic and equilibrium relations compared. A numerical model is used to both calculate breakthrough curves using the experimentally determined adsorption-desorption data, and to determine the necessary adsorption-desorption relationship to ensure good experimental-numerical comparisons.

24. Cushman, J.H. (1979), An analytical solution to solute transport near root surfaces for low initial concentration I. Equations development, *Soil Sci. Soc. Am. J.*, *43*, 1087-1090.
An analytical solution is developed for a non-dimensional form of the governing partial differential equation for radial flow of solute (nutrient) in the root zone. Mass flow, diffusion and absorption are considered. Water flow is steady-state.

25. Cushman, J.H. (1979), An analytical solution to solute transport near root surfaces for low initial concentration II. Applications, *Soil Sci. Soc. Am. J.*, *43*, 1087-1095.
The analytical solution is used to study the influence of the root size, absorption ability and transpiration rate on solute (nutrient) distribution.

26. Dagan, G. & Bresler, E. (1979), Solute Dispersion in unsaturated heterogeneous soil at field scale I. Theory, *Soil Sci. Soc. Am. J.*, *43*, 461-467.

Quasi-analytical solutions to non-reactive solute flow under vertical, steady-state soil water flow in unsaturated, heterogeneous soil are presented. Field heterogeneity is described in terms of the statistical distribution of the hydraulic parameters, implying a corresponding distribution of the solute concentration.

27. Dahiya, I.S., Singh, M., Singh, M. & Hajrasuliha, S. (1980), Simultaneous transport of surface-applied salts and water through unsaturated soils as affected by infiltration, redistribution and evaporation, *Soil Sci. Soc. Am. J., 44*, 223-228.
Laboratory column studies on the effects of water application rate and initial water content on the leaching of chloride salt. Comparisons are made between three soil types - sand, sandy loam and clay.

28. Davidson, J.M., Baker, D.R. & Brusewitz, G.H. (1975), Simultaneous transport of water and adsorbed solutes through soil under transient flow conditions, *Trans. ASCE, 18*, 535-539.
Simultaneous solutions of finite difference approximations for water (implicit) and reactive solute (explicit) under unsteady and steady flow conditions are presented. Non-linear adsorption/desorption relations are used, based on the Fruendlich equilibrium relationship. Comparisons are made between the numerical and an analytical (steady-state water flow) solution, and with experimental results for a constant applied water flux. The model is used to study an infiltration/redistribution/evaporation sequence for a slug of reactive solute.

29. Davidson, J.M., Brusewitz, G.H., Baker, D.R. & Wood, A.L. (1975), *Use of Soil Parameters for Describing Pesticide Movement Through Soils*, U.S. Environ. Protect. Agency EPA-660/2-75-009 Report R-800364.
Explicit finite difference models describing reactive solute transport through unsaturated porous media are presented for both steady- and unsteady-state water flow conditions, and solved simultaneously with the water flow equations. Experimental results from laboratory and field studies are used to test the numerical solutions under infiltration conditions.

30. Day, P.R. & Forsythe, W.M. (1957), Hydrodynamic dispersion of solutes in the soil moisture stream, *Soil Sci. Soc. Am. Proc., 21*, 477-480.
Experimental study of solute dispersion under saturated, steady-state water flow conditions. A statistical analysis is presented to determine the amount of dispersion, and dispersion coefficients and indicies are compared for a range of soil types.

31. De Smedt, F. & Wierenga, P.J. (1978), Solute transport through soil with nonuniform water content, *Soil Sci. Soc. Am. J., 42*, 7-10.
An approximate analytical solution is presented for steady leaching of solute (salt) through soil with a nonuniform water content. The solution compares favourably with a numerical solution, and the approximate analytical and the numerical solutions agree with an analytical solution for soils with a uniform water content distribution.

32. De Smedt, F. & Wierenga, P.J. (1978), Approximate analytical solution for solute flow during infiltration and redistribution, *Soil Sci. Soc. Am. J., 42*, 407-412.
An approximate analytical solution is developed to describe non-reactive solute flow in soil during infiltration and redistribution.

The solute dispersion coefficient is a linear function of pore water velocity. Comparisons are made with a set of experimental results and with numerical solutions.

33. De Smedt, F. & Wierenga, P.J. (1979), A generalised solution for solute flow in soils with mobile and immobile water, *Water Resour. Res.*, *15*, 1137-1141.
An approximate analytical solution is developed to describe non-reactive solute flow in soil during steady-state leaching in one dimension. The solution takes into account transfer into an immobile water fraction, and is examined for different sets of boundary conditions.

34. Elrick, D.E., Laryea, K.B. & Groenevelt, P.H. (1979), Hydrodynamic dispersion during infiltration of water into soil, *Soil Sci. Soc. Am. J.*, *43*, 856-865.
A power series solution is developed for the dispersion of solute during one dimensional infiltration and a (CSMP) computer program presented to solve the resulting equations for water and solute movement. The dispersion coefficient is assumed to be a function of water content only. A comparison between experimental data and theoretical predictions is given for a clay loam soil.

35. Fried, J.J. & Combarnous, M.A. (1971), Dispersion in porous media, *Advances in Hydroscience*, *7*, 169-282.
A comprehensive 'state of the art' which includes the historical development of dispersion theory, descriptions of both dispersion and diffusion processes and their significant parameters, conceptual models, experimental studies, extensions to stratified and heterogeneous media, analytical and numerical methods to solve the dispersion equations, experimental techniques used in dispersion studies, and a methodological approach for treating real problems.

36. Gaudet, J.P., Jégat, H., Vachaud, G. & Wierenga, P.J. (1977), Solute transfer with exchange between mobile and stagnant water through unsaturated sand, *Soil Sci. Soc. Am. J.*, *41*, 665-671.
An experimental and numerical study of non-reactive solute transport through unsaturated sand under steady soil water flow conditions. Solute is allowed to transfer between mobile and immobile soil water phases. The numerical model uses an explicit finite difference technique. Coefficients needed for simulation are obtained at different water contents by curve fitting observed and calculated concentrations at one depth.

37. Gelhar, L.W. & Collins, M.A. (1971), General analysis of longitudinal dispersion in non uniform flow, *Water Resour. Res.*, *7*, 1511-1521.
An analytical method is proposed which allows evaluation of the effects of flow non-uniformity and variable dispersion coefficients on longitudinal dispersion in porous media. One-dimensional saturated, steady-state flow conditions apply. The approximate analytical solution is compared to a numerical solution of the exact equation.

38. Gershon, N.D. & Nir, A. (1969), Effects of boundary conditions of models on tracer distribution in flow through porous mediums, *Water Resour. Res.*, *6*, 830-39.
A study of the influence of different initial and boundary conditions on the distribution of a tracer in time and distance for several one-dimensional systems. Saturated flow under steady and unsteady-state

conditions, with hydrodynamic dispersion, diffusion, radio-active decay and simple chemical interactions are all considered. Exact and approximate analytical solutions are used.

39. Ghuman, B.S. & Prihar, S.S. (1980), Chloride displacement by water in homogeneous columns of three soils, *Soil Sci. Soc. Am. J., 44*, 17-21.
Column laboratory experiments are used to study the effect of initial soil wetness, amount and rate of surface water application and redistribution on the displacement of chloride in three soil types - loamy sand, sandy loam, silt loam. Experimental results are compared with the quasi-analytical solution (extended) of Warrick et al (1971).

40. Ghuman, B.S. & Prihar, S.S. (1980), Chloride displacement by water in layered soil columns, *Aust. J. Soil Res., 18*, 207-14.
A study of solute displacement by water during infiltration and redistribution in two-layered, air-dry soil profiles. Various combinations of loamy sand, sandy loam and silt loam soils are used, under high and low rates of water application.

41. Glas, T.K., Klute, A. & McWhorter, D.B. (1979), Dissolution and transport of gypsum in soils I. Theory, *Soil Sci. Soc. Am. J., 43*, 265-268.
A numerical model using the method of characteristics is developed to describe the movement of gypsum in one dimension under saturated, steady-state flow conditions. Results showing the effect of the various model parameters on calculated concentration-time profiles are presented.

42. Glas, T.K., Klute, A. & McWhorter, D.B. (1979), Dissolution and transport of gypsum in soils II. Experimental, *Soil Sci. Soc. Am. J., 43*, 268-273.
Experimental information on the dissolution of gypsum and transport of dissolved species in a saturated soil water system under steady-state flow conditions is compared with two mathematical models - one based on equilibrium and the other on kinetic dissolution principles. The dissolution process appeared to be kinetically controlled and could not be described by the solubility-product relationship as assumed in the equilibrium model.

43. Gray, W.G. & Pinder, G.F. (1976), An analysis of the numerical solution of the transport equation, *Water Resour. Res., 12*, 547-555.
The relative merits of finite difference and finite element methods for solving the one-dimensional convective-dispersive equation are examined. An explanation for the commonly observed shortcomings in each approach is presented. See also comment and author's reply in the same journal, Vol. 13, 219-220 (1977).

44. Gupta, S.P. & Greenkorn, R.A. (1973), Dispersion during flow in porous media with bilinear adsorption, *Water Resour. Res., 9*, 1357-1368.
An implicit finite difference model is presented for the transport of reactive solutes in water saturated, steady-state flow fields, where convection, diffusion, dispersion and bilinear adsorption are considered. Solutions are presented for a range of variables covering practical values for one-dimensional flow, and compared with a known analytical solution.

45. Gupta, S.P. & Greenkorn, R.A. (1974), Determination of dispersion and nonlinear adsorption parameters for flow in porous media, *Water Resour. Res., 10,* 839-846.
Different methods for calculating the dispersion coefficient from experimental data are discussed. The dispersion-velocity data are correlated using two dispersivity models and the influence of different proportions of clay studied. Two types of adsorption models are used for fitting the static adsorption data. A method is then presented to determine the adsorption parameters for dynamic experiments. 51.

46. Gupta, R.K., Millington, R.J. & Klute, A. (1973), Hydrodynamic dispersion in unsaturated porous media. I. Concentration distribution during dispersion, *J. Indian Soc. Soil Sci., 21,* 1-7.
An experimental study of non-reactive solute movement in an unsaturated porous medium during steady-state water flow. Various combinations of water content and pore water velocity are used, and the resulting solute concentration profiles examined. A glass bead media is used. 52.

47. Gureghian, A.B., Ward, D.S. & Cleary, R.W. (1979), Simultaneous transport of water and reacting solutes through multilayered soils under transient unsaturated flow conditions, *J. Hydrology, 41,* 253-278.
A one-dimensional unsteady-state implicit finite difference model for the simultaneous flow of water and reactive solute through multilayered soil systems under unsaturated flow conditions is presented. Infiltration, redistribution and evaporation are considered. The numerical solutions are compared with analytical and experimental results for particular flow conditions. 53.

48. Hassan, F.A. & Ghaibeh, A.Sh. (1977), Evaporation and salt movement in soils in the presence of water table, *Soil Sci. Soc. Am. J., 41,* 470-478.
The emphasis in this paper is on water flow. Evaporation from homogeneous and stratified soil columns under steady-state flow conditions and in the presence of a shallow water table is studied experimentally and compared with a quasi-analytical solution. The movement of salts initially present in the soil during evaporation above the water table is studied for different evaporation rates, and the total dispersion coefficient calculated as a function of pore water velocity. 54

49. Hornsby, A.G. & Davidson, J.M. (1973), Solution and adsorbed fluometuron concentration distribution in a water-saturated soil: experimental and predicted evaluation, *Soil Sci. Soc. Am. Proc., 37,* 823-828.
An experimental technique is described for measuring solution and adsorbed phases of a reactive solute in a saturated soil column under steady-state conditions. A numerical finite difference (CSMP) model developed to describe the movement of a sorbing material through a porous medium is evaluated in terms of the experimental results for both high and low pore-water velocities. 55

50. Jones, M.J. & Watson, K.K. (1980), Solute movement in soil under an intermittent water application regime, *Hydrology & Water Resour. Symp. Adelaide, 4-6 Nov.,* 1-5. 56
An explicit finite difference model for non-reactive solute transport in unsaturated soils is solved simultaneously with an implicit finite

difference model for water movement under one-dimensional unsteady flow conditions. The significance of soil-water hysteresis and the solute dispersion coefficient are studied for a sandy loam soil.

51. Jury, W.A., Gardner, W.R., Saffigna, P.G. & Tanner, C.B. (1976), Model for predicting simultaneous movement of nitrate and water through a loamy sand, *Soil Sci.*, *122*, 36-43.
Numerical finite element model of dispersion, convection, plant uptake, nitrification and mineralisation - a water balance approach for three soil zones between the surface and the water table. Primarily designed for use in field studies - non-uniform water flows, heterogenity etc. Model predictions of nitrate movement are reasonable in some cases only.

52. Kirda, C., Nielsen, D.R. & Biggar, J.W. (1973), Simultaneous transport of chloride and water during infiltration, *Soil Sci. Soc. Am. Proc.*, *37*, 339-345.
A combined experimental and numerical study of non-reactive solute transport during infiltration, for different initial soil water content and water application rates and for solute either initially present (leaching) or added at the surface. Non-destructive measuring techniques are used for the experimental work, and the numerical program simultaneously solves the water and solute movement equations using finite difference techniques. The solute dispersion coefficient is assumed constant.

53. Kirda, C., Nielsen, D.R. & Biggar, J.W. (1974), The combined effects of infiltration and redistribution on leaching, *Soil Sci.*, *117*, 323-330.
An experimental study of the transport of a non-reactive solute (chloride) under infiltration and redistribution conditions. Non-destructive measurements are used, and the solute is either spread on the surface or initially dispersed throughout the soil and leached with 'pure' water. The effects of water application rate and initial soil water content on solute transport are observed.

54. Krupp, H.K., Biggar, J.W. & Nielsen, D.R. (1972), Relative flow rates of salt and water in soil, *Soil Sci. Soc. Am. Proc.*, *36*, 412-417.
An analytical solution is presented to describe the mixing of two miscible solutions in a porous media under saturated, steady-water flow conditions. The model differentiates between mobile and immobile soil water regions, and includes the effects of ion exclusion on solute transport. The influence of pore water velocity and total solution concentration is studied. Predictions are compared with experimental results.

55. Kurtz, L.T. & Melsted, S.W. (1973), Movement of chemicals in soils by water, *Soil Sci.*, *115*, 231-239.
A general discussion paper with an emphasis on leaching and soil development. Includes a review of laboratory studies using various tracers, with discussion on their chemical interactions (ion exchange, adsorption).

56. Lapidus, L. & Amundson, N.R. (1952), Mathematics of adsorption in beds. VI. The effect of longitudinal diffusion in ion exchange and chromatographic columns, *J. Physical Chem.*, *56*, 984-988.
Analytical solutions are presented for transport of reactive solutes in saturated, steady-state water flow. Both equilibrium and first order kinetic adsorption are considered.

57. Lawson, D.W. (1971), Improvements in the finite difference solution of two-dimensional dispersion problems, *Water Resour. Res.*, *7*, 721-725.
Two improvements are presented for the implicit finite difference solution of solute transport in two dimensions in a steady, saturated flow field.

58. Lehner, F.K. (1979), On the validity of Fick's law for transient diffusion through a porous medium, *Chem. Eng. Sci.*, *34*, 821-825.
The method of spatial averaging is applied to derive a macroscopic form of Fick's law for unsteady-diffusion through a saturated rigid porous medium. The restrictions on the validity of this form are determined.

59. Lin, S.H. (1977), Nonlinear adsorption in porous media with variable porosity, *J. Hydrology*, *35*, 235-243.
A numerical procedure is presented to allow the prediction of reactive solute dispersion and adsorption in heterogeneous porous media. Different forms of porosity variation are used, and the resulting simulations compared to determine the influence of porosity variation on solute concentration distribution. Comparison is also made between an analytical solution and the numerical method.

60. Lin, S.H. (1977), Longitudinal dispersion in porous media with variable porosity, *J. Hydrology*, *34*, 13-19.
A procedure is presented to allow prediction of non-reactive solute dispersion in porous media with variable porosity under steady-state flow conditions. Results generated from an analytical solution using a constant average porosity provide the basis for assessment of the effects of different porosity functions on the solute predictions. The porosity variations are specified as a function of the space co-ordinate and the resulting equations solved numerically using an implicit finite difference technique.

61. Lindstrom, F.T., Haque, R., Freed, V.H. & Boersma, L. (1967), Theory on the movement of some herbicides in soils, *Environ. Sci. Technol.*, *1*, 561 - 565.

62. Lindstrom, F.T. (1976), Pulsed dispersion of trace chemical concentrations in a saturated sorbing porous medium, *Water Resour. Res.*, *12*, 279-238.
A rather simple yet complete mathematical model is presented for the pulsed dispersion of reactive solutes in water saturated, steady-state flow systems. The model includes the effects of convection, dispersion, adsorption-desorption and first order decay. A typical example is discussed with the aid of concentration distribution curves.

63. Lindstrom, F.T. & Boersma, L. (1971), A theory on the mass transport of previously distributed chemicals in a water-saturated sorbing porous medium, *Soil Sci.*, *111*, 192-199.
Models developed to predict the mass transport of reactive solutes in saturated, steady-state flow systems commonly represent the actual pore size distribution by some average pore size. This paper proposes that improvements can be obtained when the actual pore size distribution is considered, and the existing theory is extended to include pore size dependent diffusion coefficients.

64. Lindstrom, F.T. & Boersma, L. (1975), A theory of the mass transport of previously distributed chemicals in a water-saturated sorbing porous medium: 4. Distributions, *Soil Sci., 119,* 411-420.
A quantitative analysis of the mass transport of reactive solutes in a water saturated, steady-state flow field. Solutions are presented for a pulse of solute in an initially solute free soil, and then for leaching of the resulting distribution of solute by water. Convection, dispersion and sorption are considered.

65. Lindstrom, F.T., Boersma, L. & Stockard, D. (1971), A theory on the mass transport of previously distributed chemicals in a water saturated sorbing porous medium: isothermal cases, *Soil Sci., 112,* 291-300.
The theory previously presented is expanded by considering three sorption models coupled with the convective-dispersive equation. Hydrodynamic effects for a range of pore sizes are taken into account, and the theoretical results obtained with each sorption model compared. See also experimental evaluation of the model in the same journal, Vol. 118, 238-242 (1974).

66. Lucas, J.N. (1980), The transport of a radioactive salt through a semi-infinite column of porous medium: a physical model, *Water Resour. Res., 16,* 387-390.
Laboratory column studies of the transport of radioactive salt through saturated sand. Mathematical equations are derived to describe the effluent concentrations for a semi-infinite column with constant and variable input solute concentrations. Predicted and measured breakthrough curves are compared for both cases.

67. Marino, M.A. (1974), Distribution of contaminants in porous media flow, *Water Resour. Res., 10,* 1013-1018.
A mathematical analysis is presented for the simultaneous dispersion and adsorption of solute within homogeneous, isotropic, saturated porous media in semi-infinite, steady, unidirectional flow fields. The solutions predict the distribution of contaminants resulting from variable source concentrations.

68. Marino, M.A. (1978), Flow against dispersion in nonadsorbing porous media, *J. Hydrology, 37,* 149-158.
Analytical solutions are developed for solute dispersion in finite, one-dimensional, horizontal, steady-state saturated water flow fields where flow and dispersion are opposed. Radioactive decay of solute is considered. Time-dependent solute concentration is maintained at the input boundary. The solutions are useful for analysing possible prevention of the spread of contaminated water by a flow of fresh water.

69. Marino, M.A. (1978), Flow against dispersion in adsorbing porous media, *J. Hydrology, 38,* 197-205.
A mathematical analysis is presented for the simultaneous dispersion and adsorption of a solute in finite porous media where water flow and solute dispersion are opposed. The flow field is one-dimensional, heterogeneous and steady-state. Solute adsorption is included in the analysis. Solute concentrations varying with time are enforced at one boundary. The solutions are useful for analysing possible prevention of the spread of contaminated water in an adsorbing media by a flow of fresh water.

70. Melamed, D., Hanks, R.J. & Willardson, L.S. (1977), Model of salt flow in soil with a source-sink term, *Soil Sci. Soc. Am. J., 41,* 29-33.
An implicit finite difference model of non-reactive solute transport under unsteady, unsaturated flow conditions is presented. The model is solved simultaneously with a water flow model, and includes the effects of convection, dispersion and also a sink/source term. Model predictions with and without the sink/source term are compared with field and laboratory results.

71. Miller, R.J., Biggar, J.W. & Nielsen, D.R. (1965), Chloride displacement in panoche clay loam in relation to water movement and distribution, *Water Resour. Res., 1,* 63-73.
A field study of the leaching of a slug of non-reactive solute during infiltration and redistribution sequences. Parallel studies for different methods of surface water application are presented.

72. Millington, R.J. & Shearer, R.C. (1971), Diffusion in aggregated porous media, *Soil Sci., 111,* 372-378.
Aggregation or under-dispersion of either the solid or void components of a porous medium imposes additional restrictions on the flow of fluid through the medium. A mathematical model is presented which permits calculation of diffusion coefficients in aggregated porous solids, either saturated or partially saturated with water. Calculated gas diffusities are compared with experimental data.

73. Molz, F.J., Davidson, J.M. & Tollner, E.W. (1979), Unsaturated-zone water, *Reviews of Geophysics & Space Physics, 17,* 1221-1239.
General review of research advances in unsaturated zone hydrology: 1974-1978. Covers soil water flow in both rigid and swelling media, hysteresis, multi-phase flow, point and line sources and sinks, saturated- unsaturated interaction, coupled solute and water flow, frozen soil transport, coupled water-heat-vapour transport, soil-root interaction, and developments in numerical methods and simulation.

74. Molz, F.J. & Hornberger, G.M. (1973), Water transport through plant tissues in the presence of a diffusable solute, *Soil Sci. Soc. Am. Proc., 37,* 833-837.
The theory of non-equilibrium thermodynamics is used to develop a quantitative description of water transport through plant tissues containing both permeating and non-permeating solutes.

75. Murali, V. & Aylmore, L.A.G. (1979), Predicting the movement of solutes in soil profiles, *Hydrology & Water Resour. Symp. Perth,* 210-214.
A brief review of the limitations of previous analytical approaches, and an illustration of the ability of numerical methods to describe reactive solute transport in soils. Experimental results are given which illustrate the importance of modelling, where the complexities of flow and solute-soil reactions can be taken into account.

76. Nielsen, D.R. & Biggar, J.W. (1961), Miscible displacement in soils: I. Experimental information, *Soil Sci. Soc. Proc., 25,* 1-5.
An experimental study of non-reactive solute movement in three different porous media under saturated and unsaturated, steady-state horizontal flow conditions, for different flow rates. Results are presented as solute concentration breakthrough curves, and their positions and shapes compared and discussed in terms of physical differences and flow conditions. This paper is essentially a re-write of Biggar & Nielsen (1960) in J. Geophys. Res.

77. Nielsen, D.R. & Biggar, J.W. (1962), Miscible displacement: III. Theoretical considerations, *Soil Sci. Soc. (Am) Proc., 26,* 216-221.
Several analytical models are examined for their usefulness in describing miscible displacement in porous media. These models are discussed for different types of porous media at various water contents and for different flow velocities, under steady-state conditions, with specific reference to experimental data.

78. Nielsen, D.R., Starr, J.L., Kirda, C. & Misra, C. (1973), Soil-water and solute movement studies, *Isotope & Radiation Techniques in Soil Physics & Irrigation Studies Proc. Symp.*, I.A.E.A. & F.A.O. Vienna, 117-133.
The simultaneous transport of water and solutes through soil profiles is examined theoretically and experimentally using isotopic tracers for selected conditions in the absence of plants. A methodology for incorporating the effects of appropriate physical, chemical and microbiological processes is presented. A detailed examination of steady-state leaching with nitrogen transformations, leaching during infiltration and redistribution, and soil solution sampling is presented.

79. Oster, C.A., Sonnichsen, J.C. & Jaske, R.T. (1970), Numerical solution to the convective diffusion equation, *Water Resour. Res., 6,* 1746-1752.
A numerical solution to the convective diffusion equation is discussed. An implicit finite difference model is presented for two dimensional non-reactive solute transport which is solved simultaneously with the equation for water flow.

80. Paetzold, R.F. & Scott, H.D. (1978), Determination of the apparent dispersion coefficient of solutes in unsaturated soil, *Soil Sci. Soc. Am. J., 42,* 874-877.
A method is presented to determine the apparent dispersion coefficient of a solute in unsaturated soils at relatively low soil water flow rates.

81. Parlange, J.-Y. & Starr, J.L. (1978), Dispersion in soil columns: effect of boundary conditions and irreversible reactions, *Soil Sci. Soc. Am. J., 42,* 15-18.
A closed form approximate analytical solution is presented which describes solute transport under steady soil water flow conditions, including the effects of convection, dispersion and adsorption. Detailed discussion on the effect of a finite length of soil column on solute displacement is given.

82. Passioura, J.B. (1971), Hydrodynamic dispersion in aggregated media 1. Theory, *Soil Sci., 111,* 339-344.
The dispersion of non-reactive solutes in saturated, aggregated media under steady-state water flow conditions is examined. A simplified model, where the effect of aggregation (described by adding a sink term) is expressed in terms of a dispersion coefficient, is presented. This approach allows the use of the 'diffusion' equation with its numerous analytical solutions. The applicability of the resulting coefficient and its effect on breakthrough curves is discussed.

83. Passioura, J.B. & Rose, D.A. (1971), Hydrodynamic dispersion in aggregated media. 2. Effects of velocity and aggregate size, *Soil Sci., 111,* 345-351.

Experimental results for dispersion in saturated, aggregated media under steady-state water flow conditions are presented, and discussed in relation to the theory presented in part I. Three different materials are studied over a wide range of mean flow velocities, and the dependence of the dispersion coefficients on mean velocity and aggregate size discussed. The criteria for breakdown of the theoretical model of part I is also studied.

84. Passioura, J.B., Rose, D.A. & Haszler, K. (1970), 'Lognorm' - A program for analysing experiments on hydrodynamic dispersion, *Technical Memorandum 70/6 C.S.I.R.O. Div. Land Res. Canberra.*
An analysis of breakthrough curves for solute transport under saturated, steady-state flow conditions to determine the coefficients of hydrodynamic dispersion is presented. A computer program (Fortran) which calculates the Brenner numbers for any displacement experiment, and which is essential to the analysis, is also given.

85. Peck, A.J. (1971), Transport of salts in unsaturated and saturated soils, *Salinity and Water Use*, Ed. T. Talsma and J.R. Philip, MacMillan, 109-123.
An introductory review paper describing the processes and their relative importance on salt transport, particularly in the plant environment. Considers molecular diffusion, convection, adsorption, ion exchange as well as the effects of porous medium structure and unsaturated flow. Leaching and surface accumulation of salts are mentioned as typical applications of salt transport theory.

86. Perkins, T.K. & Johnston, O.C. (1963), A review of diffusion and dispersion in porous media, *Soc. Pet. Eng. J., 3*, 70-84.
An extensive review of studies of dispersion in saturated porous media. Molecular diffusion, dispersion, and a number of variables which can influence dispersion are discussed.

87. Pinder, G.F. & Cooper, H.H. (1970), A numerical technique for calculating the transient position of the saltwater front, *Water Resour. Res., 6*, 875-882.
A numerical method using characteristics is presented to determine the unsteady-movement of the saltwater front in coastal aquifers. The A.D.I. method is used to solve the groundwater flow equation for the two dimensional problem. The method readily extends to irregular geometry, and to non-homogeneous aquifers. Numerical results are compared with two analytical solutions.

88. Pinder, G.F. & Gray, W.G. (1976), Is there a difference in the finite element method?, *Water Resour. Res., 12*, 105-107.
The convective-diffusive transport of a non-reactive solute is analyzed to demonstrate the relationship between the finite element and finite difference methods of approximating the differential equations.

89. Pinder, G.E. & Shapiro, A. (1979), A new collocation method for the solution of the convection-dominated transport equation, *Water Resour. Res., 15*, 1177-1182.
An orthogonal collocation method using a modified hermitian basis function is developed which, when solving the one-dimensional convection-dominated solute transport equation, provides an accurate, efficient and oscillation free solution with little numerical diffusion.

90. Rao, P.S.C., Davidson, J.M., Jessup, R.E. & Selim, H.M. (1979), Evaluation of conceptual models for describing nonequilibrium adsorption-

desorption of pesticides during steady flow in soils, *Soil Sci. Soc. Am. J.*, *43*, 22-28.
Experimental breakthrough curves are used to evaluate two conceptual models for describing the non-equilibrium adsorption-desorption of pesticides in porous media under steady-state saturated flow conditions.

91. Rose, D.A. (1977), Hydrodynamic dispersion in porous materials, *Soil Sci.*, *123*, 277-283.
A discussion of aspects of the hydrodynamic dispersion of a tracer in porous media under steady, saturated flow conditions. The use of superposition to obtain breakthrough curves for pulsed and periodic tracer inputs, the form of dispersion coefficients in terms of dimensionless groups of parameters, and the mechanisms underlying dispersion are discussed.

92. Rose, D.A. & Passioura, J.B. (1971), The analysis of experiments on hydrodynamic dispersion, *Soil Sci.*, *111*, 252-257.
A procedure for analysing experiments on hydrodynamic dispersion when under steady-state, saturated flow conditions. The analysis can only treat dispersion caused by interactions between molecular diffusion and convection, and not complex chemical interactions. The analysis is supported by experimental evidence. Several conditions which cause deviations from the analysis are discussed, as are alternative methods of analysis.

93. Ross, B. & Koplik, C.M. (1979), A new numerical method for solving the solute transport equation, *Water Resour. Res.*, *15*, 949-955.
A numerical model for solute transport in a saturated, steady-state quasi three-dimensional porous media is presented, and its use illustrated by a case study. The water flow field is approximated by a network of stream tubes and a Green's function solution used for each streamtube. Effects of mass transport, chemical interaction, hydrodynamic dispersion and radioactive decay are incorporated. The approach permits computational efficiencies and ease of representation of small discontinuities with more physically-oriented results compared to previous methods.

94. Rubin, J. & James, R.V. (1973), Dispersion-affected transport of reacting solutes in saturated porous media: Galerkin method applied to equilibrium-controlled exchange in unidirectional steady water flow, *Water Resour. Res.*, *9*, 1332-1356.
The relevant equations of reactive solute transport are formulated, and their solution described using a Galerkin finite element method. One-dimensional saturated, steady-state flow conditions apply. The utility of the numerical solution is demonstrated by means of several computed examples, and the role of some of the relevant system characteristics explored.

95. Saffman, P.G. (1959), A theory of dispersion in a porous medium, *J. Fluid Mech.*, *6*, 321-349.
A theory is presented for dispersion of a non-reactive solute flowing through a saturated porous medium under steady-state fluid flow conditions when dispersion is primarily due to mechanical dispersion. Theoretical results are compared with published experimental data, and remarks made concerning dispersion when Darcy's law is not obeyed.

96. Saffman, P.G. (1959), Dispersion due to molecular diffusion and macroscopic mixing in flow through a network of capillaries, *J. Fluid Mech.*, *7*, 194-208.
A theory is presented for dispersion of a non-reactive solute under saturated, steady-state flow conditions for the case where both molecular diffusion and mechanical dispersion are important. Comparisons are made between theoretical results and experimental observations of dispersion in flow through granular beds.

97. Sauty, J.P. (1980), An analysis of hydrodispersive transfer in aquifers, *Water Resour. Res.*, *16*, 145-158.
An analysis of the transport of non-reactive solute in saturated porous media for slug and continuous injection of solute in one and two dimensional uniform flow fields, and converging and diverging radial flow fields. A series of dimensionless type curves of concentration vs time are presented to permit direct analysis of field data (dispersivity and kinematic porosity) using curve matching techniques.

98. Schwartz, F.W. (1977), Macroscopic dispersion in porous media: the controlling factors, *Water Resour. Res.*, *13*, 743-752.
The dispersive character of natural groundwater systems resulting from large scale variations in hydraulic conductivity is investigated using stochastic analysis. Several controlling parameters are identified and their significance and influence demonstrated. A theoretical method for estimating dispersion within large scale geological systems using statistical techniques is suggested.

99. Scott, H.D. & Paetzold, R.F. (1978), Effects of soil moisture on the diffusion coefficients and activation energies of tritiated water, chloride and metribuzin, *Soil Sci. Soc. Am. J.*, *42*, 23-27.
Diffusion coefficients for tritiated water, chloride and matribuzin are determined in captina silt loam as functions of soil water content and soil temperature.

100. Selim, H.M., Davidson, J.M. & Rao, P.S.C. (1977), Transport of reactive solutes through multilayered soils, *Soil Sci. Soc. Am. J.*, *41*, 3-10.
A study of reactive solute transport through saturated and unsaturated multilayered soils using laboratory experiments and a numerical finite difference model. Steady-state water flow conditions apply, and the model includes convection, dispersion, adsorption/desorption and sink/source effects.

101. Selim, H.M. & Mansell, R.S. (1976), Analytical solution of the equation for transport of reactive solutes through soils, *Water Resour. Res.*, *12*, 528-532.
Mathematical solutions for reactive solute transport under steady-state flow conditions in a finite column are presented for a number of surface boundary conditions. The effects of convection, dispersion, linear adsorption and a sink/source term are included. Comparisons are made with other solutions subject to different boundary conditions. See also comment by Parlange and Starr and author's reply in same journal, Vol. 13, 701-704.

102. Shamir, U.Y. & Harleman, D.R.F. (1967), Numerical solutions for dispersion in porous mediums, *Water Resour. Res.*, *3*, 557-581.
A numerical implicit finite difference method is presented for solving problems of dispersion in steady, saturated three-dimensional

flow fields where the miscible fluids have the same density and viscosity. The model is developed and tested for two-dimensional problems where exact or approximate analytical solutions exist, then extended to three-dimensions. An emphasis is placed on the efficiency of the numerical scheme, which is shown to be independent of the flow fluid geometry.

103. Skopp, J. & Warrick, A.W. (1974), A two-phase model for the miscible displacement of reactive solutes in soils, *Soil Sci. Soc. Am. Proc., 38,* 545-550.
Reactive solute transport with convection, diffusion and adsorption under saturated, steady-state water flow conditions is studied using an analytical model. A distinction is made between mobile and immobile soil-water regions, and the solution gives solute concentration breakthrough curves. Comparisons are made with published experimental data.

104 Smiles, D.E., Perroux, K.M., Zegelin, S.J. & Raats, P.A.C. (1981), Hydrodynamic dispersion during constant rate absorption of water by soil, *Soil. Sci. Soc. Am. J., 45,* 453-458.
Experimental study of dispersion of salt under unsaturated unsteady, constant flux adsorption into an initially uniform soil. Quasi-analytical methods are presented which predict the water and solute profiles using a constant solute dispersion coefficient. The data presents no evidence to reject the piston flow model during transient flow at relatively low soil water contents.

105. Smiles, D.E. & Philip, J.R. (1978), Solute transport during absorption of water by soil: laboratory studies and their practical implications, *Soil Sci. Soc. Am. J., 42,* 537-544.
An experimental study of non-reactive solute transport during absorption into uniform horizontal soil columns under unsteady constant moisture concentration flow conditions in a sand. Various initial moisture contents with either displacement of concentrated soil solution by dilute solution or vice versa are included. Both water and solute preserve similarity in terms of distance divided by the square root of time. The dispersion coefficient could be considered velocity independent and moisture content independent. Observed piston-like displacement of initial water by the adsorbed water questions basis of mobile and immobile water fractions (in this material at least).

106. Smiles, D.E., Philip, J.R., Knight, J.H. & Elrick, D.E. (1978), Hydrodynamic dispersion during absorption of water by soil, *Soil Sci. Soc. Am. J., 42,* 229-234.
Experimental study of hydrodynamic dispersion of low concentration non-reactive solute during absorption into horizontal columns of sand with initially uniform moisture and solute contents. The initial soil solution contains a relatively high solute concentration. Both water and solute concentration profiles preserve similarity in terms of distance divided by the square root of time implying that the dispersion coefficient is insensitive to pore water velocity.

107. Starr, J.L., De Roo, H.C., Frink, D.E. & Parlange, J.-Y. (1978), Leaching characteristics of a layered field soil, *Soil Sci. Soc. Am. J., 42,* 386-391.
A field study of leaching characteristics of a layered soil (fine sandy loam over coarse sand) above a water table. The effect of air

entrainment on the rate of infiltration under ponded conditions is observed. The movement of a slug of solute under ponded infiltration conditions is measured under steady-state conditions. Solute movement is in fingers of flow below where the flow becomes unstable. Effects of field spatial heterogeneity, untrapped air, and experimental techniques on the observed results are discussed.

108. Starr, J.L. & Parlange, J.-Y. (1976), Solute dispersion in saturated soil columns, *Soil Sci., 121,* 364-372.
An experimental study of non-reactive solute dispersion in vertical, water saturated soil columns. The influence of flow rate, direction of flow, and the density difference of the displacing solution on the amount of dispersion are studied. An explicit finger model is postulated to explain the failure of the diffusion model to predict breakthrough curves for the neutrally and overstable configurations, (ie when the density difference between the solutions is zero, and dense over less dense respectively) and to explain changes in shape of the breakthrough curves for the unstable configuration.

109. Starr, J.L. & Parlange, J.-Y. (1979), Dispersion in soil columns: the snow plow effect, *Soil Sci. Soc. Am. J., 43,* 448-450.
The exchange and transport of cations are studied in a saturated soil column under steady flow conditions. The soil has a low cation exchange capacity. Displacement of a labelled solute is by an unlabelled solution of much greater solute concentration. A theoretical approximation is developed which predicts the phenomenon adequately.

110. Tang, D.H. & Babu, D.K. (1979), Analytical solution of a velocity dependent dispersion problem, *Water Resour. Res., 15,* 1471-1478.
An analytical solution assuming radial flow for the convective-dispersive transport of solute under saturated, steady fluid flow conditions is developed. The solution is significantly different to existing approximate analytical solutions.

111. Terkeltoub, R.W. & Babcock, K.L. (1971), A simple method for predicting salt movement through soil, *Soil Sci., 111,* 182-187.
A simplified model is presented to calculate the distribution of salt in a porous medium at the end of an infiltration period.

112. Todd, R.M. & Kemper, W.D. (1972), Salt dispersion coefficients near an evaporating surface, *Soil Sci. Soc. Am. Proc., 36,* 539-543.
An experimental study of salt and water movement near an evaporating surface under steady, unsaturated water flow conditions for both a clay loam and a sand.

113. Umari, A., Willis, R. & Liu, P.L.F. (1979), Identification of aquifer dispersivities in two dimensional transient groundwater contaminant transport: an optimization approach, *Water Resour. Res., 15,* 815-831.
A finite element model of the water and solute transport equations for saturated, two-dimensional unsteady-conditions is presented. An optimization algorithm is developed to allow unknown aquifer dispersivities to be calculated to minimize the discrepancy between calculated and observed values of the concentration field. The reverse problem of choice of data input to calculate the concentration field is studied, and attention given to the model sensitivity for each of the input parameters.

114. Vachaud, G., Wierenga, P.J., Gaudet, J.P. & Jegat, H. (1976), Simulation of miscible displacement in unsaturated porous media, *System Simulation in Water Resources*, Ed. G.C. Vansteenkiste, North Holland, 129-140.
A review of a number of physical approaches toward solving solute dispersion problems in saturated and unsaturated porous media, and a discussion on the relative merits of these approaches.

115. Van de Pol, R.M., Wierenga, P.J. & Nielsen, D.R. (1977), Solute movement in a field soil, *Soil Sci. Soc. Am. J., 41,* 10-13.
A study of non-reactive solute (chloride and tritium) and water movement under field conditions with steady-state soil water flow. Results are compared to an analytical solution.

116. Van Genuchten, M.Th., Davidson, J.M. & Wierenga, P.J. (1974), An evaluation of kinetic and equilibrium equations for the prediction of pesticide movement through porous media, *Soil Sci. Soc. Am. Proc., 38,* 29-35.
An experimental and numerical study of reactive solute transport in a saturated loam soil under steady-state water flow conditions. An explicit finite difference (CSMP) solute model is used to compare numerical results using three different absorption-desorption relationships with the experimental data, for a range of pore water velocities. An empirical model is developed which gives reasonable comparisons over the range of pore water velocities. This includes a mobile-immobile water distinction.

117. Van Genuchten, M. Th. & Wierenga, P.J. (1974), *Simulation of One-Dimensional Solute Transfer in Porous Media,* New Mexico State Univ. Ag. Exp. Stn., Bulletin 628.
An explicit finite difference model (CSMP) of one-dimensional reactive solute flow under steady water flow conditions is presented. Problems of numerical dispersion, stability and boundary conditions are discussed. Examples of the model's use are presented, and comparisons made between analytical and numerical solutions.

118. Van Genuchten, M. Th. & Wierenga, P.J. (1976), Numerical solution for convective dispersion with intra-aggregate diffusion and non-linear adsorption, *System Simulation in Water Resources,* Ed. G.C. Vansteenkiste, North Holland, 275-291.
An explicit finite difference (CSMP) model of reactive solute transport in unsaturated, steady flow conditions where intra-aggregate diffusion and hysteretic non-linear adsorption/desorption are included, is presented. The model differentiates between mobile and immobile water to account for the observed asymmetry in the effluent concentration curves. Comparisons are presented with analytical and experimental results.

119. Van Genuchten, M.Th. & Wierenga, P.J. (1976), Mass transfer studies in sorbing porous media I. Analytical solutions, *Soil Sci. Soc. Am. J., 40,* 473-480.
An analytical solution is presented for the movement of reactive solutes through a sorbing porous medium under unsaturated steady-state water flow conditions. The liquid phase is divided into mobile and immobile regions. The solution gives the effluent concentration-time relationship and depends upon four dimensionless parameters, and a study of the solution sensitivity to each parameter is presented.

120. Warrick, A.W., Biggar, J.W. & Nielsen, D.R. (1971), Simultaneous solute and water transfer for an unsaturated soil, *Water Resour. Res.*, *7*, 1216-1225.
The simultaneous flow of water and solute during infiltration is studied both in the field and numerically. Two approximate quasi-analytical solutions are presented and used to study the influence of the initial soil water content and the infiltration rate on solute movement.

121. Warrick, A.W., Kichen, J.H. & Thames, J.L. (1972), Solutions for miscible displacement of soil water with time-dependent velocity and dispersion coefficients, *Soil Sci. Soc. Am. Proc.*, *36*, 863-867.
Simplified analytical solutions are presented to describe non-reactive solute flow for both step and slug inputs during infiltration. Numerical calculations are made and compared using both constant and time-dependent pore water velocities and solute dispersion coefficients. The approximate analytical solutions are used to predict experimental breakthrough curves.

122. Weeks, O.L., Stewart, G.L. & Weeks, M.E. (1976), Measurement of non-exchanging pores during miscible displacement in soils, *Soil Sci.*, *122*, 139-144.
An experimental study of non-reactive solute movement under steady-state, saturated conditions for solute infiltration and solute leaching under different flow velocities. The study is designed to estimate the proportion of pore space not readily exchangeable with the displacing solution, and to determine whether previously reported values reflect primarily non-exchanging pore space or only slowly conducting pore space.

123. Wierenga, P.J. (1977), Solute distribution profiles computed with steady-state and transient water movement models, *Soil Sci. Soc. Am. J.*, *41*, 1050-1055.
Solute concentration distributions obtained using a steady-state and an unsteady-state model are compared. A numerical study and experimental data is used to illustrate that the steady-state model could adequately predict solute profiles and effluent concentration distributions following sequences of infiltration/redistribution, even when the infiltration interval varies. Adequate predictions rely on suitable choices for the average water content and a constant dispersion coefficient, and the paper discusses the basis for these choices.

124. Wood, A.L. & Davidson, J.M. (1976), Fluometuron and water content distributions during infiltration: measured and calculated, *Soil Sci. Soc. Am. Proc.*, *39*, 820-825.
An explicit finite difference model for reactive solute flow coupled with an implicit finite difference model for water flow under unsteady, unsaturated flow conditions are solved simultaneously. Solute is allowed to be adsorbed/desorbed using a Freundlich equilibrium type relationship. The influence of initial soil water content and water application rate on the transport of reactive solute is studied numerically and experimentally.

125. Wooding, R.A. (1972), Perturbation analysis of the equation for the transport of dissolved solids through porous media I. Linear problems, *J. Hydrology*, *16*, 1-15.

The technique of matched asymptotic expansions is applied to reactive solute transport in steady one-dimensional flow fields assuming linear exchange equilibrium and constant diffusivity. Three cases illustrative of the perturbation technique are treated.

126. Wooding, R.A. (1972), Perturbation analysis of the equation for the transport of dissolved solids through porous media II. Basic non-linear problem, *J. Hydrology, 16*, 105-116.
Singular perturbation methods are used to treat analytically the transport of reactive solute in steady one-dimensional flow fields in a porous column assuming non-linear exchange equilibrium and a concentration dependent diffusion coefficient.

127. Wooding, R.A. (1972), Perturbation analysis of the equation for the transport of dissolved solids through porous media III. Influence of boundary conditions, *J. Hydrology, 16*, 241-245.
The asymptotic properties of solute transport involving first-order irreversible reaction in a finite column of porous material are described for a linearized system when the Danckwerts boundary conditions apply.

128. Yule, D.F. & Gardner, W.R. (1978), Longitudinal and transverse dispersion coefficient in unsaturated plainfield sand, *Water Resour. Res., 14*, 582-588.
The relationship between longitudinal and transverse dispersion coefficients, pore water velocity and the effective diffusion coefficient is determined experimentally for a range of pore water velocities in a vertical, unsaturated column of sand under steady flow conditions.

APPENDIX B

SOLUTION OF TRIDIAGONAL EQUATIONS USING THE THOMAS ALGORITHM

The set of tridiagonal simultaneous equations to be solved was given by equation 2.10 and is

$$\begin{aligned} A_2h_1 + B_2h_2 + C_2h_3 &= D_2 \\ A_3h_2 + B_3h_3 + C_3h_4 &= D_3 \\ A_4h_3 + B_4h_4 + C_4h_5 &= D_4 \\ \cdots\cdots\cdots\cdots\cdots\cdots & \\ A_Nh_{N-1} + B_Nh_N + C_Nh_{N+1} &= D_N \end{aligned} \qquad \text{B.1}$$

The solution of this set of N-1 equations in N+1 unknowns requires the application of a top and bottom boundary condition to eliminate the terms in h_1 and h_{N+1} respectively. The method of solution involves two sweeps through the equations as follows:

(a) *Preparatory Sweep*

For the first equation, A_2h_1 is rewritten in terms of h_2 and h_3 by the application of the top boundary equation giving

$$B_2h_2 + C_2h_3 = D_2 \qquad \text{B.2}$$

$$h_2 = \frac{D_2}{B_2} - \frac{C_2}{B_2}h_3 = Z_2 - Y_2h_3 \qquad \text{B.3}$$

where

$$Z_2 = \frac{D_2}{B_2} \qquad \text{B.4}$$

$$Y_2 = \frac{C_2}{B_2} \qquad \text{B.5}$$

For the second equation

$$A_3(Z_2 - Y_2h_3) + B_3h_3 + C_3h_4 = D_3$$

$$(B_3 - A_3Y_2)\,h_3 = D_3 - A_3Z_2 - C_3h_4 \qquad \text{B.6}$$

$$h_3 = \frac{D_3 - A_3Z_2}{B_3 - A_3Y_2} - \frac{C_3}{B_3 - A_3Y_2}h_4$$

$$= Z_3 - Y_3h_4 \qquad \text{B.7}$$

where $$Z_3 = \frac{D_3 - A_3 Z_2}{B_3 - A_3 Y_2} \qquad \text{B.8}$$

$$Y_3 = \frac{C_3}{B_3 - A_3 Y_2} \qquad \text{B.9}$$

Similarly for the third equation

$$h_4 = Z_4 - Y_4 h_5 \qquad \text{B.10}$$

where $$Z_4 = \frac{D_4 - A_4 Z_3}{B_4 - A_4 Y_3} \qquad \text{B.11}$$

$$Y_4 = \frac{C_4}{B_4 - A_4 Y_3} \qquad \text{B.12}$$

Therefore in general

$$h_i = Z_i - Y_i h_{(i+1)} \qquad \text{B.13}$$

where $$Z_i = \frac{D_i - A_i Z_{(i-1)}}{B_i - A_i Y_{(i-1)}} \qquad \text{B.14}$$

$$Y_i = \frac{C_i}{B_i - A_i Y_{(i-1)}} \qquad \text{B.15}$$

The definitions of Z_2 and Y_2 for the first equation conform if Z_1, $Y_1 = 0$.

(b) *Solution Sweep*

For the last (Nth) equation the term $C_N h_{N+1}$ is eliminated by the application of the bottom boundary condition. Therefore

$$h_N = Z_N \qquad \text{B.16}$$

Knowing h_N we can obtain

$$h_{(N-1)} = Z_{(N-1)} - Y_{(N-1)} h_N \qquad \text{B.17}$$

or in general

$$h_{(i-1)} = Z_{(i-1)} - Y_{(i-1)} h_i \qquad \text{B.18}$$

The solution then progresses backwards to give the values of h between h_N and h_2. Since the boundaries are at 1 and N+1, the boundary condition equation must be solved using the values of h just determined to give h_1 and h_{N+1}.

APPENDIX C

CURVE FITTING USING SPLINE TECHNIQUES

Introduction

The numerical solution of either equation 2.1 or 2.2 requires that the hydrologic characteristics $h(\theta)$ and $K(\theta)$ be defined over the range covered by the simulation. These characteristics are determined experimentally, and usually cannot be represented by simple algebraic relationships. A convenient and accurate method of defining the characteristics is given by the interpolating spline technique.

A mathematical spline is a piecewise polynomial of degree 'm' which has continuous derivatives at the junction points where two polynomials meet. The cubic spline ($m = 3$) is preferred because of its smoothness and its ability to accurately reflect localised variations. Its use in the present context, for defining $h(\theta)$ and $C_s(h)$ characteristics, has been detailed by Erh (1972). However a cubic spline occasionally produces extraneous inflection points in the curve. To remove these unwanted inflections an approach, which mathematically approximates the applying of a tension to the curve by pulling on its end points, was developed by Schweikert (1966) and Cline (1974α). The resulting 'spline in tension' is still constrained to pass through the given points. By varying the amount of 'tension' a range of interpolating curves can be determined, from a highly curved low tension spline indistinguishable from the ordinary cubic spline, to a nearly-polygonal high tension spline.

The 'spline in tension' is developed from a differential equation, which involves values of the spline's second derivative for several values of the independent variable. A tridiagonal set of linear equations for the unknown second derivatives results from the requirement that the function and its first two derivatives are continuous. These must be solved before the spline can be evaluated.

Theory

Consider a set of n data points x_i where $x_1 \leq x_i \leq x_n$. The corresponding set of functional values is $y_1 \leq y_i \leq y_n$ where in general $y_i = f(x_i)$. A constant, non zero 'tension factor' equal to σ is also defined. The desired function f must be real-valued and have two continuous derivatives.

Let $f'' - \sigma^2 f$ (which is necessarily continuous) vary linearly over each interval $[x_i, x_{i+1}]$, $i = 1,\ldots,n$. Then for $x_i \leq x \leq x_{i+1}$,

$$f''(x) - \sigma^2 f(x) = [f''(x_i) - \sigma^2 y_i][x_{i+1} - x]/\kappa_i + [f''(x_{i+1}) - \sigma^2 y_{i+1}][x - x_i]/\kappa_i \qquad C.1$$

where $\kappa_i = [x_{i+1} - x_i]$ for $i = 1,\ldots,(n-1)$

The solution to equation C.1 is

$$\begin{aligned} f(x) = {} & [f''(x_i)/\sigma^2]\sinh[\sigma(x_{i+1} - x)]/\sinh(\sigma\kappa_i) \\ & + [y_i - f''(x_i)/\sigma^2][x_{i+1} - x]/\kappa_i \\ & + [f''(x_{i+1})/\sigma^2]\sinh[\sigma(x - x_i)]/\sinh(\sigma\kappa_i) \\ & + [y_{i+1} - f''(x_{i+1})/\sigma^2][x - x_i]/\kappa_i \end{aligned} \qquad C.2$$

for $x_i \le x \le x_{i+}$. That equation C.2 is the solution of equation C.1 is readily shown by differentiation. Clearly f is continuous over the interval $x_i \le x \le x_{i+1}$, and it follows from equation C.1 that f'' and thus f' are continuous, provided a unique solution exists for $f''(x_i)$, i = 1,...,n.

Differentiating equation C.2 and rearranging gives

$$\begin{aligned} f'(x) = {} & [f''(x_i)/\sigma^2]\{1/\kappa_i - \sigma \cosh[\sigma(x_{i+1} - x)]/\sinh(\sigma\kappa_i)\} \\ & + [f''(x_{i+1})/\sigma^2]\{\sigma \cosh[\sigma(x - x_i)]/\sinh(\sigma\kappa_i) - 1/\kappa_i\} \\ & + [y_{i+1} - y_i]/\kappa_i \end{aligned} \qquad \text{C.3}$$

Evaluating and equating the right and left sided derivatives at x_i, for i = 2,...,(n-1), and rearranging gives

$$\begin{aligned} & [y_{i+1} - y_i]/\kappa_i - [y_i - y_{i-1}]/\kappa_{i-1} \\ & = [f''(x_{i-1})/\sigma^2]\{1/\kappa_{i-1} - \sigma/\sinh(\sigma\kappa_{i-1})\} \\ & \quad + [f''(x_i)/\sigma^2]\{\sigma \cosh(\sigma\kappa_i)/\sinh(\sigma\kappa_i) - 1/\kappa_i \\ & \quad + \sigma \cosh(\sigma\kappa_{i-1})/\sinh(\sigma\kappa_{i-1}) - 1/\kappa_{i-1}\} \\ & \quad + [f''(x_{i+1})/\sigma^2]\{1/\kappa_i - \sigma/\sinh(\sigma\kappa_i)\} \end{aligned} \qquad \text{C.4}$$

To complete the solution, the boundary conditions need to be specified. If the derivatives y_1' and y_n' are known, then f must satisfy $f'(x_1) = y_1'$ and $f'(x_n) = y_n'$. Differentiating equation C.2 at $x = x_1$ and $x = x_n$, and then equating to y_1' and y_n' respectively, gives

$$\begin{aligned} y_1' = {} & [f''(x_1)/\sigma^2][1/\kappa_1 - \sigma \cosh(\sigma\kappa_1)/\sinh(\sigma\kappa_1)] \\ & + [f''(x_2)/\sigma^2][\sigma/\sinh(\sigma\kappa_1) - 1/\kappa_1] + [y_2 - y_1]/\kappa_1 \end{aligned} \qquad \text{C.5}$$

and

$$\begin{aligned} y_n' = {} & [f''(x_{n-1})/\sigma^2][1/\kappa_{n-1} - \sigma/\sinh(\sigma\kappa_{n-1})] \\ & + [f''(x_n)/\sigma^2][\sigma \cosh(\sigma\kappa_{n-1})/\sinh(\sigma\kappa_{n-1}) - 1/\kappa_{n-1}] \\ & + [y_n - y_{n-1}]/\kappa_{n-1} \end{aligned} \qquad \text{C.6}$$

The tridiagonal linear system defined by equations C.4 to C.6 for the unknown $f''(x_i)/\sigma^2$, i = 1,...,n is strictly diagonally dominant and thus nonsingular. The solution of equations C.4 to C.6 is equivalent to the solution of the original differential equation C.1 with its boundary conditions. Once the $f''(x_i)/\sigma^2$, i = 1,...,n are determined, the solution is given by equation C.2.

For the extreme values of the tension factor σ, it is seen from equation C.1 that if $\sigma \to 0$, f'' is continuous and varies linearly between the data points

x_i, i = 1,...,n. This is the standard cubic spline. As $\sigma \to \infty$, equation C.1 reduces to f, and is linear from point to point, or piecewise linear in general. Hence the splines under tension will approach cubic splines for low tension factors and piecewise linear functions for large tension factors. For $\sigma' < 0.001$ the resulting curve is virtually indistinguishable from a cubic spline, and for $\sigma' > 50$ it is almost piecewise linear. A usual value is $\sigma' = 1$.

The use of σ as detailed above results in nonlinear behaviour, because all the data points x_i and hence κ_i are multiplied by a constant factor. This is eliminated by using a 'normalised' tension factor σ' where

$$\sigma' = \sigma(x_n - x_1)/(n - 1) \qquad C.7$$

Structure of the Spline Function Subprograms

Two computer subprograms are used to implement the spline under tension. The first is called once only for a given set of data, and sets up and solves the tridiagonal system to determine the spline function. It incorporates a routine to compute the end slopes y_1' and y_n' by quadratic interpolation using the first three and last three data points respectively. The second subprogram interpolates a curve at a given point (x) using the spline in tension determined from the first subprogram. A further call to the second subprogram calculates the value of the derivative at the specified point (x).

The computer routines were kindly supplied by D. Doran of the School of Civil Engineering, University of N.S.W. (personal communication) and are based upon those given by Cline (1974*b*).

Application

A preliminary spline function is fitted to the raw soil water pressure (the x_i values) and water content (the y_i values) data. The corresponding first derivative function (this corresponds to the specific water capacity which is also required for the solution of equation 2.1 or 2.2) is then calculated. Any irregularities in the first derivative function are then removed by making small adjustments to the x_i values until a smooth first differential curve is obtained. The resultant spline function is then ready for use in the soil water program of Chapter 2.

References

Cline, A.K. (1974*a*), Scalar- and planar-valued curve fitting using splines under tension, *Comm. ACM, 17,* 218-220.

Cline, A.K. (1974*b*), Algorithm 476 - Six subprograms for curve fitting using splines under tension, *Comm. ACM, 17,* 220-223.

Erh, K.T. (1972), Application of the spline function to soil science, *Soil Sci., 114,* 333-338.

Schweikert, D.G. (1966), An interpolation curve using a spline in tension, *J. Math. and Physics, 45,* 312-317.